The cell-secreted microenvironment: shaping embryonic stem cell self-renewal and differentiation

by

Laralynne M. Przybyla
B.S., Biochemistry and Molecular Biology, Purdue University 2006

SUBMITTED TO THE DEPARTMENT OF BIOLOGY IN PARTIAL FULFILLMENT OF THE REQUIREMENTS FOR THE DEGREE OF

DOCTOR OF PHILOSOPHY
AT THE
MASSACHUSETTS INSTITUTE OF TECHNOLOGY

JUNE 2012

Signature of Author_____
Laralynne Przybyla
Department of Biology
May 10, 2012

Certified by_____
Joel Voldman
Associate Professor of Electrical Engineering and Computer Science
Thesis Supervisor

Accepted by_____
Robert T. Sauer
Salvador E. Luria Professor of Biology
Co-Chair, Biology Graduate Committee

The cell-secreted microenvironment: shaping embryonic stem cell self-renewal and differentiation

by

Laralynne M. Przybyla

Submitted to the Department of Biology on May 10, 2012 in partial fulfillment of the requirements for the degree of Doctor of Philosophy in Biology

ABSTRACT

The objective of this work is to obtain an in depth understanding of how embryonic stem cell-secreted signals contribute to their identity. We analyze the contribution of broad and specific signals present in the cell-secreted microenvironment using techniques that can easily be applied to studies of other cell types and signaling systems. Determining the effects of external signals produced endogenously by stem cells is important for understanding fundamental biological processes regarding cell communication and for implementing more sophisticated manipulation protocols for future clinical applications. Harnessing the ability of stem cells to generate specific cell types is necessary for many regenerative medicine and tissue engineering applications and would be enhanced by a more thorough understanding of the signaling pathways required to maintain stem cell self-renewal and to initiate an exit from the self-renewing state.

In this thesis, we describe work showing that mouse embryonic stem cell (mESC)-secreted signals are required to maintain self-renewal, as cells enter a primed, epiblast-like state of early differentiation when microfluidic perfusion is used to deplete soluble cell-secreted signals. We show that this phenotypic change can be used to our advantage for directed differentiation, and further demonstrate that remodeling the endogenous extracellular matrix halts the exit from the self-renewing state that occurs in mESCs growing under perfusion. Matrix remodeling is then shown to be both necessary and sufficient for maintaining mouse embryonic stem cell self-renewal in the absence of other external cues, and we demonstrate a method for assessing the relative contributions of soluble versus matrix-based cues.

Together, our data indicate the importance of mESC-secreted factors in contributing to cell survival, self-renewal, and differentiation in normal cultures. Beyond furthering our understanding of intrinsic signaling mechanisms, this information can be used to devise better culture systems for directed differentiation of pluripotent cells. In addition, the techniques developed and implemented here for assessing the contributions of endogenous signals can all be applied generally to any adherent cell type for studies of how the cell-secreted microenvironment contributes to signaling processes and ultimately to cell phenotype.

Thesis Supervisor: Joel Voldman
Title: Associate Professor of Electrical Engineering and Computer Science

Acknowledgements

The work described in this thesis would not have been possible without the help and support of a great many people. First, I want to thank Dr. Joel Voldman, who agreed to let me join his lab despite my lack of experience and always enthusiastically supported my research. I admire and value his willingness to simultaneously pursue several diverse projects, which has given me the opportunity to learn about fields of research I may never have encountered otherwise. Thanks also to my thesis committee, Dr. Frank Gertler, Dr. Alex Meissner, and especially Dr. Laurie Boyer, who has graciously allowed me to attend and present at her group meetings for the past four years and whose lab has provided me with valuable input and essential experimental advice.

Many members of the Voldman lab have made my experience in grad school more meaningful and enjoyable. Thanks to Lily Kim and Alison Skelley for first introducing me to stem cells and microfluidics. Also thanks to Lily and Katarina Blagovic for helping with design of the perfusion device that was used in many of the experiments described here. In addition to the device, Katarina also contributed significantly to the lab environment and my growth as a scientist, as did Mike Vahey, Salil Desai, and Pat Sampattavanich. I also had experimental help from Joseph Kovac and Tao Sun, who helped me with polymerization experiments, and Yi-Chin Toh who shared her expert knowledge on immunofluorescence staining. Thanks also to Brian Taff, Nick Mittal and Melanie Hoehl, who I am glad to have worked with.

Lab members who are currently contributing to making the Voldman lab an interesting and collegial environment include my officemate Catherine Lo, the ever-enthusiastic Hao-Wei Su, the lively post-docs Marc Castellarnau and Javier Prieto, Sarvesh Varma, who shares in my continuous frustration over perfusion but is friendly and accommodating nonetheless, and Burak Dura, Aalap Dighe, and Thibault Honegger, all of whom I wish I had a chance to overlap with more in lab. I owe special thanks to everyone mentioned in this paragraph for not only putting up with me in lab during the last few months of finishing my thesis, but also for being very supportive and helpful as I looked to the next stage in my academic career.

Beyond the scientific help already mentioned above, I have also worked directly with some people for generating portions of this thesis. I would like to thank Eloise Shaw for being a fantastic summer student who did great work trying to separate ESC colonies based on morphology, found in Chapter 6.3. In addition, Thor Theunissen, a post-doc from Rudolf Jaenisch's lab, helped with some experiments described in Chapter 7 involving epiblast stem cells and with in vivo experiments. The Flow Cytometry and BioMicro center core facilites have been invaluable, especially Fugen Li who helped with analyses of RNA sequencing data. Finally, the Boyer lab has provided many reagents, including the H2A-GFP cell line used in this work.

Beyond scientific support, I have also been lucky to have great friend and family support without whom my time here at MIT would not have been nearly as rewarding. My entering graduate class still includes many great friends who I feel fortunate to have shared this experience with. My parents John and Michelle Przybyla have been nothing but supportive of my personal and professional choices, which I do and will continue to value. My siblings Ben, Becki, and Stephanie Przybyla are three of the cleverest, most talented people I know and I appreciate the competitive spirit I'm sure they helped instill in me. And finally, thanks to Luke, for everything.

Table of Contents

Figures and Tables

Commonly used abbreviations

BMP4 – Bone morphogenetic protein 4

EB – Embryoid body

ECM – Extracellular matrix

ERK – Extracellular signal-regulated kinase

ESC – Embryonic stem cell

EpiSC – Epiblast stem cell

FGF – Fibroblast growth factor

GFP – Green fluorescent protein

GSK3 – Glycogen synthase kinase 3

HSPG – Heparan sulfate proteoglycan

ICM – Inner cell mass

JAK – Janus kinase

LIF – Leukemia inhibitory factor

MEF – Mouse embryonic fibroblast

MMP – Matrix metalloproteinase

PD03 – PD0325901, a MEK/ERK inhibitor

PDMS - Polydimethylsiloxane

PEGDA – Polyethylene glycol diacrylate

STAT3 – Signal transducer and activator of transcription 3

TGFβ – Transforming growth factor, beta

VEGF – Vascular endothelial growth factor

Chapter 1 Introduction

1.1 Significance

Cell phenotype is defined in part by the extracellular signals encountered by the cell, whether it is a cell growing in culture, a cell growing in the body performing normal functions, or an abnormal cell that exploits extracellular signals to disrupt cellular functions. The in vivo extracellular microenvironment, or niche, consists of basement membranes and extracellular matrix, cell-cell contacts, and soluble signals that travel from other cells throughout the body. The niche is particularly important for stem cell microenvironments, as subtle signal changes can lead to significant downstream fate adjustments. Understanding the composition and contributors to the in vivo niche is required for successful recapitulation of stem cell microenvironments in vitro.

In recent years, the ability to grow and maintain many diverse types of cells in culture has significantly advanced due to technical developments allowing for more sophisticated cell culture systems. Tools that can successfully manipulate the in vitro microenvironment can be used to learn more about how extracellular signals act to regulate fate choice and thus provide platforms to further our understanding of the biological and functional impacts of particular signals. This information can be useful for generating in vitro models of in vivo events and for establishing conditions for maintenance of stem cells as multipotent entities in vitro.

In this thesis, we use embryonic stem cells (ESCs) as an unbiased model stem cell system and apply various methods to disrupt the endogenous extracellular microenvironment in an effort to learn more about how embryonic stem cell-secreted signals contribute to the remarkable ability of these cells to self-renew indefinitely while retaining the ability to differentiate into any cell type found in an adult organism. Our results highlight the importance of the cell-secreted microenvironment on stem cell growth, self-renewal, and differentiation, and show that cell fate can be strongly influenced by altering microenvironmental cues. The utility of this work lies in its broad applicability to other stem cell systems, its use as a potential tool to direct differentiation or maintain self-renewal, and its uncovering of novel endogenous mechanisms used by stem cells in culture to balance differentiation and self-renewal cues.

1.2 Embryonic stem cells

ESCs are pluripotent cells—they are able to differentiate into all lineages—derived from the inner cell mass (ICM) of a blastocyst. In addition to being pluripotent, they are also able to self-renew by dividing while maintaining their pluripotent state, or to differentiate by dividing and exiting their pluripotent state to adopt other phenotypes. ESCs have been derived from several mammals (Evans and Kaufman, 1981; Martin, 1981; Thomson et al., 1998, 1995; Iannaccone et al., 1994; Hayes et al., 2008; Schneider et al., 2007), but mouse (Evans and Kaufman, 1981; Martin, 1981) and human (Thomson et al., 1998) ESCs (mESCs and hESCs, respectively) are most commonly studied. ESCs are readily available from cell banks and can be derived *de novo*, are relatively straightforward to culture, and can divide indefinitely in culture without losing their pluripotency. Pluripotent stem cells can also be derived from somatic cells by reprogramming, which has been shown for both mouse (Takahashi and Yamanaka, 2006; Wernig et al., 2007; Okita et al., 2007) and human (Yu et al., 2007; Takahashi et al., 2007). These cells, called induced pluripotent stem (iPS) cells, share most features with ESCs and can be derived from patient-specific backgrounds. Because they can be generated from cells with specific disease backgrounds, iPS cells provide an opportunity to study disease progression from development onward. The ability of pluripotent cells to differentiate into all tissues in the adult explains their clinical significance, in that they have the potential to form cells or tissues for regenerative medicine.

Self-renewal is the most fundamental process that ESCs undergo, and is interesting both from a basic cell biological view (i.e., how do ESCs decide to stay as ESCs) and biotechnological (i.e., how do we design bioprocesses that allow expansion of ESCs to therapeutic scales while maintaining pluripotency). Thus, significant effort has been expended over the last 30 yrs to understand ESC self-renewal, resulting in the identification of exogenous signals important for this process. ESCs are derived from mouse at embryonic day 3.5 (E3.5), at which point the inner cell mass is formed but not organized and implantation has not yet occurred. By E4.5, the embryo has segregated to form the trophectoderm, epiblast, and primitive endoderm, and begins the process of attachment and implantation. By E6.5, the embryo is implanted and gastrulation begins, whereby the epiblast forms the primitive streak and generates cells of the mesoderm and endoderm lineages. The epiblast itself goes on to generate cells of the ectoderm lineage, which

differentiate into epidermal and neuronal cells, while the mesoderm forms cells of the circulatory system and muscle, and endoderm forms the gut, liver, pancreas and lungs.

It was recently demonstrated that pluripotent cells could be isolated from the mouse later than E3.5 when epiblast stem cells (EpiSCs) were isolated from the post-implantation epiblast (E5.5-5.75) (Tesar et al., 2007; Brons et al., 2007). While EpiSCs can differentiate into tissues from all three germ layers, they cannot contribute to all tissues in the developing organism after injection into a blastocyst, indicating that they are not fully pluripotent. mEpiSCs and mESCs also have different exogenous requirements for maintaining their self-renewal due to their different origins, and mEpiSCs more closely resemble hESCs in terms of morphology and self-renewal requirements, indicating that hESCs may be derived from a human developmental stage equivalent to the E5.5 stage in mice.

The work done in this thesis is centered around mESCs, which are conventionally maintained on a mouse embryonic fibroblast feeder layer with addition of leukemia inhibitory factor (LIF) and serum (Nichols et al., 1990). Many ESC lines have been adapted to not require a feeder layer, but are grown in media with LIF and serum. Various types of serum-free media have also been developed, and the variant I refer to in this thesis is N2B27 media supplemented with LIF and bone morphogenetic protein 4 (BMP4) (Ying et al., 2003b). The common component among all these methods for maintaining mESCs in a self-renewing state is LIF, a cytokine originally isolated based on its ability to inhibit growth and induce differentiation into macrophages in the mouse leukemic cell line M1 (Hilton et al., 1988). LIF was found to share this ability with a previously identified cytokine, IL-6, and it was thus found that the two signals shared a common receptor component in gp130 (Gearing et al., 1992; Ip et al., 1992). Along with gp130, the LIF receptor forms a heterodimer that allows the LIF signal to be transmitted internally. This family of cytokine receptors was found to activate tyrosine kinase activity when stimulated, and the specific tyrosine kinases that bind to dimerized gp130 are in the Janus kinase (JAK) family (Silvennoinen et al., 1993). JAK family tyrosine kinases then go on to phosphorylate signal transducer and activator of transcription (Stat) family proteins, the first identified being Stat3, which is phosphorylated and translocates into the nucleus within minutes after gp130 activation (Wegenka et al., 1993). For mESC maintenance, Stat3 is the most relevant Stat family member downstream of LIF, as it acts as a transcription factor to regulate genes necessary for the

maintenance of mESC self-renewal, including Klf4 and Nanog (Darnell, 1997; Jiang et al., 2008) (Figure 1-1).

In contrast to the signaling elements that act to maintain mESC self-renewal, the primary extracellular signaling requirements for both mEpiSCs and hESCs are fibroblast growth factor 2 (FGF2) and Activin/Nodal/TGFβ family ligands. FGF2 is typically added to mEpiSC cultures to maintain their self-renewal, and EpiSCs have been shown to also require autocrine Activin/Nodal signaling, which signals through Smad2/3 to activate self-renewal signals, including Nanog (Greber et al., 2010) (Figure 1-1). FGF2 is also added to hESC cultures, where it may act to reinforce autocrine production of FGF2 (Eiselleova et al., 2009). TGFβ/Activin signaling has also been proposed as an autocrine loop for maintenance of hESC self-renewal (Xu et al., 2008), and Activin addition may induce autocrine FGF2 production in hESCs (Xiao et al., 2006). GDF3, also in the TGFβ superfamily, is secreted from hESCs and acts to block BMP and thus inhibit differentiation (Levine et al., 2009), while autocrine levels decrease during differentiation (Levine and Brivanlou, 2006). Though the extracellular regulatory processes are different in mouse and human ESCs, likely due to differences in the developmental stage at which they are isolated, both types of cells share some elements of the core self-renewal regulatory circuitry, including autoregulatory control by the transcription factors Oct4, Sox2, and Nanog (Boyer et al., 2005).

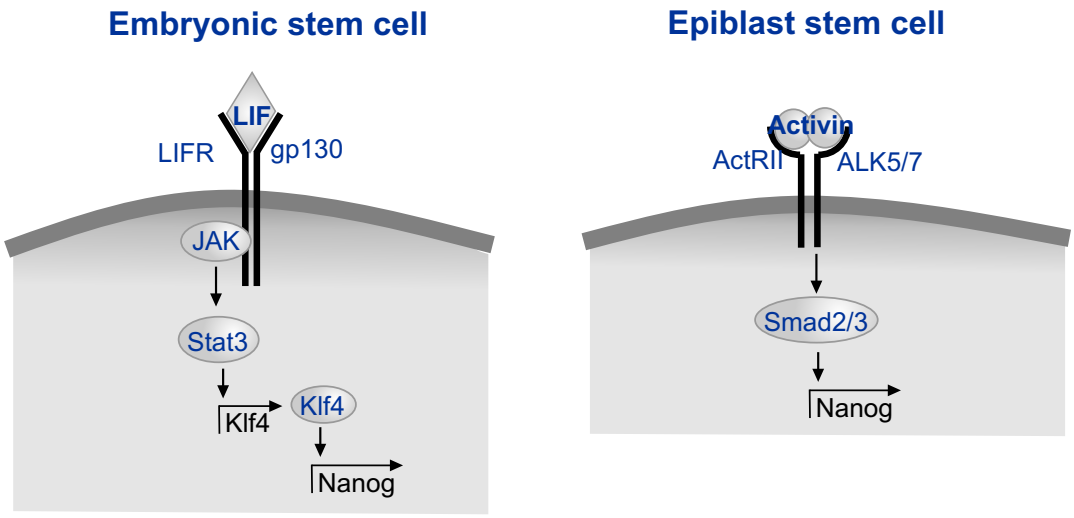

Figure 1-1 Model figure depicting major pathways by which transcription of the crucial self-renewal transcription factor Nanog is upregulated in mouse embryonic (left) and epiblast (right) stem cells.

Neither mouse nor human ESCs are homogenous under normal culture conditions. Part of the mechanism by which exogenous FGF2 acts to maintain hESC cultures is thought to be due to a paracrine loop that forms after some fraction of the population differentiates to a more fibroblast-like state that then secretes IGF-II in response to exogenous FGF2, which in turn serves to keep the remaining hESCs in a self-renewing state (Bendall et al., 2007). mESC cultures are also heterogeneous, with cells maintaining a balance between naïve and primed states, the latter of which allows the cells to be ready for differentiation. Cells in the naïve state express specific ESC markers such as Klf4 and Rex1, while primed cells have markers more similar to that of the epiblast stem cell state, including FGF5 and Dnmt3b (Lanner et al., 2010; Kunath et al., 2007). This heterogeneity has been shown to be functional, as in the case of Rex1 high- and low-expressing mESC populations with different differentiation potentials after FACS separation (Toyooka et al., 2008), which was also seen for the self-renewal marker Nanog (Kalmar et al., 2009) and the visceral endoderm marker Hex (Canham et al., 2010). Maintaining a balance between the naïve and primed states in mESC culture is thought to be important for maintenance of pluripotency, as cells trapped in a naïve state are unable to properly differentiate to all three germ layers (Kunath et al., 2007; Lanner et al., 2010).

Besides addition of LIF, other culture systems have also been shown to maintain mESC self-renewal, the best characterized being addition of inhibitors of the FGF4-ERK signaling pathway and glycogen synthase kinase 3 (GSK3) (Ying et al., 2008), but the maintenance of self-renewal under these conditions is still enhanced by addition of LIF, a media formulation known as 2i/LIF. We will not fully understand the process of self-renewal until we determine the signals that are both necessary and sufficient to maintain self-renewal. Embryonic stem cells are a useful model cell type in which to study microenvironmental cues, as these cells have a dynamic and robust capacity for intercellular signaling, and functional assays can be performed to convincingly test both necessity and sufficiency of a particular signaling environment to maintain self-renewal and pluripotency.

1.3 Cell-secreted microenvironment

To test sufficiency of signals for any cellular process, it is imperative to either know the identity of or develop the ability to control the relevant signals secreted from the cells themselves. One

important type of cell-secreted signals are soluble signals that travel through the culture media to signal to other cells in the environment, but cells can also signal through direct contact with other cells or by extracellular matrix-based signals.

Soluble signals consist of autocrine or paracrine signals, which canonically refer to signals produced by cells to which they respond (autocrine) or to which neighboring cells respond (paracrine) (Sporn and Todaro, 1980). Here, I will use the term autocrine signaling to refer to signals secreted by a cell that may bind to that cell or to a neighboring cell of similar phenotype, while paracrine signaling refers to signals produced by a cell to which that cell type cannot respond, but other cell types can. These soluble signals can include growth factors, which are defined as having a positive effect on proliferation and/or differentiation, cytokines, which constitute other signaling molecules with diverse functions in intercellular communications, and hormones, which are generated at specific sites in vivo and typically act in a limited range with tightly controlled secretion levels. Different types of soluble signals also have different rates of uptake, as the number of cytokine receptors on the cell surface is usually on the order of 10^2 to 10^3, a hundred times less than that of hormone or growth factor receptors (Kishimoto, 2005).

Contact-mediated signals, also known as juxtacrine signals, require two adjacent cells to be in contact, as these types of signals are not secreted extracellularly from the producing cell. Such signals can be transmitted through transmembrane receptors or through membrane channels. Notch signaling is an example of a juxtacrine mechanism in which the ligand and receptor are both transmembrane proteins such that cells must be in direct contact for signaling to occur. Notch is activated by Delta, Jagged, or Serrate proteins in an adjacent cell and is then cleaved, at which point it translocates to the nucleus and binds and activates transcription factors (Schroeter et al., 1998). Small soluble signals (less than 15 kD) can also be directly transmitted between cells through gap junctions made up of connexin proteins that create a pore between cells through which ions can freely pass (Peracchia and Dulhunty, 1976).

Once adherent cells are attached to a substrate, they begin to produce an extracellular matrix (ECM) consisting of many types of signals that become an important part of the extracellular microenvironment. The ECM includes structural proteins, connective proteins, glycoproteins, signaling proteins, etc., all contained in a dense and dynamic structure. Fibronectin is a large

glycoprotein that serves as a general adhesive molecule, linking cells to their substrate and to each other (Yamada and Olden, 1978). The extracellular matrix present in vivo surrounding epithelial tissue generally includes a dense region called the basal lamina, which consists of laminin and collagen along with glycoproteins such as heparan sulfate proteoglycans (Sanes et al., 1990; Jenniskens et al., 2000). Heparan sulfate proteoglycans (HSPGs) are important ECM components that are thought to act as a reservoir of signaling proteins such as growth factors (Hynes, 2009), and also affect the signaling of molecules such as Wnt, vascular endothelial growth factor (VEGF) and fibroblast growth factor (FGF) (Rosen and Lemjabbar-Alaoui, 2010). The developmental signal sonic hedgehog binds vitronectin in the ECM (Pons and Martí, 2000), and core ECM components such as integrins and laminins have been shown to act as signaling molecules themselves. Integrins are essentially transmembrane fibronectin receptors that bind to cytoskeletal proteins on the inside of a cell, thus integrating the extracellular and intracellular scaffolds (Tamkun et al., 1986).

In addition to acting as a substrate on which cells can grow and directly or indirectly providing signals from its structural molecules or by binding growth factors, the ECM has physical properties that can also influence cells. For uncommitted progenitor cells, the stiffness of the matrix has been shown to influence differentiation trajectory in a variety of systems, including for mesenchymal stem cells (Engler et al., 2006), neural stem cells (Keung et al., 2011), and embryonic stem cells (Chowdhury et al., 2010), and increased matrix stiffness has also been implicated in cancer cell migration and proliferation (Ulrich et al., 2009). Manipulating the rigidity of the ECM can alter availability of autocrine signals, as seen with myofibroblasts and autocrine TGFβ accessibility (Wells and Discher, 2008). ECM composition is also affected endogenously by cell-secreted proteinases, including matrix metalloproteinases (MMPs), a disintegrin and metalloproteinase with thrombospondin motifs (ADAMTS) family proteins, and serine proteases, which have the potential to affect any of the ECM-based signaling mechanisms described above. Of these, the MMP family includes the major secreted proteins that dynamically regulate the ECM both in vitro and in vivo during development (Vu and Werb, 2000), the significance of which will be described in the next section.

1.4 Embryonic stem cell and in vivo microenvironment: soluble and ECM-based signals

Proper embryonic development requires specific regulation of a series of signaling events emanating from within the embryo or maternally. At early stages of development, many of these signals are identical to the ones used for maintenance or early differentiation of embryonic stem cells cultured in vitro. Here, we detail what is known about the functionality of ESC in vitro endogenous extracellular signals and then describe several relevant examples of signaling events required for proper development in the early embryo.

Embryonic stem cells divide rapidly and secrete high levels of proteins, both in terms of soluble ligand secretion and extracellular matrix formation. Several mESC autocrine factors have been identified that influence proliferation (Figure 1-2), including Activin, Nodal and Cyclophilin A (Ogawa et al., 2007; Mittal and Voldman, 2011). LIF has also been shown to act in an autocrine fashion (Davey et al., 2007; Davey and Zandstra, 2006; Zandstra et al., 2000), though not at levels sufficient to maintain self-renewal, while autocrine Wnt signaling has been shown to be required but not sufficient for mESC self-renewal (ten Berge et al., 2011). Autocrine differentiation-inducing signals have also been identified, the most studied example being FGF4, which signals through extracellular signal-regulated kinase 1 and 2 (ERK1/2). FGF4-null mES cells were found to be more likely to express pluripotency markers and less likely to express differentiation markers, and a similar phenotype was observed in $ERK2^{-/-}$ cells (Kunath et al., 2007), while disruption of both FGF4 and ERK signaling in the absence of LIF caused cells to stagnate in a reversible primitive ectoderm state in which no further differentiation is possible (Stavridis et al., 2007). At the transcriptional level, the ERK pathway has been implicated in the repression of the pluripotency-related transcription factor Nanog (Hamazaki et al., 2006). Many of the functional identified autocrine signals acting in hESCs differ from those in mESCs, which have been described in chapter 1.2 and are also summarized in Figure 1-2.

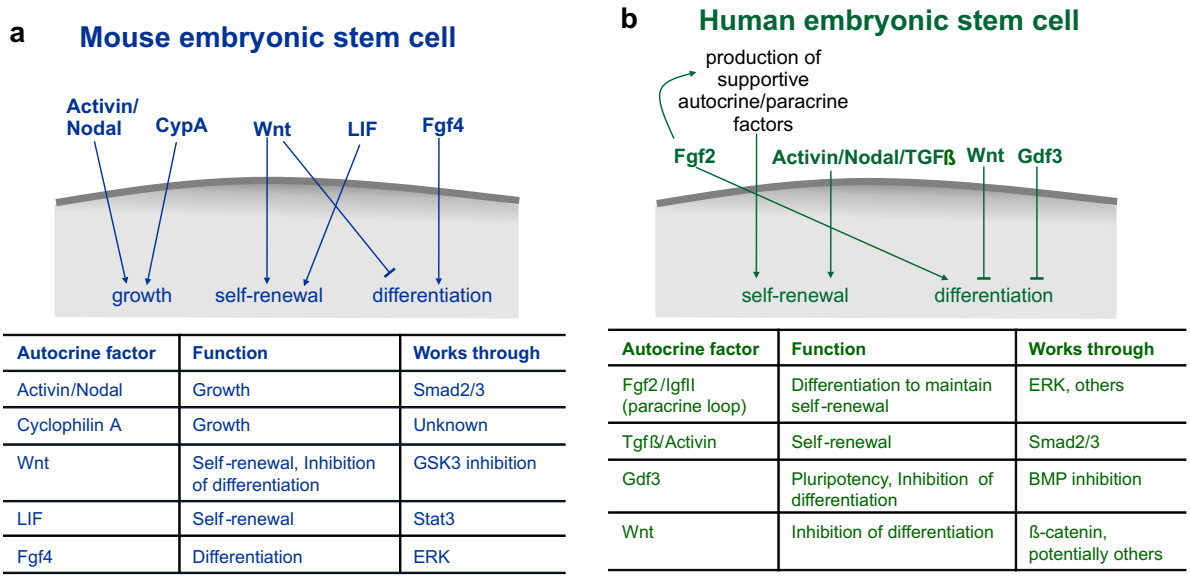

Autocrine factor	Function	Works through
Activin/Nodal	Growth	Smad2/3
Cyclophilin A	Growth	Unknown
Wnt	Self-renewal, Inhibition of differentiation	GSK3 inhibition
LIF	Self-renewal	Stat3
Fgf4	Differentiation	ERK

Autocrine factor	Function	Works through
Fgf2/IgfII (paracrine loop)	Differentiation to maintain self-renewal	ERK, others
Tgfß/Activin	Self-renewal	Smad2/3
Gdf3	Pluripotency, Inhibition of differentiation	BMP inhibition
Wnt	Inhibition of differentiation	ß-catenin, potentially others

Figure 1-2 Functional autocrine-acting signals that have been identified in mESCs (a) and hESCs (b) and their roles.

While a variety of natural and synthetic matrices have been used to influence ESC self-renewal or differentiation, and ESCs also deposit a rich matrix of their own, the mechanisms behind how extracellular matrix affects cell fate are largely unexplored. Autocrine FGF4 has been shown to require ECM-based HSPGs for signaling to ESCs, and disruption of FGF4 binding leads to increased self-renewal of mESCs (Lanner et al., 2010). Other autocrine signals such as Wnts have also been shown to bind in the ECM and to HSPGs (Schryver et al., 1996; Fuerer et al., 2010), but no functional role for the ECM in mESC autocrine Wnt signaling has been conclusively shown. Mechanically, it has been shown that softer matrices, at similar stiffnesses to mESCs themselves, are able to maintain mESCs in the absence of LIF for multiple passages (Chowdhury et al., 2010), indicating the possibility for a direct mechanical role of ECM in ESC self-renewal, but the mechanism behind this phenomenon is unknown. A direct role for ECM in maintaining self-renewal has been further characterized in hESCs, where their survival and self-renewal in defined media requires growth on an exogenous ECM, mediated by the binding of endogenous integrins with exogenously supplied vitronectin (Braam et al., 2008). ESCs will differentiate into heterogenous cultures if not passaged regularly, signifying that regular breakdown and rebuilding of the ECM is important in maintaining a more homogenous undifferentiated state.

Although ESCs do not directly correspond to cells found in a developing embryo, uncovering autocrine signals present in vitro is important for understanding early embryonic development, as the pluripotent state in vivo is transient and proper development requires an exit from this state as a result of maternal and embryonic autocrine and paracrine signaling (Figure 1-3). Much is known about the signals generated in vivo that contribute to embryonic development, implantation, and gastrulation, but many of these studies have been performed in non-mammalian systems, so this section will highlight the relevant soluble and ECM-based signals that contribute to early mammalian embryonic development.

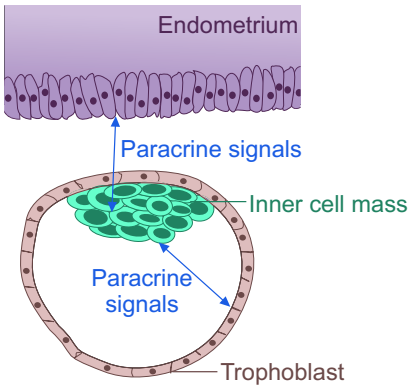

Figure 1-3 Origin of paracrine signals involved in developmental specification in the early embryo.

In terms of soluble signaling, paracrine communication between cells that make up the inner cell mass and the trophectoderm or between extraembryonic cells and adjacent epiblast cells has been shown to be an important part of early mouse embryonic growth (Murohashi et al., 2010; Mesnard et al., 2011), and blastocyst implantation requires paracrine LIF expression in the uterus (Stewart et al., 1992). Signals within the embryo itself are also important, for example, it has been shown that the anterior visceral endoderm inhibits Nodal signaling to ensure proper formation of the primitive streak during gastrulation (Bertocchini and Stern, 2002; Perea-Gomez et al., 2002). FGF signaling is also important within the embryo, as it is in ESC differentiation. Embryos lacking FGFR1 die at gastrulation (Deng et al., 1994; Yamaguchi et al., 1994), and both FGF4 and FGF8 are required for early embryonic development, as their disruption results in abortive postimplantation development and disrupted gastrulation, respectively (Feldman et al., 1995; Sun et al., 1999). Endogenous FGF signaling has recently been more specifically identified as the signal required for segregation of the primitive endoderm and epiblast cells during ICM maturation (Yamanaka et al., 2010).

Direct cell contacts such as gap junctions are also important in development, for example, before the blastocyst even forms, the first eight blastomere cells are connected by gap junctions, forming physiological compartments within the developing embryo (Kalimi and Lo, 1988). The gap junctions regulate the compaction of the blastomeres to form the blastocyst, as inhibiting connexins inhibits further embryonic development (Lo and Gilula, 1979). Defects in cell-cell adhesion in the early mammalian embryo due to knockout of a specific myosin chain affected production of epiblast-derived cells in the post-implantation embryo and resulted in embryonic death by E7.5 (Conti et al., 2004).

Cell adhesion and migration are essential mechanisms involved in embryonic implantation and gastrulation, and these mechanisms depend on the ability of cells to attach to extracellular matrices. Cell-cell and cell-ECM adhesion molecules that have been shown to act during gastrulation in mouse include E-cadherins and integrins (Hammerschmidt and Wedlich, 2008), and both their extra- and intracellular domains are required for proper gastrulation movements (Lee and Gumbiner, 1995; Kühl et al., 1996). Integrin interaction with fibronectin plays a large role in cell migration that occurs during gastrulation, while other known integrin ligands such as collagens and laminins are expressed at the end of or after this process (Bökel and Brown, 2002). Preceding this, the development of the epiblast prior to implantation requires proper basement membrane assembly between epiblast cells and their underlying epithelial layer (Murray and Edgar, 2000), and integrin- and laminin-deficient cells are unable to form basement membranes and thus do not undergo epiblast differentiation (Li et al., 2002). While ECM may not directly contribute to intracellular signaling during development, it is an important regulator of signals such as those from the TGFβ, Wnt, and Hedgehog protein families, all important secreted mediators of cell patterning and fate determination in early embryos (Brown, 2011). Matrix remodeling is important in vivo as it is in vitro, as MMPs and MMP inhibitors were found to be expressed at high levels in mouse blastocysts and play a role in embryonic implantation (Alexander et al., 1996), with a significant increase in MMP production during the peri-implantation period (Chen et al., 2007).

1.5 Manipulating extracellular signaling

Cell-secreted autocrine and paracrine factors comprise a significant fraction of available soluble signals, particularly in serum-free cultures, but their identity and significance are challenging to study. When specific factors or receptors that are part of an autocrine/paracrine signaling pathway are known, the best way to investigate the contributions of the pathway is via inhibition with knockout cell lines or specific inhibitors. Many small molecule inhibitors have been identified that are specific to receptors or downstream signaling molecules, and blocking antibodies can be developed to target known proteins or receptors. Cell lines can also be derived with specific secreted proteins or receptors knocked out. With these reagents, one can perform the definitive experiments to identify and characterize an autocrine loop (Figure 1-4a). By measuring ligand in the media and characterizing phenotype with and without receptor-blocking antibody, one can determine that (1) the cells are secreting ligand, (2) the ligand binds to the receptor, and (3) ligand binding alters phenotype (DeWitt et al., 2001; Joslin et al., 2007). Importantly, all these methods are limited to studies of known factors.

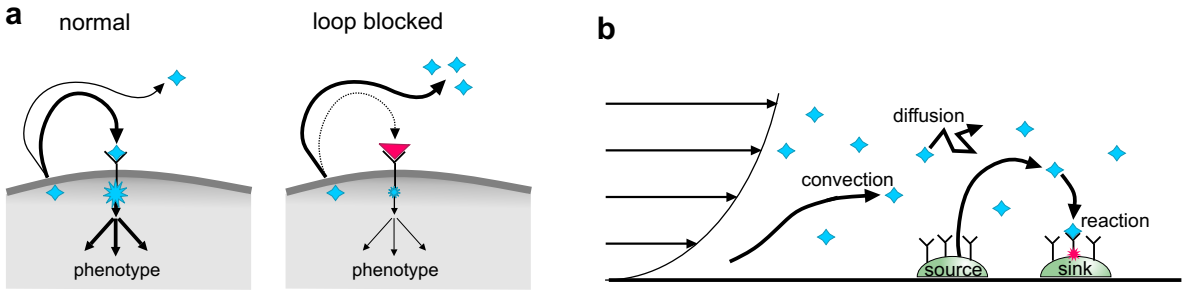

Figure 1-4 Methods for investigating autocrine/paracrine signaling. (a) As autocrine factors are secreted from a cell, they bind to receptors to trigger a downstream response (left), unless the receptor is blocked, in which case autocrine signals accumulate in the surrounding media (right). (b) Transport modes for cell-secreted soluble signals, including diffusion, reaction, and convection of ligands from sources to sinks.

What is currently known about autocrine signaling in ESCs has primarily been determined using these methods. For example, when autocrine Wnt signals were identified to be necessary for mESC self-renewal, it was found that addition of either a Wnt antagonist or an inhibitor of Wnt signal production were able to halt self-renewal, an effect that could be reversed with exogenous Wnt addition (ten Berge et al., 2011). An alternative to varying cell density is to use conditioned media assays. Experiments in which media that has been exposed to one population of cells to condition it (i.e., to load it with cell-secreted factors) and then transferred to a separate cell population have been used in studies of both autocrine and paracrine signaling. In studies of autocrine signaling, conditioned media can be used as a surrogate for cell density, as cells can be

grown sparsely and then conditioned media added to simulate culture at high density; this approach has been used to find that autocrine factors are important for maintenance of a short G1 cell cycle phase in hESCs (Becker et al., 2010). Conditioned media studies are even more powerful when studying paracrine signaling. Many in vitro protocols for differentiation of ESCs rely on conditioned media or on co-culture with other cell types (Banerjee et al., 2011; Kawasaki et al., 2000; Lam et al., 2010). One common method involves use of a transwell, an insert that allows paracrine signals to pass between cells cultured in a single well but separated by a protein-permeable membrane. Though useful, conditioned media assays may suffer from inconsistency, as the complement of growth factors present may vary based on cell seeding density, growth time, and preparation and storage of conditioned media.

In addition to these conventional cell culture methods, microtechnologies that enable cell patterning and organization have also been adopted to investigate cell-cell signaling, either within colonies of cells or between colonies of the same or different cell types. Micropatterning has been used to study density-dependent autocrine signaling in ESCs by allowing for control over colony size, which in turn affects ligand source and sink levels. Modulating signaling by altering colony size can help to remove source/sink variations in autocrine signals while also indicating whether cell fate is density-dependent. For example, Peerani and colleagues patterned hESCs into different-sized colonies using microcontact printing and assessed the ESCs' phenotype using quantitative immunocytochemistry, ultimately implicating endogenous BMP2 and GDF3 as modulators of self-renewal (Peerani et al., 2007). Related studies with mESCs patterned at different colony sizes indicated the importance of endogenous Stat3 activation on self-renewal and showed that transcription downstream of Stat3 can be regulated by colony size (Peerani et al., 2009). Control of cell placement has also been used to manipulate and study contact-mediated signaling with mechanical control and micrometer precision (Hui and Bhatia, 2007), a technique that could feasibly be applied to studies involving stem cells.

In addition to their utility in placing cells to alter levels of secreted ligands, patterning techniques can also be used to pattern islands of specific matrix-associated molecules to limit their exposure within a population. ECM binding of cell-secreted factors limits their diffusion, which can be mimicked by attaching such factors to the surface on which cells are growing. For example, Shh attached to a polymer hydrogel surface was shown to promote the ostogenic differentiation of

mesenchymal stem cells (Ho et al., 2007), while attachment of EGF was able to sustain ERK signaling in these cells to promote cell spreading and survival (Fan et al., 2007). In addition to signaling molecules, structural ECM proteins can also be patterned and shown to be functional, as was shown for neuronal stem cells, which showed enhanced neuronal and astrocytic differentiation on immobilized fibronectin molecules but not laminins (Nakajima et al., 2007). Cell and substrate patterning techniques have also been combined to create experimentally convenient in vitro models of vivo environments. Bio-flip chip cell patterning creates patterns by overturning a cell-loaded microwell array onto a recipient substrate, whereupon the cells fall out of the well and onto the recipient substrate while maintaining their arrangement (Rosenthal et al., 2007), and this technique has been combined with stenciling to pattern mESCs along with other cell populations found in the early embryo to create developmental models to study early embryonic patterning events in vitro (Toh et al., 2011).

The endogenous extracellular matrix can itself be disrupted to determine its broad roles or the roles of specific molecules or classes of molecules, though relatively few studies exist that specifically probe endogenous matrix functionality. The disruption of proper heparan sulfate proteoglycan sulfation has been shown to cause neonatal lethality in vivo and to inhibit the ability of mESCs to differentiate properly in vitro (Ringvall et al., 2000; Lanner et al., 2010). As mentioned above, HSPG sulfation is known to be important for its binding function of many cytokines and growth factors (Bernfield et al., 1999), and the inability of ESC developmental progression in the absence of this function was primarily attributed to a lack of FGF4 signaling (Lanner et al., 2010). In this case, matrix disruption caused a matrix-based signal to no longer signal properly. Conversely, matrix remodeling can allow for proteins trapped within the matrix to be released, thereby increasing levels of available cell-secreted signals in the extracellular signaling environment (Taipale and Keski-Oja, 1997).

1.6 Microfluidic approaches to study cell-secreted signaling

While conventional approaches provide methods for uncovering the presence of autocrine and paracrine signaling pathways, revealing their importance, and identifying specific intercellular molecules involved, recent technological advances in microfluidic technology have enabled a more precise quantitative understanding of spatial and temporal parameters, thus allowing for

more controlled studies of the cell-secreted signaling environment. This section is adapted from a recently published review article (Przybyla and Voldman, 2012a).

To control cell-secreted signaling, the modes by which secreted molecules are transported in liquids need to be considered. In general, ligand is produced by "source" cells at some rate (molecules/sec), and then can bind to cell surface receptors (reaction sink), diffuse away, or be convected away (e.g., by fluid flow) (Figure 1-4b). To directly control transport of ligand in the media, nondimensional numbers can be used to compare different modes of transport, and thus determine the appropriate microfluidic operation regime. A diffusion velocity can be estimated by D/L, where D is the ligand diffusivity (for a ~20 kD cytokine, $D \sim 10^{-6}$ cm^2/s), and L is a characteristic length (e.g., the chamber height). Similarly, a reaction velocity can be defined as $k_{on}R_s$, where k_{on} is the ligand binding on-rate (in $M^{-1}s^{-1}$), R_s is the receptor density (in mol/m^2), and the convection velocity is simply v, the characteristic fluid velocity in the system. Ratios of these values lead to previously defined nondimensional numbers known as the Peclet number (convection/diffusion, vL/D), the Damkohler group I number (reaction/convection, $k_{on}R_s/v$) and the Damkohler group II number (reaction/diffusion, $k_{on}R_sL/D$). By altering these transport phenomena, one can alter the balance between diffusion, convection, and reaction, and in turn modulate the activity of autocrine loops to discover their effects on cell state.

Microfluidics allows a decrease of L and the application of v, and thus allows tuning of both diffusion and convection. To decrease soluble signaling, one wishes to decrease the effect of reaction, which can be accomplished by increasing convection. The fundamental requirement of microfluidic systems used for removing soluble signals is that they have some mechanism for exchanging the medium in the culture chamber. Thus, these systems are typically comprised of polydimethylsiloxane (PDMS) microfluidic chambers with inlets and outlets, and often have valves (King et al., 2007; Unger et al., 2000) and debubblers (Kang et al., 2008) to provide additional functionality.

Several microfluidic platforms have been described for the culture of ESCs, primarily to minimize reagent volumes for screens (Kamei et al., 2009; Villa-Diaz et al., 2009). Flow has also been used in microscale cultures to periodically replace the media in cell cultures to minimize nutrient depletion while allowing periodic accumulation of secreted factors, as was shown for

hESCs grown on a feeder layer that required a short pulse of media every 2-4 hours (Korin et al., 2008). Determination of the cell-secreted signals that are sufficient and necessary to maintain ESC self-renewal can also be aided by the precise control afforded by microfluidics. The use of microfluidics to control soluble factor mass transport has been demonstrated for both hESCs (Cimetta et al., 2009) and mESCs (Kim et al., 2006; Blagovic et al., 2011). For hESCs, a system was developed that could be tuned to operate in either a convection- or diffusion-dominated regime, resulting in different percentages of differentiated cells (Cimetta et al., 2009). This effect was primarily attributed to the effects of shear in the convection-dominated regime, but also to a decrease in soluble signaling due to the fact that the relative amount of differentiation was density-dependent.

In our lab, microfluidic techniques for controlling mESC soluble cell-secreted microenvironment were initially developed by Lily Kim, who demonstrated the first continuous, logarithmically scaled perfusion of mESCs for several days and showed that different perfusive flow rates affected mESC growth and colony size (Kim et al., 2006). A perfusion device designed by Lily Kim and Katarina Blagovic for growing mESCs at a single flow rate with two separate media conditions in triplicate chambers was then used to differentiate mESCs toward a neuroectodermal fate under perfusion (Blagovic et al., 2011). The viability of mESCs during this process was found to require cell-secreted factors beyond autocrine-acting FGF4. These studies laid the groundwork for using microfluidic perfusion to test the sufficiency and necessity of cell-secreted factors on the self-renewal of mESCs, which is the basis of much of the work described below.

1.7 Thesis specific aims and overview

In this thesis, I will discuss my work involving manipulating the endogenous embryonic stem cell extracellular signaling environment and assessing the effects on embryonic stem cell fate. These studies involve implementation of conventional techniques and development of novel methods for disruption of ESC-secreted signals, combined with downstream assays of the resulting phenotypic and functional consequences. The work can be broadly categorized into three specific aims, as follows:

1. Determining the effects of globally depleting soluble mESC-secreted signals and exploiting these effects to control ESC fate
2. Assessing the independent contributions of soluble and matrix-based endogenous signals with broad manipulations
3. Identifying and mechanistically analyzing functional endogenous components of the ESC extracellular matrix

In chapter 2, I describe the design and implementation of a microfluidic perfusion device for growth of mESCs under a continuous depletion of cell-secreted factors in serum-free culture, as part of aim 1. I discuss the motivation behind the device's initial application as studying how cell-secreted signaling influences heterogeneity in mESC cultures. I then show that mESCs exposed to decreased levels of cell-secreted soluble signals exit their self-renewing state and exhibit marker expression and signal responsiveness indicative of a more primed epiblast-like state.

Chapter 3 continues aim 1 by using the information gained from a depletion of ESC signals to manipulate and further characterize cells growing under perfusion. I first show results indicating that rapid directed differentiation is possible under perfusion given the right culture conditions, and I then describe a method for modeling and identifying the signals being removed under perfusion.

In chapter 4, I turn towards different cell-secreted signals, those emanating from the extracellular matrix. To address aim 2, I disrupt soluble signaling using perfusion in combination with broad disruption of the extracellular matrix, and show that these two types of signaling act in generally different pathways and adjust cell fate in different ways. While disrupting soluble signals causes cells to exit their self-renewing state, disrupting ECM-based signals does the opposite, and these opposing actions can be reconciled by realizing the importance of cell-secreted signals that act to disrupt the matrix in normal cultures.

An interesting conclusion from chapter 4 is further probed in chapter 5, as the sufficiency of matrix remodeling is demonstrated by exogenously adding matrix-remodeling proteins and

showing that they are able to maintain long-term LIF-independent mESC self-renewal, a result that I go on to explore mechanistically to address aim 3.

Chapter 6 describes a novel technique and a new application for an existing technique, both aimed at assessing the origin and significance of heterogeneity in mESC populations and within mESC colonies by manipulating or exploiting different aspects of the cell signaling microenvironment, to further address aim 2.

Finally, chapter 7 includes the broad conclusions that can be drawn from this work as a whole and describes several future directions that can be pursued using results and evidence described in the previous chapters.

Chapter 2 Effects of manipulating soluble ESC signaling under perfusion

2.1 Introduction

Determining the precise contributions of autocrine or paracrine signals to a particular process is difficult if the full complement of signals involved is unknown. Currently, such studies involve varying cell density or patterning cells at specific locations to find density-dependent responses (Lauffenburger and Cozens, 1989; Peerani et al., 2007). However, these methods are often incomplete due to the fact that autocrine loops can be self-sufficient even at clonal density (Van Zoelen et al., 1989). Further complicating matters, fluctuations in autocrine ligand concentration both within colonies and between colonies occur in a culture dish, leading to different levels of downstream pathway activation. Such differences in local concentrations of extracellular signals can cause and be exacerbated by population-wide heterogeneity.

In mESC cultures, heterogeneity is due in part to the fact that ESCs are constantly shifting between naïve and primed states (Chambers et al., 2007; Enver et al., 2009), which have different ligand and receptor expression and production levels. While naïve ESCs are primarily dependent on LIF signaling through Stat3 to maintain self-renewal (Darnell, 1997; Jiang et al., 2008), primed ESCs are closer to being in an epiblast-like state in which they may be more dependent on autocrine-acting Activin for maintenance of self-renewal (Greber et al., 2010). These opposing states cause heterogeneity in ligand production and uptake within mESC cultures, which can lead to difficulties when studying specific cell-secreted signaling pathways. Heterogeneity has been assessed within ESC colonies via specific marker expression (Singh et al., 2007; Toyooka et al., 2008), and this has been quantified in terms of how radial position within a colony relates to marker expression (Davey and Zandstra, 2006; Peerani et al., 2007). Building on these studies, we developed and tested a method to quantify the extent to which diffusible signaling affects heterogeneity in mESC cultures, showing that inhibition of MEK/ERK signaling causes mESC cultures to be more homogenously naïve. Because heterogeneity is due in large part to local differences in the cell-secreted extracellular signaling microenvironment, we sought to deplete cell-secreted signaling in general to determine whether other signals also contribute to heterogeneity.

We use a microfluidic perfusion system in which cells can be cultured under continuous media perfusion to remove cell-secreted soluble signals, thus providing a more neutral background with reduced signaling noise. In this chapter, we describe the characterization of this device in terms of transport parameters and practical operation with cells, and then we show that cells can successfully be cultured in the device. In order to analyze the phenotype of cells grown under perfusion, it is essential to compare them to cells grown in static culture under identical conditions. Thus, all experiments performed using perfusion involve cells grown in the device on polystyrene slides coated with gelatin, and these cells are compared to cells grown in gelatin-coated standard polystyrene culture dishes at identical cell density in cells/mm^2. To provide cells with a neutral signaling background, it is also important to use defined culture media, as use of feeder cells or addition of serum would create a noisier background that could obscure the contributions of cell-secreted factors.

Using this device affords us the opportunity to test how a global depletion of ESC-secreted factors affects cells in terms of their fundamental characteristics. We use a combination of population-wide assays to assess mRNA levels and single-cell measurements to quantify relative intracellular levels of a protein of interest to assess the resulting phenotype after cells have undergone perfusion, and compare this to the phenotype seen in static cultures. We can also use this system to add in factors individually or together to test their specific effects in the neutral background of perfusion. Here, we describe how depleting cell-secreted soluble signals in mESC populations compares to inhibiting the specific intracellular signal ERK, and go on to further characterize the cells that result from several days of growth under continuous perfusion.

Sections 2.2, 2.3, 2.5, and 2.6 of this chapter are adapted from Przybyla and Voldman (Przybyla and Voldman, 2012b).

2.2 Microfluidic device specifications and transport parameters

The microfluidic perfusion device used in all subsequent perfusion studies (Figure 2-1) is made from the transparent, biocompatible polymer polydimethylsiloxane (PDMS), a material commonly used for microfluidic cell culture (Meyvantsson and Beebe, 2008) that we have previously shown is suitable for culture of mESCs (Kim et al., 2006). Certain parameters need to be taken into consideration when designing a device and choosing operating conditions in order

to ensure that cell-secreted factors are removed while cells are not being affected in other ways by device operation. To ensure secreted factor removal, we consider the three molecular transport mechanisms that act on secreted molecules, namely convection, diffusion, and reaction (i.e., ligand binding to receptor) (Figure 1-4b). In order for molecules to be removed, convection must dominate over reaction and diffusion. To compare the importance of the different transport mechanisms, we make use of established non-dimensional parameters.

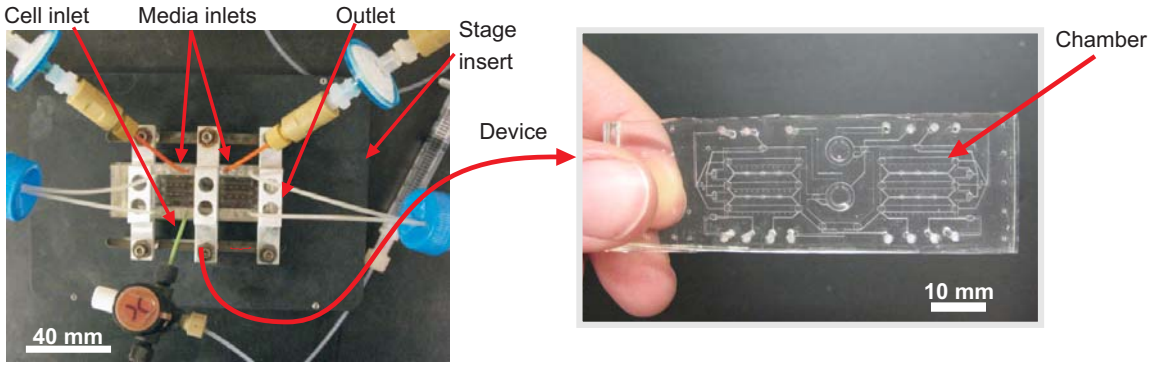

Figure 2-1 Microfluidic device setup. Left panel shows the device, inlets and outlets clamped to an insert for imaging on the microscope. Right panel shows the PDMS device.

Pe is given by vh/D, where v is a characteristic fluid velocity in the system (in our case, the average velocity, ~0.0296 mm/s), h is a characteristic length (in our case, half the chamber height, 125 µm), and D is the diffusivity of a relevant molecules (for a ~20 kD cytokine, $D \sim 10^{-6}$ cm^2/s). This results in *Pe* ~37, where *Pe*>1 indicates a convection-dominated regime. The ratio of the Peclet number and the Damkohler number *Da* is given by $v/k_{on}R_s$, where k_{on} is the ligand binding on-rate (~10^6 $M^{-1}s^{-1}$ for a strong interaction) and R_s is the receptor density (which we take to be ~12 receptors/μm^2 for a 8 µm radius cell with ~10000 receptors). This results in *Pe*/*Da* of ~1500, indicating that convection dominates over reaction. As medium flows by the autocrine-secreting cells, the axial convection and transverse mass transport will induce a concentration boundary layer above the cells, increasing in thickness along the length of the chamber (Squires et al., 2008). The boundary layer in general will decrease flux to and from the surface, and thus the concentration of secreted factor at the cell surface will be higher at the cell outlet than the inlet. The thickness of the boundary layer in microsystems such as ours generally scales as $1/Pe^{1/3}$ and thus will get thinner at higher *Pe*, while the flux through the boundary layer increases as $Pe^{1/3}$, therefore motivating operation at high *Pe* and use of short chambers, along

with experiments assessing axial heterogeneity. Together, these calculations suggest that secreted proteins that detach from the cell surface will be convected away and not recaptured.

Using these transport parameters, the shear at the culture surface is ~0.007 dynes/cm^2, two orders of magnitude lower than what is considered low fluid shear stress for cells (Grabowski and Lam, 1995), and also much lower than the shears of 5-25 dyn/cm^2 used to induce ESC-derived endothelial cells to begin expression of endothelial and tight junction markers (Nikmanesh et al.), or to induce endothelial cell-specific genes in mouse embryonic endothelial cells (Egorova et al., 2011). While mESCs have been shown to sense shear stress and respond to it dose-dependently at stresses from 0.016-16 dyn/ cm^2 (Toh and Voldman, 2011), ESCs have been grown indefinitely in bioreactors without any effects on self-renewal properties at shears up to 6.1 dyn/cm^2 (Cormier et al., 2006; Fok and Zandstra, 2005). In terms of cell removal, the detachment shear stresses for fibroblasts are ~30-50 dyn/cm^2 (Crouch et al., 1985), and shear stresses of 5 dyn/cm^2 have been applied to an endothelial monolayer for a week without noticeable cell detachment (Dewey et al., 1981), indicating that the shear required to detach adherent cells from substrates are typically >>1 dyn/cm^2. For mESCs in particular, removal shear stresses have been reported to be >6.5 dyn/cm^2 (Fok and Zandstra, 2005).

Furthermore, our chamber height (250 μm) was chosen to be substantially higher than the colony heights (55 μm) to minimize the effects of cell or colony height or morphology on flow patterns. To account for any flow rate differences in the chambers that could result from the presence of three-dimensional cell colonies, we use a previously described model (Gaver III and Kute, 1998). In general, for a cell or colony whose height is less than 30% of the chamber height (for our 250-μm high chambers, this corresponds to a 75 μm high colony), there is only a minor effect (0.05%) on flow rate realized in the system, due to increasing flow resistance from the decreased gap size between the colony and the chamber walls. Cells or colonies present in the chambers will also affect the shear stress, specifically increasing the surface shear stress as compared to the shear stress on a flat surface. However, Gaver and Kute demonstrate that the cells/colonies increase shear by a maximum of 3× with respect to a flat surface when the cell/colony height is <1/4 of the channel height (corresponding to 62 μm for our chambers). We measured colony heights in our chamber using optical microscopy to be 25-55 μm (average 40 μm), smaller than the 62 μm or 75 μm thresholds. Thus, for our chamber geometry, any cells or colonies smaller

than 62 µm in height would negligibly affect the flow and would have surface shear stresses well below shear stresses that have been shown to negatively affect cells.

2.3 Minimal requirements for ESC growth under microfluidic perfusion

To use microfluidic perfusion as a tool with which to characterize the contributions of ESC-secreted signals, it was first necessary to determine the minimal media required to successfully culture healthy cells. As stated above, use of serum-free, defined media was essential to this study, but ESCs generally do not grow as well or as reliably in the absence of serum. While mESCs in static culture can be induced to differentiate into neuronal precursors in defined media known as N2B27 (Ying et al., 2003b), they do not proliferate well in this defined media under perfusion where cell-secreted factors are removed (Blagovic et al., 2011). N2B27 can be used to maintain mESC self-renewal by supplementation with LIF and BMP4, and we found that this minimal defined self-renewing media did allow for growth of mESCs under perfusion (Figure 2-2). Once minimal defined conditions for mESC attachment and survival were established, we went on to show that cell-secreted factors were indeed removed and that cells growing under perfusion did not suffer any acute damage due to culture in the device.

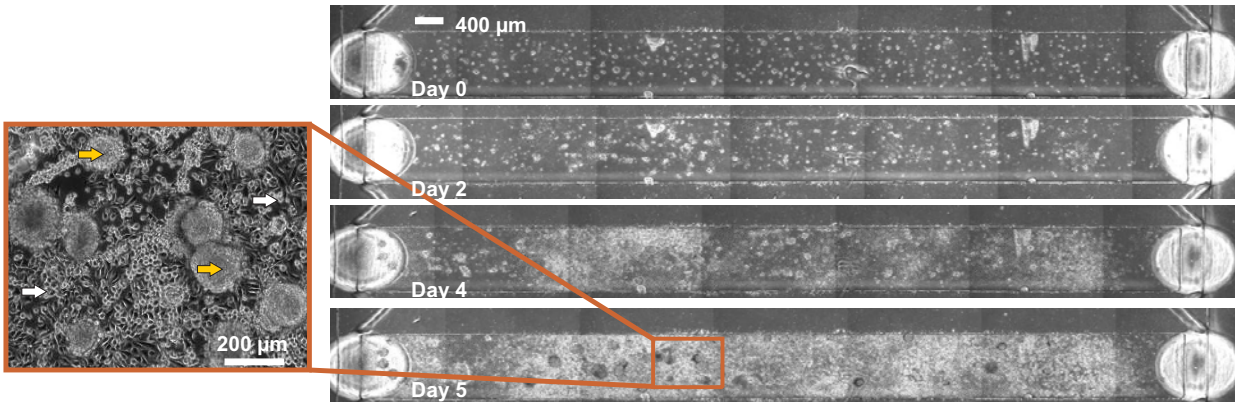

Figure 2-2 Images of cells growing for the indicated number of days in one chamber of a device. Left panel is a close-up of a portion of the chamber in, where yellow arrows represent colonies with ESC-like morphology, while white arrows represent surrounding differentiated-looking cells.

In order to experimentally verify what our theoretical predictions regarding removal of cell-secreted factors suggest, we sought evidence for soluble factor removal. A molecule known to be secreted at high levels by mESCs (Guo et al., 2006b), VEGF, was collected and levels were measured by ELISA. Interestingly, we found that levels of VEGF collected from cells under perfusion after 30 hours of culture were almost ten-fold higher than those from static cultures, in

both differentiation (N2B27) and self-renewal (N2B27 with added LIF and BMP4) medium (Figure 2-3). The increased VEGF collected from cells under perfusion is consistent with autocrine systems in which the binding of ligand to receptor is blocked (DeWitt et al., 2001). In these systems, where secreted ligand can be recaptured by its receptor, blocking that capture (via blocking antibody/small molecule (Lauffenburger et al., 1998), or in this case, by flow) causes more ligand per cell to be delivered into the bulk media and recovered (Figure 1-4a). These results verify removal and downstream recovery of secreted molecules in this system.

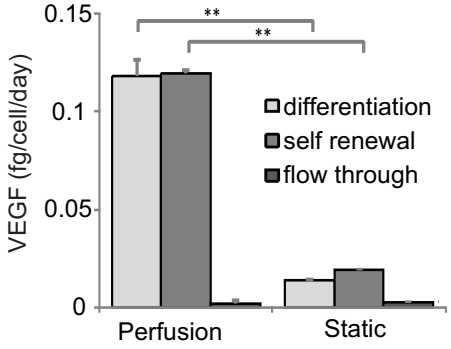

Figure 2-3 ELISA measurements of VEGF collected from mESCs cultured in static and perfused systems, either in self-renewal (N2B27+LIF+BMP4) or differentiation (N2B27) environments. Also shown are the VEGF levels measured in systems without cells ("flow through").

To show that mESCs grown under perfusion do not suffer damage as a result of being grown in the perfusion device, we characterized the cells after three days of perfusion in serum-free self-renewal conditions. We found that cells grew with normal morphology (Figure 2-2), and that expression levels of the early differentiation markers Brachyury and FGF5 were not altered as compared to static self-renewal cultures (Figure 2-4), while those markers did increase in static differentiation conditions (Figure 2-4). Thus, we show that diffusible signaling can be reduced in this system and that cells under short-term perfusion predominantly resemble self-renewing mESCs.

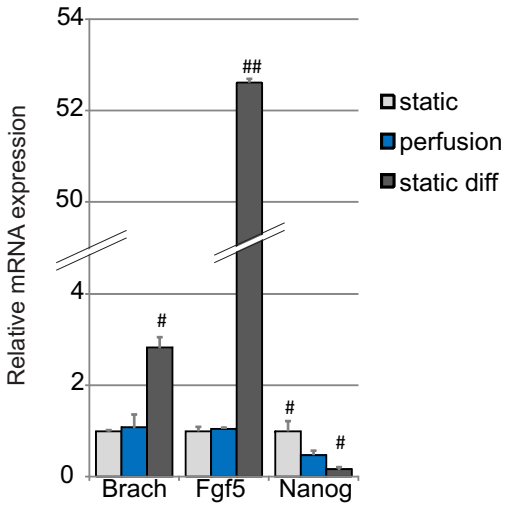

Figure 2-4 mRNA expression levels of key markers after 3 days of growth in static or perfusion self-renewal culture or in static differentiation culture.

2.4 Adjusting heterogeneity by manipulating exogenous signaling

After establishing conditions appropriate for mESC growth under perfusion, we next wanted to assess the effects of depleting soluble cell-secreted signals. We initially expected such a depletion to cause cells to become more homogenous at a population-wide level, as we assumed the cells would experience less variability in local concentrations of extracellular signals. To develop a system for measuring homogeneity, we initially performed experiments in static culture using the FGF4-ERK signaling pathway as a model system. FGF4 is one of the most well-studied functional autocrine mESC signals, and it signals through FGF receptors to activate ERK, leading to downstream changes consistent with a transition to a primed stem cell state more amenable to ectoderm differentiation (Kunath et al., 2007; Stavridis et al., 2007). It has been shown that blocking intracellular ERK signaling causes mESCs to retain a more undifferentiated morphology and to cause mESC populations to become more homogeneous (Burdon et al., 1999). Consistent with this, continuous blockage of ERK signaling, combined with blockage of signals that inhibit growth, allows for maintenance of mESC self-renewal indefinitely over repeated passage (Ying et al., 2008). We also show that blocking ERK activity with two different MEK inhibitors, PD98059 and PD0325901, reduces mESC morphological heterogeneity, even in serum-free cultures (Figure 2-5a). Because MEK and ERK are the major downstream signals of extracellular FGF4 (Kunath et al., 2007), these data indicate that

endogenous FGF4 signaling through ERK may be primarily responsible for the heterogeneity seen in mESC cultures.

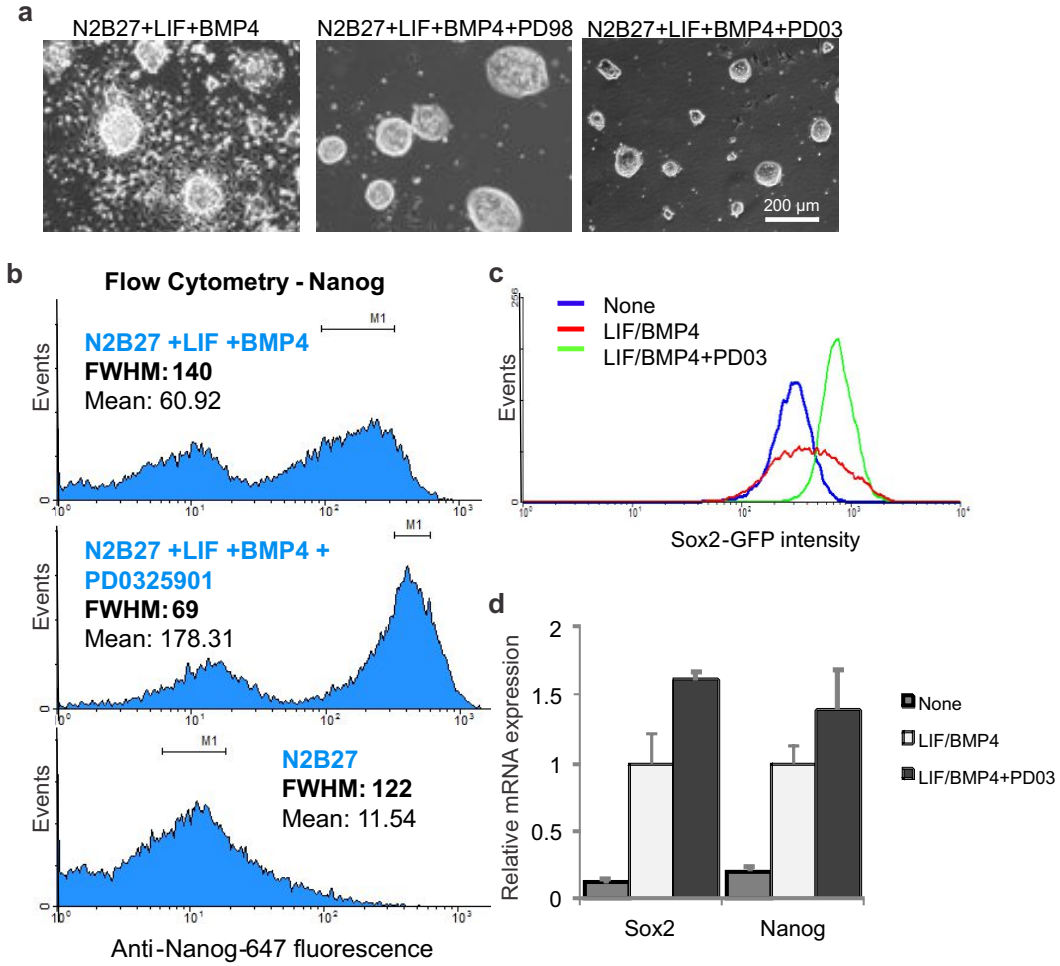

Figure 2-5 MEK inhibition increases homogeneity of mESC cultures. (a) Representative images of cells growing in the indicated conditions for five days. (b) Flow cytometry histograms showing levels of Nanog using direct immunofluorescence staining of cells grown in the indicated conditions. (c) Flow cytometry histogram of levels of Sox2 in a Sox2-GFP cell line. (d) mRNA levels of self-renewal markers from cells grown in the indicated conditions.

We can quantify the level of homogeneity in ESC cultures by measuring levels of the self-renewal marker Nanog at the single-cell level using direct intracellular immunofluorescence combined with flow cytometry (Figure 2-5b). For each population, we measured the width of the flow cytometry histogram peak at half the maximum peak height (full width at half maximum, FWHM) as a measure of homogeneity in the system – smaller FWHM indicates greater homogeneity. We found that cells grown in the presence of a MEK inhibitor exhibited a lower FWHM overall, providing quantitative confirmation of increased homogeneity in this condition.

Similarly, Sox2-GFP reporter mESCs were used to assess population-wide heterogeneity in levels of the alternate self-renewal marker Sox2 (Figure 2-5c), and we found a much broader peak in the absence of the MEK inhibitor. We confirmed these general trends in expression levels of Nanog and Sox2 by analyzing mRNA levels by qPCR (Figure 2-5d). These results indicate that inhibiting MEK-ERK signaling causes a population-wide trend towards higher levels of self-renewal markers, and generates a more homogeneous population.

Formation of a homogeneous self-renewing population could be due to a population-wide shift in expression levels or to a selective growth or survival advantage of cells with a higher propensity to self-renew. To determine whether we are selecting out a specific population, we performed cell proliferation assays. We initially performed cell cycle analysis and found that cells grown in the presence of the MEK inhibitor had more cells in G1 phase and fewer in S phase, whether in the presence or absence of LIF (Figure 2-6a), indicating that blockage of ERK signaling inhibits entrance of mESCs into S phase from G1 phase. This is consistent with previous results in which Fgf4 signaling through ERK was shown to be mitogenic (Burdon et al., 1999) and specifically to regulate the transition between G1 and S phase in a context-specific manner (Roovers and Assoian, 2000). We also found cell growth to be slower in the presence of the ERK inhibitor (Figure 2-6b), in keeping with the mitogenic action of Fgf4. To determine whether multiple populations were arising in the presence of this inhibitor such that cells with higher growth rates also expressed higher levels of the self-renewal marker Nanog, we performed flow cytometry to compare Nanog expression and Bromodeoxyuridine (BrdU) incorporation. BrdU is a thymidine analog that gets incorporated into newly replicated DNA synthesized during the S phase of the cell cycle, and thus, higher levels indicate increased proliferation. Consistent with cell cycle and counting results, levels of BrdU are lower in the presence of the inhibitor (Figure 2-6c), however, this did not correlate to Nanog protein expression levels (Figure 2-6d), indicating that higher Nanog levels do not confer a growth advantage in this system.

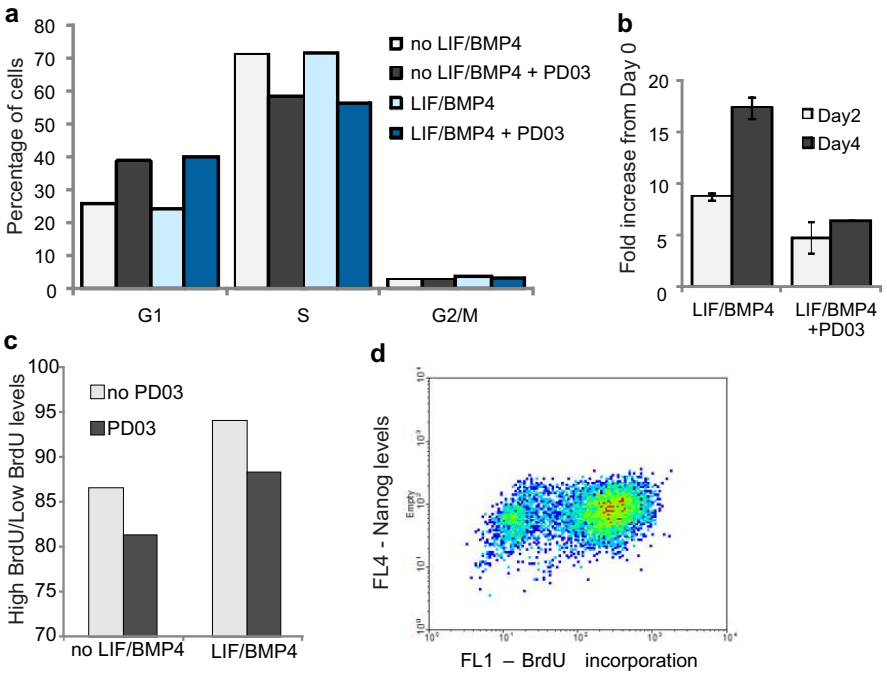

Figure 2-6 Growth and proliferation of cells grown with MEK inhibition. (a) Cell cycle analysis of fraction of cells in the indicated stages of the cell cycle. LB indicates supplementation of N2B27 media with LIF and BMP4. (b) Fold increase in cell number after the indicated number of days. (c) BrdU incorporation levels over five hours in the indicated conditions. (d) Flow cytometry plot showing relationship between Nanog immunostaining intensity and BrdU incorporation in the presence of LIF/BMP4 and PD03.

Together, these data indicate that we are able to manipulate and quantify the heterogeneity of mESCs simply by blocking FGF4 signaling through ERK. The increase in homogeneity seen when ERK is blocked can be explained in terms of the ESCs uniformly entering a more naïve state in which they are not primed for differentiation. If cells in normal self-renewing culture exist in a balance between primed and naïve states, the inhibition of a signal that has been shown to help prime cells for differentiation can push all cells towards the more naïve state without selecting out a specific population, consistent with our results. Since FGF4 is a cell-secreted molecule that has been shown to be important for this phenotype, and it is likely removed by flow, we tested whether mESCs grown under continuous microfluidic perfusion would obtain a phenotype reminiscent of populations in which FGF4 signaling through ERK is blocked. However, after five days of perfusion, ESCs did not look more homogenous based on morphology (Figure 2-7a) or based on flow cytometry histograms of Nanog or Sox2 protein expression levels (Figure 2-7b,c).

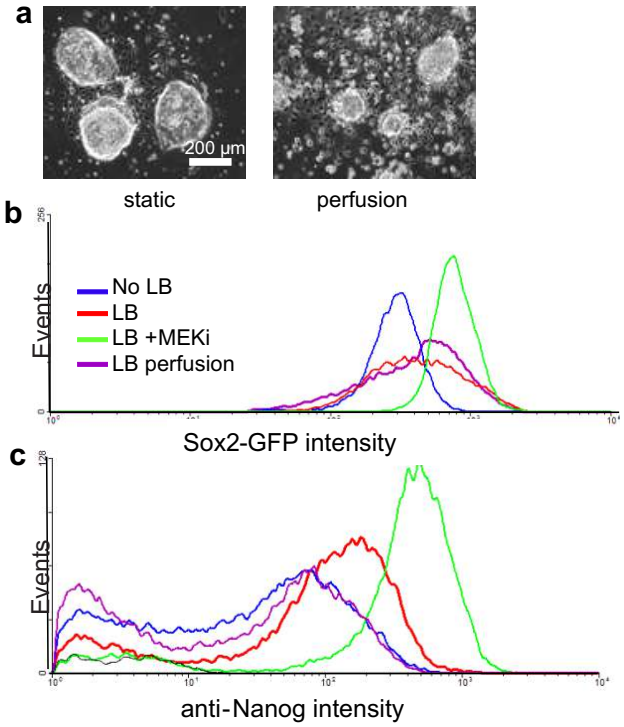

Figure 2-7 Growing mESCs under perfusion does not create a more homogeneous population. (a) Representative morphology of cells grown for five days in static or under perfusion. LB indicates supplementation of N2B27 media with LIF and BMP4. (b) Flow cytometry histograms showing levels of Sox2 in a Sox2-GFP cell line. (c) Flow cytometry histograms showing levels of Oct4 in an mESC Oct4-GFP cell line.

2.5 Exit from self-renewing ESC state under perfusion

Upon finding that mESCs growing under perfusion for several days were not becoming more homogeneous based on morphology or protein expression, but instead actually appeared to be becoming less ESC-like (Figure 2-7a), we sought to determine how this manipulation actually affected ESC characteristics. Upon continued culture under perfusion, mESC growth stagnated such that by day five, less substrate surface area was covered by cells and colony size was smaller, and differentiated-looking cells were more numerous (Figure 2-8a,b, Figure 2-2).

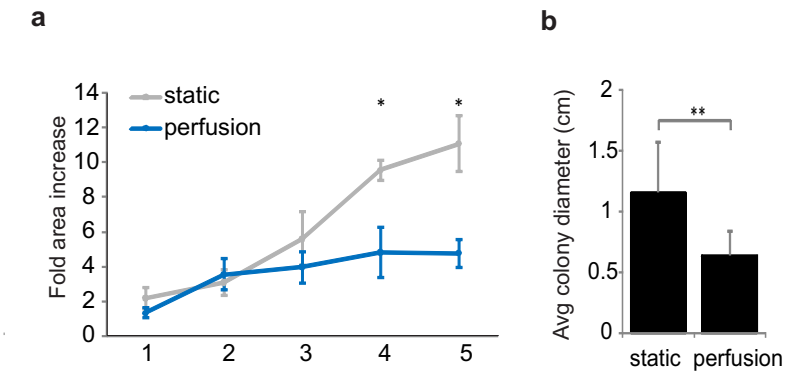

Figure 2-8 Growth characteristics of cells under perfusion. (a) Fold increase in area of static or perfusion culture surfaces covered by cells over time. A 50 mm^2 area was analyzed at each time point under each condition. (b) Day 5 average colony diameter.

When we examined the expression of key pluripotency genes in cells that were cultured for five days under perfusion in the presence of LIF and BMP4, we found that levels of the self-renewal markers Klf4, Rex1, and Nanog were downregulated (Figure 2-9a), and that Brachyury and FGF5 levels, which had been unaffected after three days of culture (Figure 2-4), were dramatically upregulated, along with levels of the differentiation marker Dnmt3b (Figure 2-9a). Oct4 and Sox2 mRNA levels did not change (Figure 2-9a), results consistent with measurements of protein levels by flow cytometry (Figure 2-9b), indicating that the cells still expressed some elements of the core stem cell transcription network. A similar expression pattern was seen between static and perfusion cultures with cells grown in static N2B27+2i/LIF media (Figure 2-9c), indicating that the perfusion phenotype is not a result of activation or block of specific signaling pathways. The differentiation potential of cells grown under perfusion in the presence of LIF and BMP4 was also altered, as embryoid bodies (EBs) formed with slightly abnormal morphology (Figure 2-9d) and increased expression of the ectoderm differentiation markers Sox1 and Nestin as compared to cells grown in static conditions (Figure 2-9d).

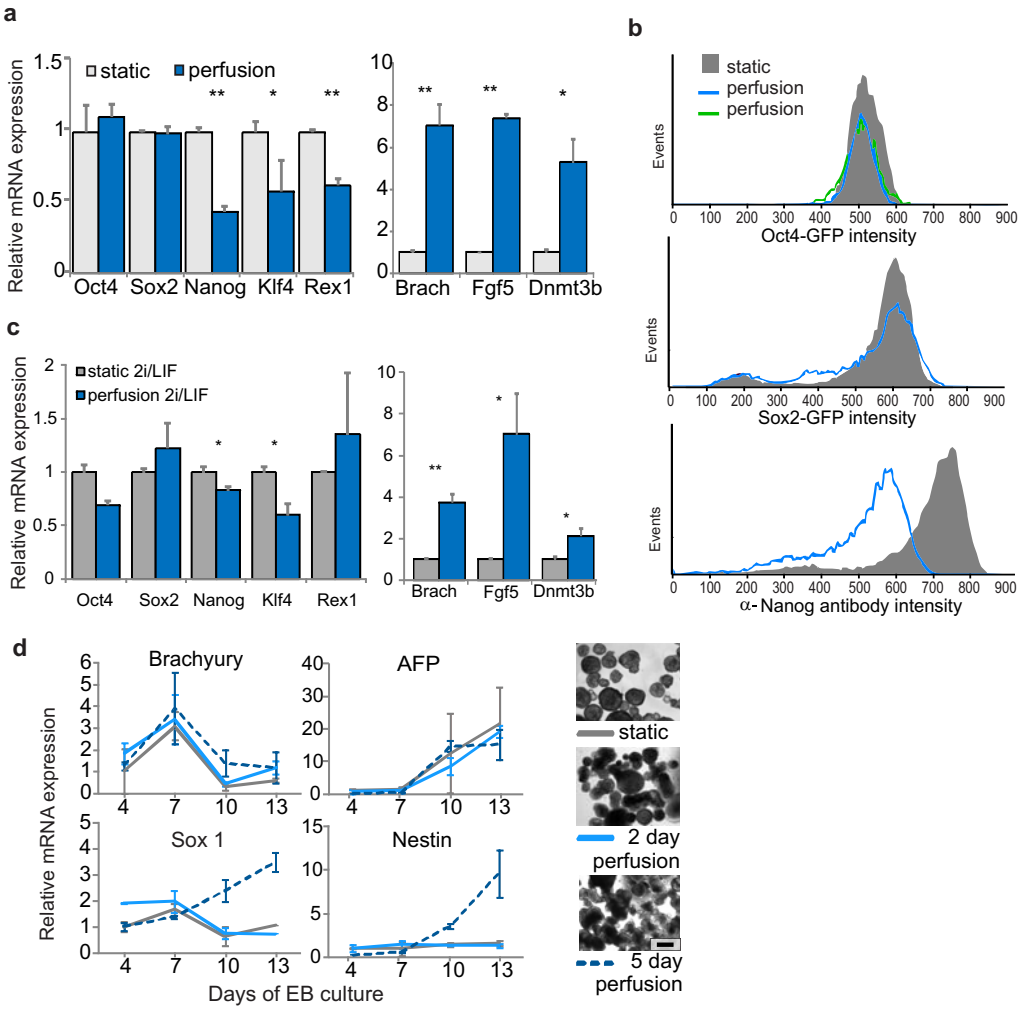

Figure 2-9 ESCs exit their stable state under long-term perfusion. (a) mRNA expression levels of self-renewal (left) or differentiation (right) markers after five days in static or perfusion culture in N2B27+LIF +BMP4. (b) Flow cytometry histograms showing levels of Oct4 in an mESC Oct4-GFP cell line (top), levels of Sox2 in a Sox2-GFP cell line (middle), and levels of Nanog using direct immunofluorescence staining (bottom), all in static and perfusion day 5 populations. (c) mRNA expression levels of self-renewal (left) or differentiation (right) markers after five days in static or perfusion culture in N2B27+2i/LIF media. (d) Embryoid body timecourse mRNA expression of EBs made from cells previously grown in static culture (gray solid line) or perfusion culture for 2 days (blue solid line), or perfusion culture for 5 days (blue dashed line). Images show representative EBs on day 5 formed from cells grown under the conditions indicated. Scale bar = 800 μm. **=p<0.001, *=p<0.05 for pairwise comparisons, all data represents averages of at least three independent experiments and error bars represent SD.

We did not observe any apparent heterogeneity in Oct4 protein levels or cell number along the length of the chamber (Figure 2-10a,b), suggesting that observed differences in phenotype are not simply due to spatially varying differentiation in the flow field. Additionally, it is unlikely that the phenotypic changes observed under perfusion were due to selection of a specific cell population, as there was no massive cell death during the culture period, the low shear rates

present in our system are >1000× below those known to cause ESC detachment (Fok and Zandstra, 2005), and in specifically designed experiments we recovered ≲600 cells released from all chambers over 5 days, which is <2% of the number of cells present in the chambers on day 5 (Figure 2-10c).

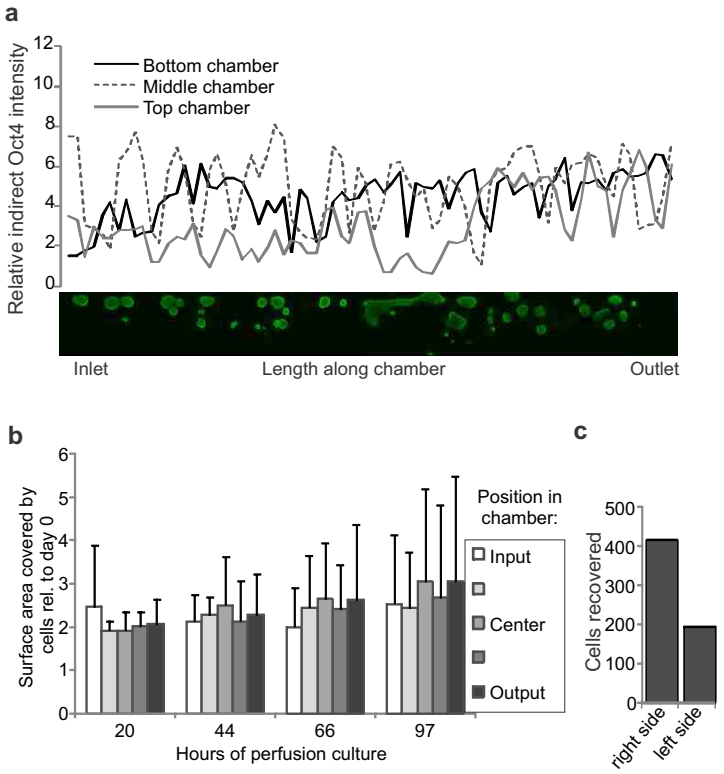

Figure 2-10 Spatial analysis and physical manipulations of cells grown under perfusion. (a) Quantification and image of Oct4 immunofluorescent staining of day 5 perfusion culture to assess the relative abundance of marker expression along the length of the chamber. No statistically significantly trend was apparent (p=0.53). (b) Quantification of surface area covered by cells over time on average between six chambers along the length of the chambers (light to dark grey). (c) Quantification of cells recovered from the perfused microdevice output over five days. Each bar represents the total number of cells recovered per chamber on either side of the device (3 chambers/side).

To ensure that the changes observed under perfusion were indeed due to removal of secreted factors, several control perfusions were performed. Increasing the LIF concentration five-fold did not restore Nanog levels (Figure 2-11a), suggesting that local concentration effects due to the perfusion transport environment are not the cause of the observed changes, while cells grown in the presence of cell-conditioned serum-containing media under perfusion did see restoration of Nanog to levels seen in static serum-containing culture (Figure 2-11b). Cells grown in a microdevice using a small-volume recirculating-loop system in which cells were fed with the

media collected under perfusion had similar marker expression to cells grown in static cultures, as did cells grown using defined feeding intervals (Figure 2-11c, recirc loop perf and pulse perf, respectively). Thus, approximating the soluble microenvironment of static culture by using recirculating loops or discrete feeding intervals to allow cells to condition the media generates a phenotype similar the static phenotype, but in a system that includes microculture and shear. Conversely, cells grown at a 4× lower perfusion rate (and thus 4× lower shear) did not show any substantial differences compared to cells grown at our normal perfusion rate (Figure 2-11c, perf 25µl/h). Thus, lowering the shear but maintaining a convection-dominated microenvironment doesn't substantially change phenotype, consistent with transport rather than shear being dominant. Together, these results further indicate that neither the microculture itself nor shear are artifactually altering the observed phenotype.

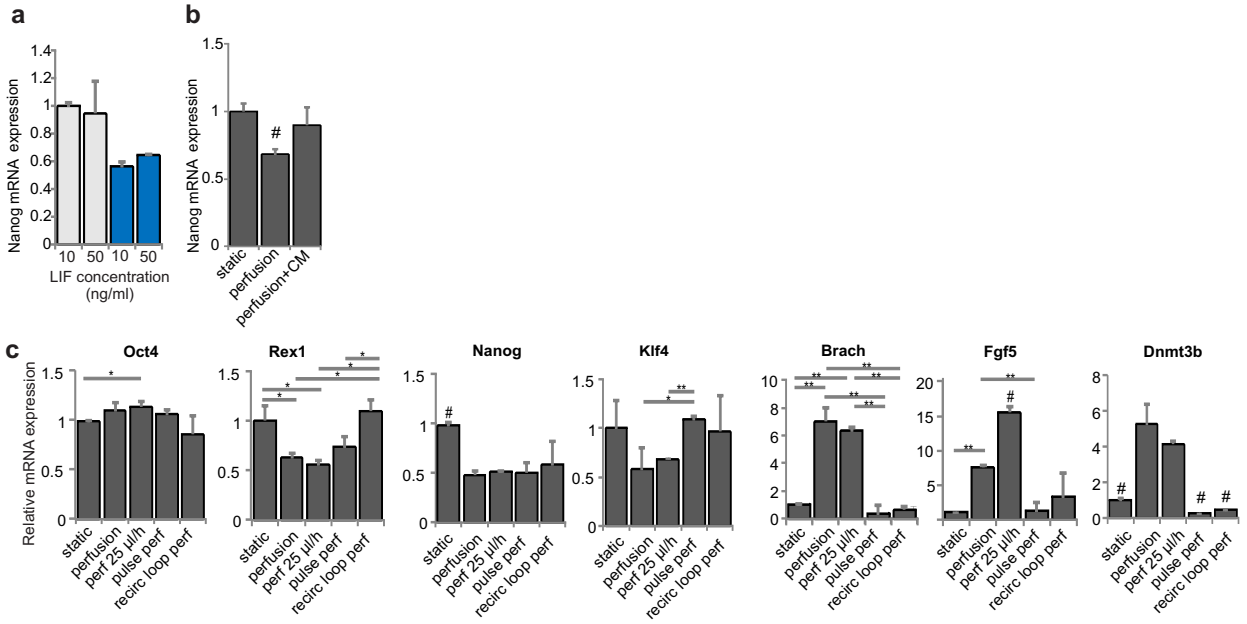

Figure 2-11 Control experiments under perfusion. (a) Nanog mRNA expression levels in static and perfusion with either 10 ng/ml LIF or 50 ng/ml LIF. (b) Nanog mRNA expression levels in static and perfusion in the presence of serum+LIF media, with or without the addition of soluble cell-secreted factors from static conditioned media (CM). (c) mRNA expression levels of self-renewal and differentiation markers in normal static and perfusion cultures compared to levels in cells grown under perfusion with 4X lower volume flowrate than normal (perf 25 µl/h), cells grown in a perfusion device with feeding intervals akin to those in static (pulse perf), and cells grown under recirculating perfusion in a total volume of 1 ml (recirc loop perf). **=$p<0.001$, * =$p<0.05$; #=$p<0.05$ for all pairwise comparisons, error bars represent SD.

These results indicate that depleting cell-secreted signals does not allow mESCs to maintain their self-renewal program even in the presence of LIF and BMP4, a finding that motivated further

study into the nature of the cells that arise out of an environment with minimal cell-secreted signaling.

2.6 Cells enter a primed epiblast-like state under perfusion

Because mouse epiblast cells and the related EpiSCs express Oct4 and Sox2 and have low levels of Klf4 and Rex1 and high levels of Brachyury and FGF5 (Bao et al., 2009), we examined whether cells under perfusion, which have a comparable expression pattern, were similar to epiblast cells. Using a qRT-PCR array, we analyzed expression of self-renewal and differentiation markers over time in static and perfused self-renewal cultures (Table 2-1). Among the most highly altered genes in cells grown under perfusion, we found many post-implantation markers indicative of epiblast (Figure 2-12a), including FGF5 (Hayashi et al., 2008), Brachyury (T) (Tesar et al., 2007), Lefty1 (Bao et al., 2009), and Dnmt3b (Hall et al., 2010) which increased relative to static, and the ESC markers Gbx2 and Cd9, which decreased (Tesar et al., 2007; Oka et al., 2002). Further growth (7 days) under perfusion results in increased expression of epiblast markers, including Eomes, Sox17, Lefty1, and Gata6 (Tesar et al., 2007) (Figure 2-12b), suggesting entrance into a stable epiblast-like state. In order to further examine whether the cells grown under perfusion are specifically differentiating towards an epiblast-like cell state or are undergoing non-specific differentiation, we compared gene expression from days 3-7 of culture under perfusion to expression in cells undergoing undirected differentiation in EB culture and to expression in mESCs cultured in conditions that induce an EpiSC-like state (culture in the presence of Activin and FGF2 (Guo et al., 2009)). We observed higher expression of genes associated with mesendoderm differentiation in day 5 embryoid bodies compared to either EpiSC-like cells, or to cells grown under perfusion, where these genes were expressed at low levels at both day 5 and day 7 (Figure 2-12c). This signifies a lack of indiscriminate differentiation in cells with minimal cell-secreted signaling and instead indicates a more directed differentiation pathway, providing further evidence for exit from the ESC state towards a state that closely resembles an epiblast-like state.

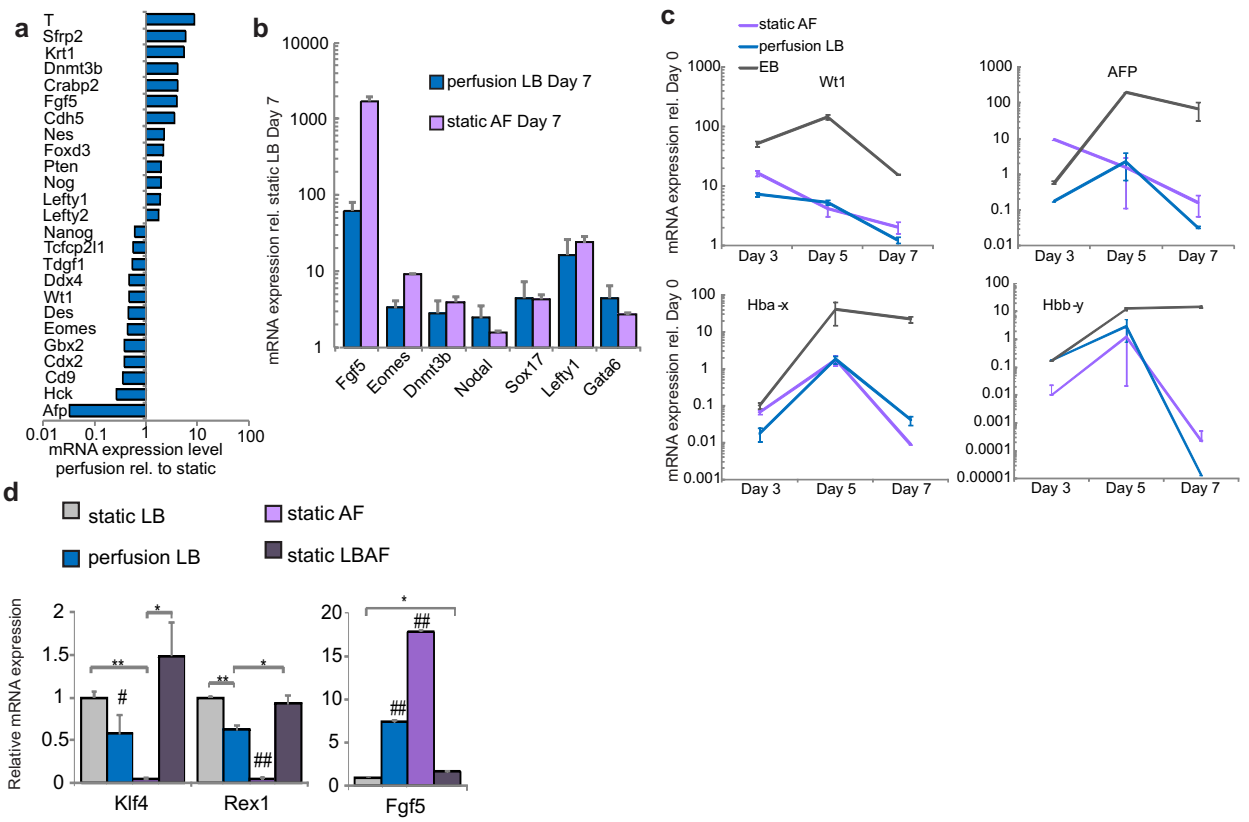

Figure 2-12 An epiblast-like state is attained upon cell-secreted factor removal. (a) mRNA expression levels of markers from a qPCR array that changed expression more than two-fold on day 5 under perfusion as compared to day 5 in static conditions. (b) mRNA expression levels of epiblast-specific markers after 7 days of growth in self-renewal media under perfusion (N2B27+LIF+BMP4, perfusion LB), or in EpiSC media in static culture (N2B27+Activin+FGF2, static AF), compared to levels at day 7 in self-renewal media in static culture. (c) mRNA expression levels of differentiation markers at 3, 5, and 7 days in either static AF, perfusion LB, or floating embryoid body culture (EB). (d) mRNA expression levels of EpiSC up- and down-regulated markers in cells grown in static or perfusion LB, or in static AF or static with all four additions (LBAF).

	Static Day 3	Perfusion Day 3	static Day 5	Perfusion Day 5
Afp	25.42	0.824	115.4	2.312
Bxdc2	0.673	0.775	0.580	0.372
Cd34	0.614	0.922	0.767	0.777
Cd9	1.231	0.990	2.259	0.705
Cdh5	1.406	12.95	4.356	18.68
Cdx2	3.449	0.961	13.89	4.588
Col1a1	1.223	1.304	2.205	3.925
Commd3	0.895	1.271	1.678	1.252
Crabp2	0.796	1.671	0.934	4.878
Ddx4	0.964	0.491	1.160	0.501

Des	1.109	0.361	1.379	0.562
Diap2	1.458	0.984	0.568	1.009
Dnmt3b	1.651	4.684	1.122	5.875
Ednrb	0.713	1.401	1.593	2.027
Eomes	2.195	1.158	2.715	1.058
Fgf4	1.366	1.003	0.976	0.767
Fgf5	22.72	30.72	23.93	115.6
Flt1	4.886	4.410	13.82	11.56
Fn1	1.600	1.120	1.060	1.296
Foxa2	3.852	5.949	9.652	10.03
Foxd3	0.518	0.827	0.356	0.867
Gabrb3	1.780	1.177	1.473	2.019
Gal	0.784	0.578	1.511	1.464
Gata4	2.021	3.251	4.336	4.038
Gata6	1.522	3.964	4.649	4.752
Gbx2	0.243	0.219	0.174	0.059
Gcg	ND	ND	ND	ND
Gcm1	1.307	ND	1.361	ND
Gdf3	0.725	0.808	0.623	0.640
Grb7	2.194	1.168	2.143	2.811
Hba-x	2.570	1.884	3.436	3.568
Hbb-y	ND	ND	ND	ND
Hck	0.641	0.193	0.557	0.123
Iapp	ND	ND	ND	ND
Ifitm1	1.743	1.163	0.831	1.067
Ifitm2	0.696	0.857	0.422	0.564
Igf2bp2	1.372	1.239	2.085	1.438
Il6st	0.712	0.726	0.721	0.752
Ins2	1.638	1.583	3.016	4.097
Kit	1.427	2.001	3.662	5.039
Krt1	1.546	3.450	1.278	8.982
Lama1	1.688	2.910	5.201	8.675
Lamb1-1	2.763	5.559	7.287	11.54
Lamc1	2.025	3.903	5.544	10.43
Lefty1	6.377	6.341	3.640	7.515
Lefty2	8.879	4.911	3.595	7.003
Lifr	0.814	0.828	1.056	1.391
Lin28	1.088	1.267	0.981	1.804
Myf5	ND	ND	ND	ND
Myod1	ND	ND	ND	ND
Nanog	0.751	0.356	0.604	0.340

Nes	1.715	1.496	3.188	8.222
Neurod1	0.950	1.723	1.190	1.505
Nodal	0.887	0.750	0.909	0.909
Nog	9.297	31.35	26.47	57.41
Nr5a2	0.597	0.595	0.375	0.343
Nr6a1	1.830	1.518	2.960	2.825
Numb	1.047	0.870	1.024	1.019
Olig2	ND	ND	3.428	3.307
Pax4	ND	ND	ND	ND
Pax6	0.928	0.401	0.715	0.616
Pdx1	1.242	1.196	1.999	1.320
Pecam1	1.311	0.896	0.954	0.708
Podxl	3.014	2.508	4.055	2.474
Pou5f1	0.668	0.607	0.580	0.672
Pten	0.909	1.183	0.860	1.899
Ptf1a	ND	ND	ND	ND
Rest	1.005	0.999	0.601	0.832
Runx2	ND	ND	ND	ND
Sema3a	ND	ND	ND	ND
Serpina1a	ND	ND	ND	ND
Sfrp2	1.432	1.648	0.466	3.535
Sox17	3.847	7.482	10.93	7.607
Sox2	1.143	0.761	0.760	0.699
Sst	ND	ND	ND	ND
Sycp3	2.686	2.454	4.031	2.902
T	0.979	1.167	1.953	23.96
Tat	1.427	2.004	3.127	3.958
Tcfcp2l1	0.777	0.477	0.592	0.308
Tdgf1	1.234	0.600	1.454	0.728
Tert	1.746	0.842	1.463	1.075
Utf1	0.910	0.968	0.704	0.930
Wt1	6.734	6.560	12.69	5.379
Zfp42	0.601	0.510	0.312	0.169

Table 2-1: Quantification of expression levels of genes in a stem cell marker panel in static and perfusion cultures at days 3 and 5 of culture, compared to expression levels on day 0. ND = Not Detected, indicating expression levels below the qPCR detection limit of 35 cycles.

This transition that occurs under perfusion is surprising given that LIF and BMP4 are still present in the culture medium, as their presence was thought to be sufficient to maintain mESC self-renewal (Ying et al., 2003a). Indeed, we found that mild induction of the EpiSC-like state using Activin and FGF2 did not alter marker expression in static culture when in the presence of

LIF and BMP4, as addition of all four factors to static cultures does not cause the reduction in Klf4 or Rex1 or the increase in FGF5 seen in the presence of Activin and FGF2 alone (Figure 2-12d). Thus, in conventional culture systems, ESCs are able to withstand state change cues as long as LIF and BMP4 are present, whereas these molecules do not have the same effect under perfusion, indicating a lack of sufficiency.

One notable difference seen in cells under perfusion as compared to EpiSCs is a decrease in Nanog expression levels under perfusion. Nanog is required for the maintenance of pluripotency in mESCs (Mitsui et al., 2003) and EpiSCs (Greber et al., 2010), but as described in chapter 1.2, the upstream regulation occurs by different processes (Figure 1-1). ESCs require Stat3 activation for upregulation of Nanog (Darnell, 1997; Jiang et al., 2008), while in EpiSCs, Stat3 is still responsive to LIF but cells are not dependent on that pathway for self-renewal (Tesar et al., 2007; Hanna et al., 2010); instead, Activin is required to upregulate Nanog through Smad2/3 signaling (Greber et al., 2010). We found that cells cultured in perfusion maintained the ability to activate Stat3 by Y705 phosphorylation in response to LIF (Figure 2-13a), but without upregulation of downstream self-renewal genes (Figure 2-9a). However, addition of Activin under perfusion causes cells to upregulate Nanog protein and mRNA levels (Figure 2-13b,c), indicating a shift from an ESC state that requires LIF+BMP4 and is Activin-insensitive to an epiblast-like cell state that is Activin-responsive and LIF-insensitive. Activin supplementation under perfusion did not upregulate Rex1 and Klf4 (Figure 2-13c) or other downstream targets of Stat3, implying that Activin supplementation does not revert perfusion cultures back to an ESC state, nor does it broadly alter marker expression in static cultures (Figure 2-13d).

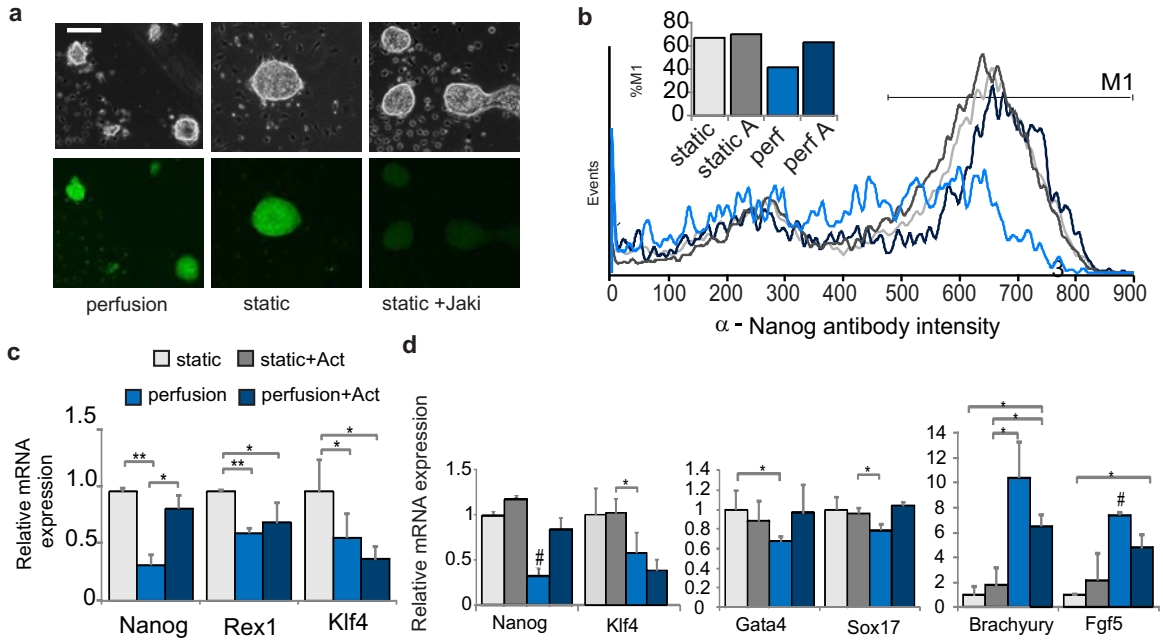

Figure 2-13 Signaling characteristics of perfused cells are representative of an epiblast-like state. (a) Phase and fluorescence images of cells grown in perfusion culture or in static culture with or without a Jak inhibitor (added 6 hrs prior to staining) and stained for phosphorylated (Y705) Stat3. (b) Flow cytometry histogram depicting Nanog protein levels in the presence or absence of Activin (A). Inset depicts percent of cells in the M1 range. (c) Self-renewal marker expression for cells cultured for five days in N2B27+LB in the presence or absence of Activin (A). (d) Relative levels of mRNA expression for self-renewal (left panel), early endoderm (middle panel), or other differentiation lineage (right panel) genes in the presence and absence of Activin under static and perfusion conditions.

To test whether addition of Activin under perfusion is able to stabilize a self-renewing state that is more epiblast-like than ESC-like, we replated cells after culture with or without added Activin into either ESC or EpiSC static self-renewal medium (Figure 2-14a). While cells that had been previously grown under perfusion in ESC medium did not replate in either ESC or EpiSC medium (Figure 2-14b, light blue lines), cells perfused with added Activin could be replated and grown in EpiSC conditions, and showed EpiSC-like colony morphology (Figure 2-14b, purple line, Figure 2-14c). Conversely, cells that had been grown in static culture (without Activin) were only able to proliferate after being replated in ESC medium (Figure 2-14b, gray lines). Additionally, cells grown in static culture with added Activin were not able to be replated in EpiSC conditions (Figure 2-14b, black line), indicating that culture in the microdevice primes cells to be receptive to Activin supplementation for maintenance of self-renewal. Cells grown under perfusion were also unable to replate and grow in N2B27+2i/LIF minimal self-renewal media (Figure 2-14d), another characteristic that these cells share with epiblast cells (Guo et al.,

2009). Together, our results demonstrate that a lack of diffusible signaling causes mESCs to leave their stable self-renewing state and enter a more epiblast-like state that is characterized by the expected marker expression profiles as well as the appropriate downstream signaling responses and state stabilization resulting from addition of Activin. However, since several self-renewing multi- or pluripotent epiblast-like states have been identified (Chou et al., 2008; Rathjen et al., 1999; Tesar et al., 2007), the precise identity of the cells with reduced soluble signaling is not known, though it is clear that depletion of cell-secreted signals induces exit from the stable ESC state in conditions that do not allow for this exit in static cultures.

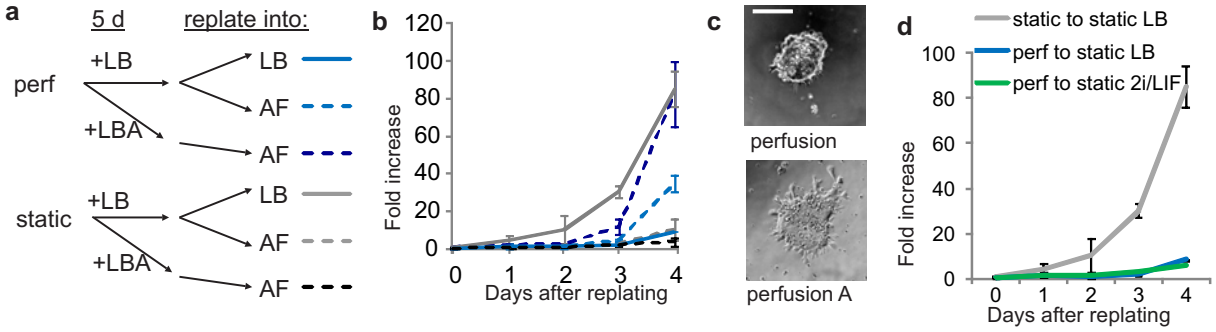

Figure 2-14 Self-renewal ability of cells grown under perfusion. (a) Schematic explaining experiment depicted in (b), where cells were grown in static or perfusion in N2B27+LB with or without Activin (A) for 5 days, then replated into either ESC (LB, solid lines) or EpiSC (Activin + FGF2 (AF), dotted lines) static culture conditions for four days. (b) Fold increase in growth of cells from conditions in (a) upon replating. (c) Images of representative colonies from replating into EpiSC medium, replated from indicated conditions, taken on day 3 after replating. Scale bar = 200 μm. (d) Fold increase in growth of cells that were replated into indicated conditions from growth in static or perfusion. **=p<0.001, *=p<0.05 for pairwise comparisons, all data represents averages of at least three independent experiments and error bars represent SD.

2.7 Discussion

It is currently thought that mESCs grown in self-renewing culture conditions exist with some level of heterogeneity due to spontaneous conversion between a naïve ESC state and a more primed epiblast-like state (Chambers et al., 2007; Enver et al., 2009). In serum-free N2B27+LIF+BMP4 media, this interconversion is thought to be a result of the opposing actions of LIF and BMP4 signaling versus autocrine/paracrine FGF4-ERK signaling (Lanner and Rossant, 2010). Here, we show results consistent with this prior work and demonstrate the ability to quantify heterogeneity by performing flow cytometry after intracellular immunofluorescent staining for the self-renewal marker Nanog and measuring the width of the curve on the resulting

histogram at half the peak height. We also show that blocking FGF4-ERK signaling in static cultures does not provide a growth or survival advantage to more self-renewing cells, but that it causes a shift in the population of cells to a uniformly naïve state.

If FGF4 was the primary cell-secreted stimulus acting in ESCs, one would expect global depletion of cell-secreted signaling to have a similar effect to ERK inhibition, maintaining ESCs in a more naïve state. To address this hypothesis, we implemented a microfluidic perfusion device for growth with mESCs in serum-free conditions and compared the cell phenotype after five days of perfusion to that after five days of growth in static cultures with ERK inhibition. Surprisingly, we find that a global reduction of cell-secreted signals does not cause ESC populations to have increased homogeneity, nor does it cause them to shift to a more naïve state. Instead, several days of continuous perfusion drives mESCs out of self-renewal and toward a defined lineage that closely resembles the epiblast state. This indicates that FGF4-ERK signaling is not the only cell-secreted signal affecting mESC differentiation.

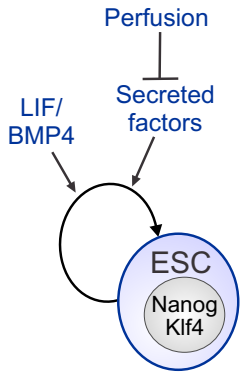

Figure 2-15 Model indicating that perfusion blocks secreted factors that in turn act to maintain the self-renewing mESC state along with LIF/BMP4.

Critically, the transition out of the ESC state seen under perfusion occurs in the presence of LIF and BMP4 or 2i/LIF, which were previously shown to be sufficient to maintain self-renewal in static culture. This indicates the presence of an additional pathway involved in ESC maintenance that utilizes cell-secreted factors (Figure 2-15). These results emphasize the power of microfluidic perfusion in uncovering previously unknown roles for cell-secreted signals. We went on to harness this device for downstream applications and to use it to probe other aspects of the cell-secreted microenvironment.

2.8 Methods

Perfusion culture device fabrication

The microdevice consists of six 1.25 mm × 13 mm × 250 μm (W × L × H) chambers, with two separate media inputs and dual addressability. The microfluidic perfusion device was molded from polydimethylsiloxane (PDMS, Corning), after mixing in a ratio of 10:1 base to curing agent and degassing in a vacuum chamber for 30 minutes. The mold was fabricated from an Autocad file using a stereolithography foundry (Fineline Prototyping). Plastic replica molds were made for fabrication of multiple devices simultaneously (Desai et al., 2009). The fluidic and vacuum layers were cured separately and bonded after exposure to oxygen plasma. Input and output fluid holes as well as vacuum line holes were punched using a 0.072 inch diameter hypo tube. The device layout consists of two sets of triplicate mm-sized enclosed culture chambers with individual addressability to enable two experimental conditions side-by-side. These chambers are connected to external syringe pumps that provide continuous pulse-free perfusion, and the chip also includes microvalves to direct liquid flow and cells to the desired locations.

Perfusion culture conditions

For all perfusion experiments, the bonded device is autoclaved and allowed to dry, then clamped on top of a polystyrene culture slide in a custom microscope stage insert. The device must be secured tightly as it is cannot be bonded to the polystyrene surface, but not so tightly that liquid flow is obstructed or valve actuation is inhibited. Tubings are then connected and gelatin is perfused through the device for 1 hour to ensure proper flow patterns and valve operation, and to remove bubbles, as assessed by microscopic observation. The device and stage are put in the incubator for at least an hour to ensure the proper temperature is attained within the device. Then, mESCs at a density of 1 x 10^6 cells/mL are loaded into the device, chambers are sealed, surrounding cells are flushed from the inlets, and the device is placed in a humidified incubator. Cellsare seeded into gelatin-coated 12-well plates at a density of 2.5 x 10^4 cells/mL for static controls. Perfusion was initiated in the device once cells were firmly attached to the surface (~ 24 hrs). Perfusion was run continuously at 0.1 ml/hr, unless otherwise noted. For pulse perfusion, 50 μl of media per side of a device (3 chambers) was perfused in a span of 30 min once every 8 h to completely replenish the media in all three chambers (~4 μl chamber volume). For recirculating

perfusion, a peristaltic pump (Rainin Dynamax) was used at a flow rate of 0.1 ml/hr with a media reservoir of 500 μl in an eppendorf tube to create a total recirculating volume of about 1 ml.

Culture conditions

For information regarding cell lines and culture additions, refer to Appendix 1. For 2i/LIF culture, CHIR99021, PD0325901, and LIF were added to N2B27 media.

Quantitative PCR

For information regarding protocols and primers for standard qRT-PCR, refer to Appendix 1. Quantitative RT-PCR array analysis was performed using a mouse embryonic stem cell-specific PCR array (PAMM-081, SABiosciences).

Flow cytometry

After harvesting cells, direct intracellular immunostaining was performed with an Alexa Fluor 647-linked anti-mouse Nanog antibody (eBioscience). Cell cycle analysis was performed on ethanol-fixed cells by adding RNAse and propidium iodide. BrdU analysis was performed after adding BrdU for five hours and fixing cells in formaldehyde. GFP-linked anti-BrdU antibody was added at 1:200 (Caltag Laboratories). Internal fluorescent intensity was measured on a FACSCaliber flow cytometer (BD Biosciences).

Immunofluorescence

For phospho-Stat3 staining, cells were incubated overnight with phosphorylated Stat3 antibody (Cell Signaling Technology) at 1:100 and secondary (anti-rabbit GFP, Invitrogen) was added for two hours at 1:1000. For Oct4, cells were incubated overnight with primary Oct4 antibody (Abcam) at 5 μg/ml and secondary (anti-goat Cy3, Abcam) was added for one hour at 1:250. Staining along the chamber was quantified using an automated MATLAB script, and differences in staining intensity in any area within the chamber was not found to be statistically significant. All cells were counterstained with 1:100000 Hoechst (Sigma).

Embryoid body formation

ESCs were harvested from culture and replated at 4 x 10^5 cells in a 60-mm ultra low attachment culture dish (Corning). Cells were grown in ESC medium with no LIF, and medium was replenished every two days.

ELISA

Enzyme-linked immunosorbent assay was performed on samples from static conditioned medium, or from the medium collected from the perfusion output. Cells were either perfused for thirty hours or remained in static culture for thirty hours, and medium was collected. Results were normalized by the average cell density (using an exponential growth model and the initial/final cell numbers) and duration to determine a secretion in grams/cell/hr under both conditions. Because of the discrepancy in volume between these two types of samples, perfusion output medium was spun down using spin filter concentrator columns with a 3 kDa molecular weight cutoff (Millipore) and reconstituted to the same volume as the static conditioned medium. VEGF ELISA was purchased from R and D Systems, and assay was performed according to manufacturer's instructions.

Cell recovery

To capture and count cells recovered from the perfusion device, cells were collected into 4% formaldehyde and transferred to 4°C twice daily. All recovered cells were combined and stained with Hoechst (Sigma), then transferred to a black-walled 96-well plate where they were automatically scanned and counted using a MATLAB script that was previously calibrated using known quantities of cells collected, treated, and counted in the same manner as the cells recovered from the device.

Chapter 3 Controlling ESC fate in the neutral background of perfusion

3.1 Introduction

Determining the effects of removing cell-secreted factors allows for an understanding of how such factors contribute to cell fate in a broad context. Microfluidic perfusion can also be used as a tool to determine the roles of specific cell-secreted factors and to manipulate cell fate accordingly, all in a system with reduced background noise. Because microfluidic platforms have the ability to provide precise control over the timing of signal addition or removal and monitor the resulting phenotype in real time, they have potential uses as screening platforms to identify and regulate endogenous or exogenous signals.

Embryonic stem cells represent an interesting system to study mechanistically, not only because of their ability to self-renew indefinitely, but also because they can be induced to leave their self-renewing state and enter down a path of differentiation toward a desired lineage. The development of methods to reprogram somatic cells into induced pluripotent stem cells in mouse (Takahashi and Yamanaka, 2006; Wernig et al., 2007; Okita et al., 2007) and human (Yu et al., 2007; Takahashi et al., 2007) has stimulated increased efforts to specifically differentiate pluripotent stem cells into cell types of interest, as this technology allows for patient-specific cells of any desired lineage to be obtained for therapeutic use. However, creating populations of specifically differentiated cells from ESCs is difficult, and even the best techniques for specific differentiation result in a heterogeneous mixture of cells that may not be appropriate to use therapeutically (Kubo et al., 2004). In addition, there are barriers to testing the functionality of differentiated cells in vivo to ensure that they act identically to the cell type they are intended to substitute for, a problem particularly relevant to neuronal directed differentiation (Hansen et al., 2011).

Many differentiation protocols use timed exposure to various exogenous growth factors (Wichterle et al., 2002; Kouskoff et al., 2005) to drive cells to particular endpoints, often in an attempt to recapitulate timing of corresponding developmental stages. However, signaling changes that occur over time in vivo are difficult to assess and the timescales on which these

changes occur may be too small to reliably recapitulate using bulk culture methods. Thus, the ability to identify and implement defined conditions in which to reproducibly and efficiently create a homogeneous population of specifically differentiated cells would be useful in many contexts. By monitoring changes in soluble extracellular signals during differentiation, we can develop a better understanding of what extracellular signals are required for specific directed changes to occur. The collection of all molecules secreted by a given cell at a given time has been referred to as the secretome (Greenbaum et al., 2001). Determining and understanding what different populations of cells secrete and why is instrumental to any complete analysis of the extracellular microenvironment. During the early stages of mESC differentiation, it has been shown that some aspects of the secretome will change in a manner consistent with the eventual fate of the cells (Farina et al., 2011). Because increased amounts of cell-secreted proteins are collected when cells are grown under perfusion as compared to static (Figure 2-3), this system represents a platform that could be further optimized for high-throughput analysis of secretome changes and their significance during differentiation and development.

Microfluidic perfusion is a powerful tool for determining the roles of specific cell-secreted signals and for adding specific signals back in a controlled manner, but to really get at how and when signals are being presented to the cells and how this relates to their resulting phenotype, it is necessary to model ligand secretion and uptake rates during perfusion as a function of cell density, flow rate, and ligand concentration. To that end, we have performed basic finite-element analysis using COMSOL to model the chambers in the perfusion device, but further analysis will be required to make testable predictions regarding specific ligand availability and signaling capacity for cells growing under perfusion. In this chapter, we provide basic experiments and analysis showing how microfluidics can address outstanding challenges in directed differentiation and in understanding regulation of endogenous signaling during differentiation processes.

3.2 Using perfusion for directed differentiation

In chapter 2, we found that mESCs grown under perfusion tend towards being more primed for differentiation. We wanted to exploit the fact that cells under perfusion were already primed by providing them with cues for directed differentiation and assessing their ability to rapidly and

homogenously differentiate. Adding in Activin under perfusion helped to stabilize this more primed epiblast-like state, so we began by adding in Activin along with two mESC-secreted proteins that have been implicated in differentiation, FGF4 and TGFβ. Together, these three proteins in conjunction with LIF and BMP4 caused a general upregulation of differentiation markers and downregulation of self-renewal markers compared to cells grown under perfusion with just LIF and BMP4 (Figure 3-1a). The most dramatic change involved an upregulation of the early mesoderm marker Brachyury (Figure 3-1b), thus we pursued this line of evidence to assess the ability of perfusion to enhance directed differentiation.

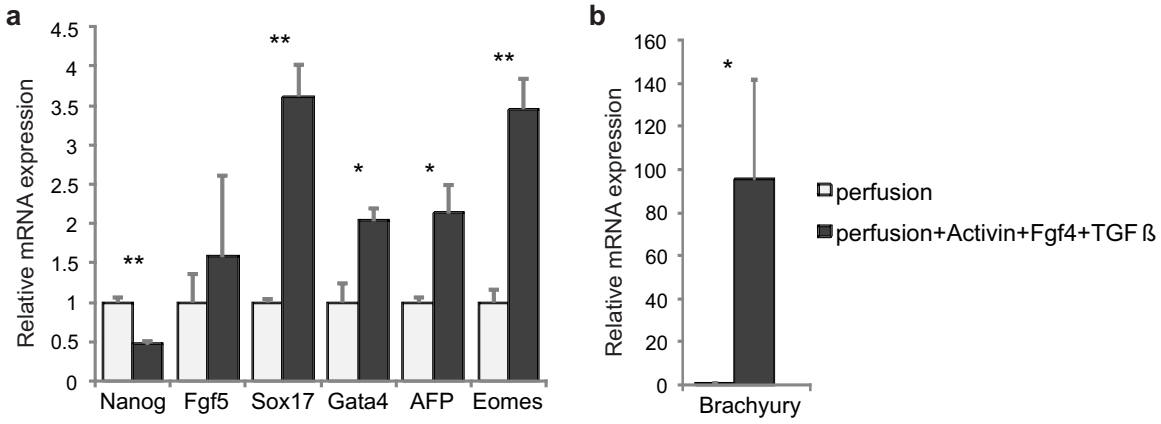

Figure 3-1 Adding proteins under perfusion. (a) Relative mRNA expression levels of the self-renewal marker Nanog and several differentiation markers in cells grown for three days under perfusion in self-renewal media with or without the indicated additions. (b) Relative mRNA expression level of Brachyury in the same conditions as in (a). **=$p<0.001$, *=$p<0.05$. Data represent the average of technical replicates and error bars represent standard deviation.

Previously described changes seen under perfusion were typically assessed at day 5, since day 3 cells did not show significant differentiation or self-renewal marker expression changes (Figure 2-4). However, after only three days of addition of FGF4, Activin, and TGFβ, we saw highly upregulated expression of the mesoderm differentiation markers Brachyury and Nkx2.5, changes that did not occur in static culture (Figure 3-2a). This dramatic upregulation did not occur in markers indicative of ectoderm (FGF5) or endoderm (Gata4, AFP) lineages (Figure 3-1). Though FGF5 levels increase with early differentiation of many lineages, they do not continue to increase in lineages other than ectoderm, which is consistent with cells under the given conditions tending towards mesoderm and not ectoderm differentiation. We went on to form embryoid bodies from cells that had been grown under perfusion for three days in the presence of FGF4, Activin, and TGFβ, and found that they formed embryoid bodies with unique

substructures (Figure 3-2b) and a higher propensity to beat as compared to embryoid bodies from normal static cultures. These results highlight the utility of perfusion in developing directed differentiation protocols, and indicate the importance of cell-secreted soluble signals in blocking exit of mESCs from self-renewal, even in the presence of differentiation-inducing cues.

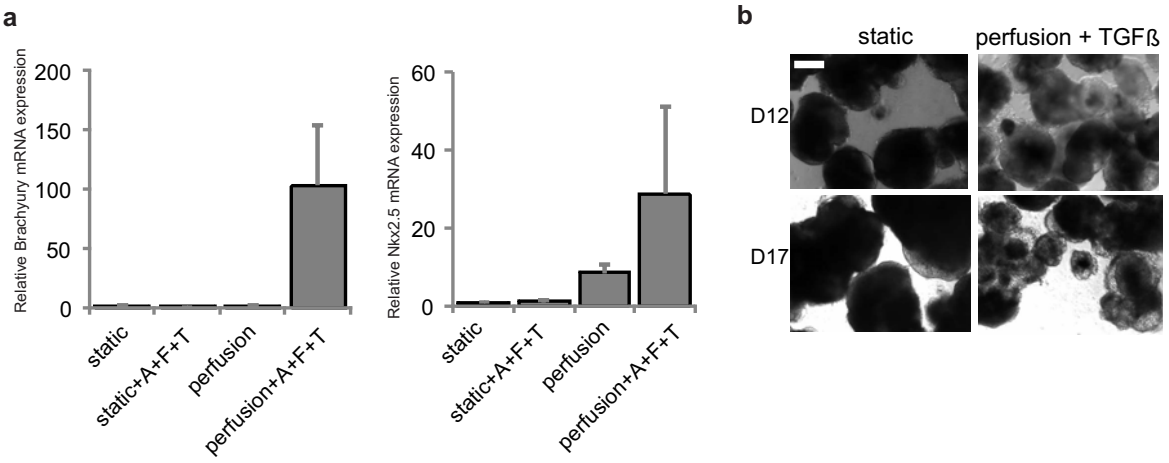

Figure 3-2 Induction of mesoderm genes under perfusion. (a) Relative mRNA expression levels of Brachyury (left) and Nkx2.5 (right) after three days of growth in static or perfusion with or without added Activin, FGF4, and TGFβ. (b) Representative images of embryoid bodies grown for 3 days in the conditions indicated on top and transferred to floating culture for the number of days indicated at left. Scale bar = 800 μm.

While the differentiation potential of these cells that express vastly higher levels of mesodermal markers has not been quantitatively monitored, we have formed embryoid bodies from normal static cultures and followed their expression of the mesodermal marker Brachyury over time using a Brachyury-GFP mESC line (Figure 3-3). A similar approach could thus be used to determine the timing and localization of Brachyury expression in embryoid bodies formed from cells initially more prone to mesodermal differentiation. Directed differentiation protocols could then be implemented to determine whether these cells are in fact more amenable to mesodermal differentiation and less amenable to differentiation towards other lineages, which could eventually lead to a more homogenous differentiated population. The proof-of-concept results showing that perfusion does allow for rapid and specific directed differentiation could be applied to direct differentiation toward other lineages, and could be used to optimize parameters for differentiation programs that are currently ill-defined.

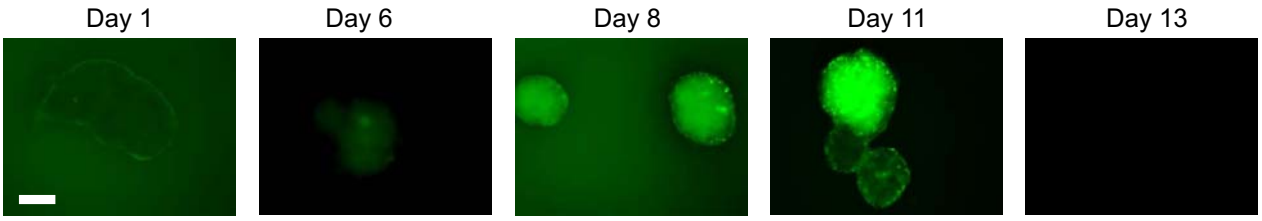

Figure 3-3 Representative fluorescent images of embryoid bodies formed from Brachyury-GFP reporter mESCs, growing for the indicated number of days. Scale bar = 800 μm.

3.3 Identifying and modeling ligands removed under perfusion

The utility of microfluidic systems exists not only in their ability to control signals on a broad scale, but also in their ability to precisely control and monitor exogenous factor addition and endogenous factor removal. However, in order to enact this precise control, a more complete understanding of a given microfluidic system's parameters and functionality in terms of its direct effects on cell signaling is crucial. For example, in order to directly manipulate the local impact of cell-secreted signals, it is imperative to quantitatively determine to what extent perfusion is removing these signals. Every candidate signal has a different mass, diffusivity, secretion level, associated receptor density, etc., so we began by attempting to establish a model system for the steady state surface concentration at the outlet versus the inlet for a molecule that is known to be secreted from mESCs, FGF4. Our model is simple but informs qualitative assumptions about removal of secreted molecules and how flow rate affects ligand exposure. Refer to (Moledina et al., 2012) for a recently published in-depth model of endogenous ESC signaling on cell fate.

For our model, we used COMSOL to solve the transient two-dimensional convection-diffusion-reaction problem in a rectangular geometry approximating our flow chambers. Specifically, we solved

$$\frac{\partial c}{\partial t} + \mathbf{u} \cdot \nabla c = \nabla \cdot (D \nabla c) + R,$$

where c is the species concentration in mol/m^3, t is time in s, $\mathbf{u}$ is linear velocity, D is the diffusivity of the reacting species in m^2/s, and R is the reaction rate expression for the species in mol/(m^3·s). This was subject to the following initial and boundary conditions:

Inlet: $c = c_0$, specified because we assume an input concentration of zero

Top of chamber: $n \cdot (-D\nabla c + c\mathbf{u}) = 0$, specified to indicate no flux into or out of the top of the chamber

Outlet: $n \cdot (-D\nabla c) = 0$, specified to indicate an outflow by convection

Flux from cells at bottom of chamber: $-n \cdot (-D\nabla c + c\mathbf{u}) = q_{sec} - (\frac{V_{max} * c}{K_m + c})$, specified to indicate that the flux of species *c* out of the bottom of the chamber (where cells are attached) is equal to the rate of species secretion minus the rate of reaction.

For these conditions, c_0 is the starting concentration, n is normal vector, q_{sec} is the rate of species secretion from the cells, V_{max} is maximum rate of species reaction, and K_m is the substrate concentration at which the reaction rate is half of V_{max}.

We specified the flow velocity to be parabolic, and used the following initial parameters:

Starting concentration	0 $mol \cdot m^{-3}$
Forward rate constant	1000 $m^3 \cdot mol^{-1} \cdot s^{-1}$
Backward rate constant	3e-4 s^{-1}
Active site concentration	4e-12 $mol \cdot m^{-2}$
Bulk ligand diffusivity	1e-9 $m^2 \cdot s^{-1}$
Surface ligand diffusivity	1e-11 $m^2 \cdot s^{-1}$
Maximum velocity	0.029 $mm \cdot s^{-1}$
Channel width	1.25 mm
Secretion rate	2.37e-16 $mol \cdot m^{-2} \cdot s^{-1}$
Chamber height	0.250 mm
Catalytic rate constant	1e-3 s^{-1}

The transport parameters are taken from chapter 2.2 and from (Huang et al., 1998; Mehta and Linderman, 2006), while the secretion rate data is from Figure 2-3.

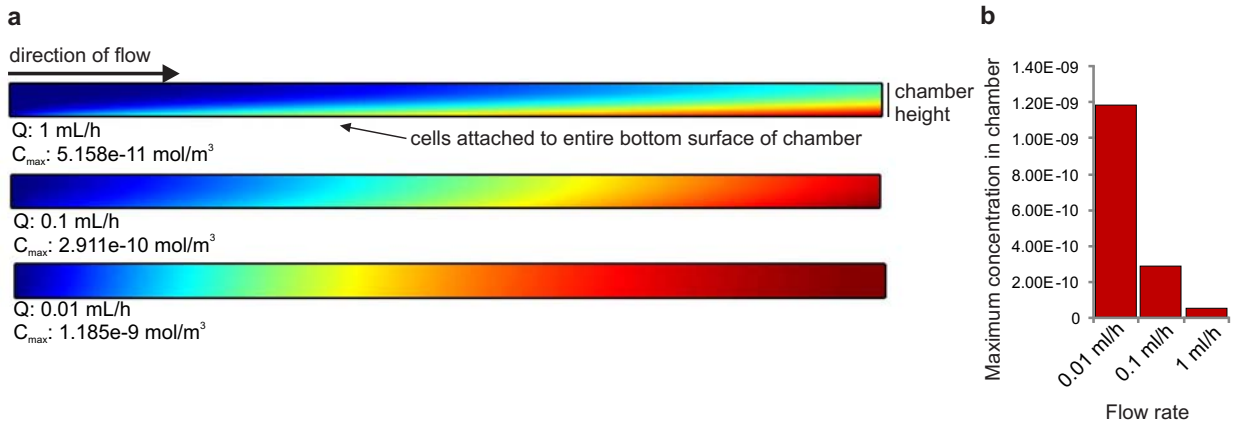

Figure 3-4 Perfusion chamber modeling results. (a) Plots show the concentration of a representative secreted ligand across the length of a perfusion chambers at a 100-fold range of flow rates (Q). The C_{max} listed under each plot indicates the highest concentration in the chamber (dark red color). The flow rate used in our system is represented by the middle plot. (b) Graph representing how the maximal concentration of ligand changes with flow rate.

Using these parameters, we profiled the steady state surface concentration of a theoretical cell-secreted ligand with characteristics similar to FGF4 at flow rate Q=0.01, 0.1, and 1 mL/h (corresponding to *Pe* = 3.7, 37, and 370), which showed expected behavior (Figure 3-4) where concentration of secreted molecules at the outlet builds up more with slower flow rates, and there is no apparent boundary layer formed at the flow rate we use. Over several flow rates, we can monitor the concentration of secreted ligand at the middle versus the end of the chamber and determine how that changes with a low density versus high density of cells (Figure 3-5). Using this data with a theoretical ligand, our flow rate (0.029 mm/s) shows that there may be some changes in ligand concentration along the length of the chamber, but that these differences are small in terms of the range of ligand concentrations seen at all flow rates. Though this analysis is rudimentary and does not take into account dynamic changes in cell growth and ligand production rates, it provides an initial framework in which to further model the relative concentration of specific ligand that is available to cells within the perfusion chamber.

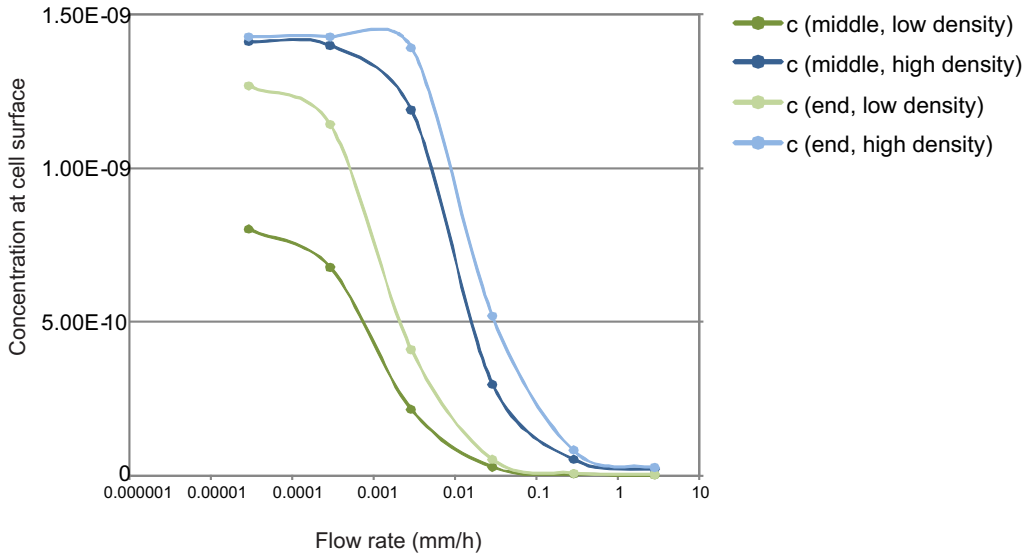

Figure 3-5 Comprehensive steady-state modeling results showing how concentration of a representative ligand changes throughout the length of the chamber according to cell density and flow rate.

To check the accuracy of the model predictions regarding removal of a candidate ligand such as FGF4, we assessed whether FGF4 appeared to be removed under perfusion. As described in chapter 2.4, autocrine/paracrine FGF4 signaling through MEK and ERK is a well-studied example of a cell-secreted factor that contributes to spontaneous differentiation of ESCs (Kunath et al., 2007; Stavridis et al., 2007; Burdon et al., 1999). Because we see an exit from self-renewal under perfusion, it is possible that FGF4 is still signaling under perfusion at levels high enough to elicit the differentiation phenotype. We thus sought to determine whether ERK signaling was still active under perfusion and thereby mediating the observed changes. We do see active ERK signaling, but LIF is known to activate ERK in a context-dependent manner (Niwa et al., 2009), and adding the potent MEK inhibitor PD0325901 (PD03) under perfusion was effective at inhibiting active ERK (Figure 3-6a). However, this addition did not cause an upregulation of the self-renewal genes Oct4, Nanog, Klf4 or Rex1 under perfusion, whereas it was effective in upregulating these genes in static cultures (Figure 3-6b), as previously reported (Ying et al., 2008). In addition, PD03 did not decrease differentiation marker expression to the level of static controls (Figure 3-6c). The fact that inhibition of downstream pathways does not affect the cells under perfusion supports the idea that perfusion is removing cell-secreted FGF4, and shows that

the transition out of the ESC state seen under perfusion is not a result of signaling through the MEK/ERK pathway.

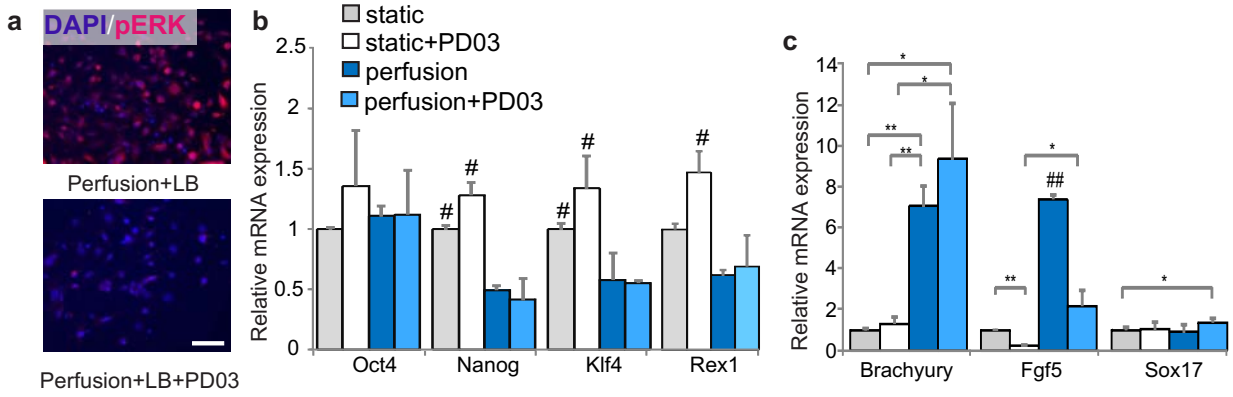

Figure 3-6 Inhibiting ERK signaling under perfusion. (a) Fluorescent images of cells grown in perfused culture in N2B27+LB with and without the MEK inhibitor PD0325901 (PD03), stained for phosphorylated ERK1/2 (red) and counterstained with DAPI (blue). Scale bar = 100 µm. (b) Expression levels of self-renewal markers after growth in static or perfusion self-renewal culture in the presence or absence of PD03. (c) Relative levels of mRNA expression for differentiation genes in the presence and absence of PD03 under static and perfusion self-renewal conditions. **=p<0.001, * =p<0.05; #=p<0.05, ##=p<0.001 for all pairwise comparisons, all data represents averages of at least three independent experiments and error bars represent SD.

As shown in Figure 2-11c, when we recirculate media from the outlet of perfusion back through the chamber, we see a reversal of the trend to exit the self-renewing state under normal perfusion conditions, indicating that proteins are being removed that are important for maintenance of self-renewal. More than one signal is likely responsible for the exit from self-renewal seen under perfusion, as the extracellular signaling environment of mESCs is very complex, and determining the combinatorial effects as well as the importance of signal presentation at the proper time and dose could benefit from the establishment of a high-throughput microfluidic screening system and from more controlled and testable model development.

3.4 Discussion

In this chapter, we discuss the utility of microfluidic perfusion in manipulating and monitoring cells. We first performed a proof-of-concept study in which mesoderm-inducing proteins were added to mESCs growing under perfusion, resulting in a dramatic upregulation of mesoderm genes after only three days. While this study is incomplete, it highlights a very promising future application for microfluidic perfusion and mESCs. Perfusion is desirable for directed differentiation as it provides a more neutral background in which cell-secreted proteins are

removed, thus eliminating factors that may inhibit or act in opposition to differentiation-inducing signals. Perfusion also allows for precisely timed factor addition and removal, which is often necessary during directed differentiation to mimic endogenous autocrine or paracrine signaling processes that occur in vivo (Murry and Keller, 2008). For example, it is known that the timing of FGF4 signaling is critical to mESC neuronal specification in vitro and epiblast formation in vivo (Stavridis et al., 2007; Yamanaka et al., 2010), and critical time windows have been found for addition of BMP4, Wnt3a, and Activin A to initiate mesodermal specification (Jackson et al., 2010). However, the temporal windows described in these examples were resolved only to days or half-days, which may not correspond to the true temporal resolution. Because the volume of our microfluidic chambers is about 4 μl, media can be exchanged very rapidly and in an automated fashion, allowing precise temporal requirements to be addressed.

Using microfluidics to mimic the in vivo environment can be extended to optimize protocols for directed differentiation and to better understand the interplay between exogenous factors and endogenous loops that operate during differentiation. Such studies are performed at moderate scale using traditional culture conditions (Purpura et al., 2008), but could potentially be performed more easily and at lower cost using microfluidics. While our device does not allow for optimization on this scale, multiplexing to a multichamber device and using an automated system for media changes on the order of minutes or seconds could be a powerful tool for screening many different additions at different concentrations and for different lengths of time. Once time windows have been narrowed down, as in some of the experiments described above, concentrations and sequential additions can be further optimized to create very precise protocols for creating or inhibiting the ability to undergo early differentiation events.

For all studies involving using microfluidic perfusion to manipulate cell signal presentation, a complete understanding of how endogenous or exogenous signals affect cells, either directly or indirectly, requires the ability to make and test predictions regarding ligand output and ligand-receptor interactions. Here we provide a simple model for determining how the concentration of a secreted ligand changes within a perfusion chamber based on flow rate and cell density, but this model is incomplete in its predictive ability. We were able to verify the fact that FGF4 signals are not functionally active in signaling through ERK under perfusion, which implies that other cell-secreted signals are contributing strongly to the exit from the self-renewing state.

However, we did not assess whether the levels of FGF4 were similar or different along the length of the chamber, nor did we determine the concentration of FGF4 removed under perfusion. Next steps would involve using an experimental setup with known levels of a secreted protein that could be tested in its ability to be removed at different flow rates and with different cell densities, and using this data to make a more complete model that could then be reapplied to predict similar outcomes with other signaling molecules.

The ability to confirm the removal of FGF4 under perfusion indicated the need to look more broadly at cell-secreted signals in order to identify the nature of the signals required to maintain self-renewal. Microfluidic perfusion of adherent cells is somewhat limited by the fact that certain types of cell-cell signaling are not addressed, such as those that act by cell-cell contact or through the extracellular matrix. In the next chapter, we will address this limitation and show that we can manipulate both cell-secreted soluble signals and extracellular matrix-based signals, with different consequences.

3.5 Methods

For information regarding cell lines, culture additions, and qPCR protocols, refer to Appendix 1. For information regarding perfusion culture or embryoid body formation, refer to the methods in chapter 2.8.

Immunofluorescence

For phospho-ERK1/2 staining, cells were incubated overnight with phosphorylated ERK1/2 antibody (BD Biosciences) at 1:100 and secondary (anti-mouse AF546, Invitrogen) was added for two hours at 1:1000. Cells were counterstained with 1:100000 Hoechst (Sigma).

Finite-element modeling

The MEMS module of COMSOL version 3.5a was used for finite-element modeling. A steady-state 2-dimensional convection and diffusion model was used, adapted from the provided Transport and Adsorption and Transport of Diluted Species models.

Chapter 4 Depletion of soluble versus extracellular matrix-based signaling

4.1 Introduction

In addition to soluble signals whose presence can be depleted using perfusion, cells also secrete extracellular matrix proteins that bind under or between the cells and thus are not affected by perfusion to the same extent as are soluble diffusible secreted signals. As described in chapter 1.3, signals emanating from the endogenous ECM are complex and can be very significant, such that the contributions of ECM-based signals cannot be ignored when discussing the cell-secreted microenvironment. It may be useful to think of the endogenous ECM as a dense mesh or a net in which the structural components such as collagen, laminin, and fibronectin can act to bind or trap endogenously secreted cytokines and growth factors (Hynes, 2009). These and other ECM proteins such as integrins and proteoglycans can also act alone as signaling proteins or as cofactors for soluble or matrix-bound proteins (Keung et al., 2010).

Heparan sulfate proteoglycans (HSPGs) function as a reservoir of growth factors in the matrix (Hynes, 2009), or as a cofactor for signaling proteins such as FGFs, BMPs, and TGFβ (Taylor and Gallo, 2006), functions that depend on the ability of proteoglycans to be properly sulfated. To manipulate this function in mESCs, Lanner et al. used multiple methods to block the sulfation of HSPGs, including a small molecule inhibitor and a sulfating enzyme knockout cell line, and found that cells grown under these conditions become more homogeneously naïve (Lanner et al., 2010). This result was reminiscent of previous results in which blocking FGF4-ERK signaling in mESCs caused a similar phenotype, and indeed, Lanner et al. found that the major extracellular signal involved in HSPG-mediated induction of a more primed state was autocrine FGF4. While we showed in chapter 3.3 that FGF4 is not a functional signal under perfusion, presumably due to its removal, other components of the ECM may still be affecting the cells undergoing perfusion. Many other aspects of the ECM could also be contributing to the perfusion phenotype, so we sought to determine the effects of manipulating ECM-based signaling using the sulfation inhibitor sodium chlorate or the enzyme collagenase, both alone and in the context of perfusion. In this way, by individually modulating both diffusible and ECM-based cell-secreted signals, we

could probe the specific roles of each, or combine the two to block signals secreted into the ECM and the mass media.

While we can manipulate the ECM exogenously by adding sulfation inhibitors or collagenase, cells also have endogenous mechanisms that they use to manipulate the ECM. The most prominent class of endogenously secreted remodeling enzymes is the MMP family (Matrisian, 1990), consisting of 23 members in mice (Nuttall et al., 2004). Each MMP has specific substrates, and some MMPs are secreted while others are transmembrane proteins, but all are initially expressed as pro-enzymes that require proteolytic cleavage to become active proteases. Secretion levels of endogenous MMPs and whether or not they have a functional role in ESC biology has not been studied extensively, but their function has been shown to be important during early embryonic development as the embryo undergoes implantation and gastrulation (Huang, 2006; Coyle et al., 2008; Das et al., 1997).

More generally from a developmental biology perspective, ECM and basement membrane production are crucial steps in proper gastrulation and embryonic development (Lu et al., 2011; Hammerschmidt and Wedlich, 2008), so understanding more general roles of ECM-based signals and how the matrix is formed and remodeled endogenously is important. Using microfluidic perfusion allows us to study ECM proteins in the absence of diffusible signals, which may normally act to obscure signaling pathways specific to ECM. Signals emanating from the ECM have been shown to regulate processes as diverse as neuronal cell migration (Perris and Perissinotto, 2000) and cancer cell invasion (Stetler-Stevenson et al., 1993), and such signals are dysregulated in muscular dystrophies (Campbell, 1995) and some forms of cardiovascular disease (Dollery et al., 1995). However, the specific functions of ECM-based and diffusible autocrine signaling in these systems is not yet well characterized, so the ability to discretely regulate both while reproducibly monitoring the outcome has wide relevance.

Sections 4.2 and 4.4 of this chapter are adapted from Przybyla and Voldman (Przybyla and Voldman, 2012b).

4.2 Extracellular matrix remodeling under perfusion

In chapter 2.5, we found that growing mESCs under constant media perfusion caused them to exit their self-renewing state, even in the presence of cues previously thought to be sufficient to maintain self-renewal. To determine the processes responsible for this exit, we looked for signals that may still be acting to elicit a state change in the absence of soluble autocrine factors. The fact that the endogenous ECM is intact under perfusion prompted us to explore the possibility that proteins trapped within the ECM could be contributing to the perfusion phenotype.

As described in chapter 1.4, the ECM has been implicated in contributing to spontaneous differentiation of mESCs by binding of cell-secreted factors (Lanner et al., 2010), or by its structural or mechanical properties (Chowdhury et al., 2010). To broadly assess the effects of disrupting the ECM under perfusion, we initially used sodium chlorate, a sulfation inhibitor that blocks the ability of most proteoglycans to act as protein tethers or reservoirs within the ECM (Baeuerle and Huttner, 1986; Humphries and Silbert, 1988). Sodium chlorate is able to remove sulfated heparan chains, as shown by staining for sulfated heparin in the presence of sodium chlorate (Figure 4-1a). As has been shown previously, disruption of heparan sulfation in static culture decreased spontaneous differentiation (Figure 4-1b). On a molecular level, disrupting heparan sulfation in static cultures caused an upregulation of the self-renewal markers Nanog and Klf4 and a decrease in levels of the differentiation marker FGF5 (Figure 4-1c). These changes in static culture are reminiscent of changes that occur when ERK is blocked (see chapter 2.4), and in terms of protein expression, Sox2-GFP reporter mESCs have a very similar flow cytometry histogram in the presence of either sodium chlorate or ERK inhibition (Figure 4-1d).

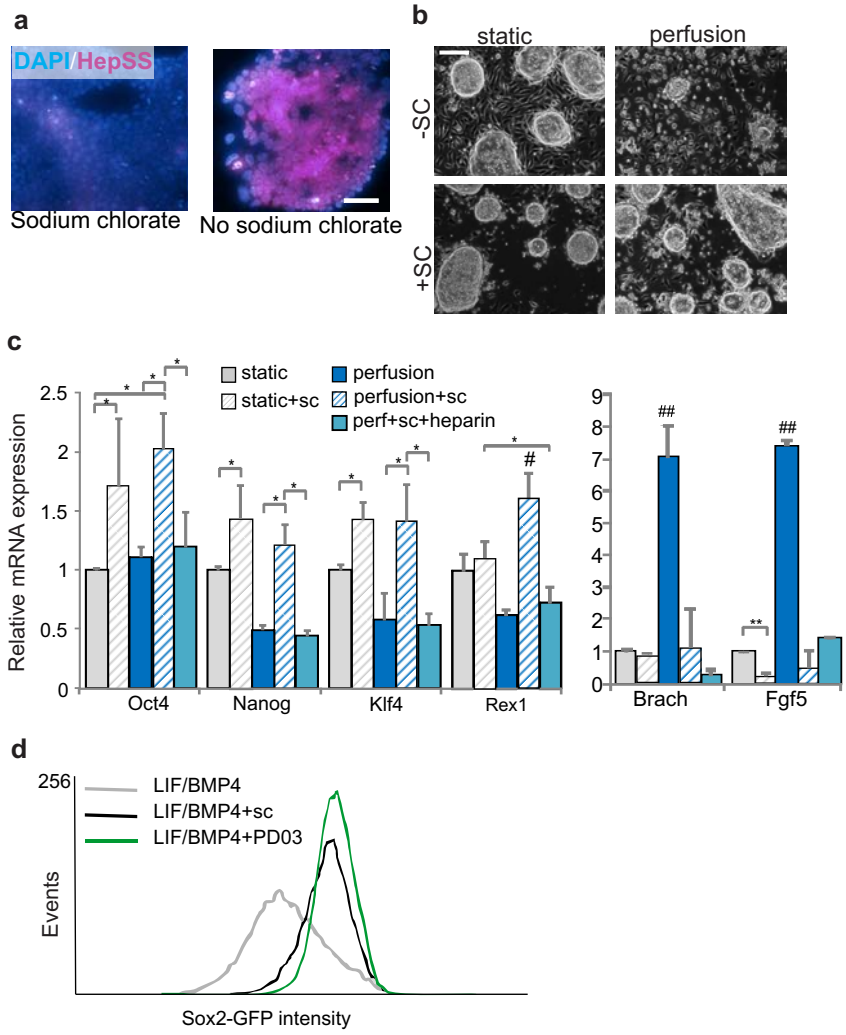

Figure 4-1 Disruption of heparan sulfation inhibits differentiation. (a) Immunofluorescence staining for sulfated heparan after five days of growth in the presence or absence of sodium chlorate. Scale bar = 100 µm. (b) Representative morphology of cells grown in static or perfusion self-renewal with or without sodium chlorate (+/- SC). Scale bar = 200 µm. (c) mRNA expression levels of self-renewal and differentiation markers in the presence and absence of sodium chlorate with or without the addition of soluble heparin in static or perfusion self-renewal. (d) Flow cytometry histograms showing levels of Sox2 in a Sox2-GFP cell line. **=p<0.001, * =p<0.05; #=p<0.05, ##=p<0.001 for all pairwise comparisons, all data represents averages of at least three independent experiments and error bars represent SD.

Whereas blocking ERK signaling under perfusion had no obvious effects on the cells (see chapter 3.3), disrupting heparan sulfate under perfusion had dramatic consequences. First, we noticed a higher prevalence of large healthy mESC colonies under perfusion in the presence of sodium chlorate compared to its absence (Figure 4-1b). In terms of marker expression, the self-renewal markers Oct4, Nanog, Klf4, and Rex1, levels of which had all decreased under perfusion, were restored to or beyond levels seen in static cultures, while differentiation markers

that had increased were restored to the low levels seen in static culture (Figure 4-1c). To show that these dramatic changes were due to functional disruption of heparan sulfate chains, we added soluble heparin along with sodium chlorate to restore the heparan sulfate binding function, and this reduced levels of self-renewal markers to the levels seen under baseline perfusion conditions (Figure 4-1c). Adding low concentrations of collagenase to disrupt the ECM produced a similar phenotype as that resulting from the addition of sodium chlorate, in terms of morphology (Figure 4-2a) and marker expression (Figure 4-2b). Interestingly, Fgf5 expression levels did not decrease in the presence of collagenase whereas it did in the presence of sodium chlorate (Figure 4-1c), indicating that this upregulation may be due to a specific heparan-sulfate binding protein that is not disrupted by collagen removal. Taken together, these data indicate that broadly disrupting the ECM by either small molecule or enzyme addition under perfusion allows ESCs to maintain their self-renewing state, while functional recovery of ECM protein binding causes cells under perfusion to exit this state, indicating the importance of ECM disruption in mESC self-renewal.

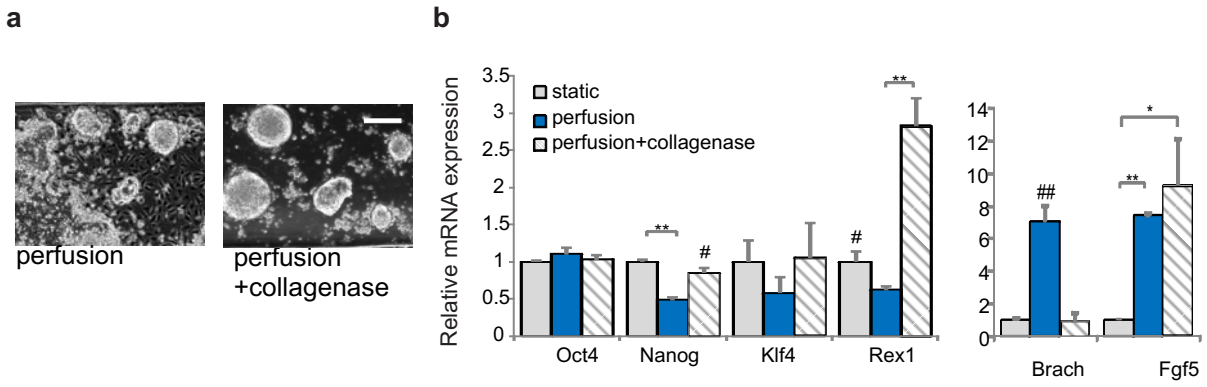

Figure 4-2 Effects of collagenase addition under perfusion. (a) Representative morphology of cells grown in the indicated conditions. Scale bar = 200 µm. (b) mRNA expression levels of self-renewal (left) and differentiation (right) markers for cells grown in static and perfusion compared to levels in cells grown in perfusion in the presence of 1 ng/ml collagenase. **=p<0.001, * =p<0.05; #=p<0.05, ##=p<0.001 for all pairwise comparisons, all data represents averages of at least three independent experiments and error bars represent SD.

Expression and production of ECM proteins is highly controlled at the transcriptional level, with many auto-regulatory loops involved to maintain appropriate levels of ECM proteins (Levenberg et al., 1998). To determine how this regulation was affected by perfusion, we used data from Table 2-1 to check expression levels of ECM structural proteins over five days in static versus perfusion. Levels of most such proteins were higher in perfusion as compared to static, even on

day 3, before many other changes were apparent (Figure 4-3). This indicates a relatively rapid misregulation of ECM formation upon depletion of soluble cell-secreted signals such that ECM proteins are produced at higher levels, which may help to explain why large-scale disruption of the matrix mitigates the phenotype seen under perfusion. Further work could involve measuring the rate and composition of endogenous matrix buildup in both static and perfusion cultures.

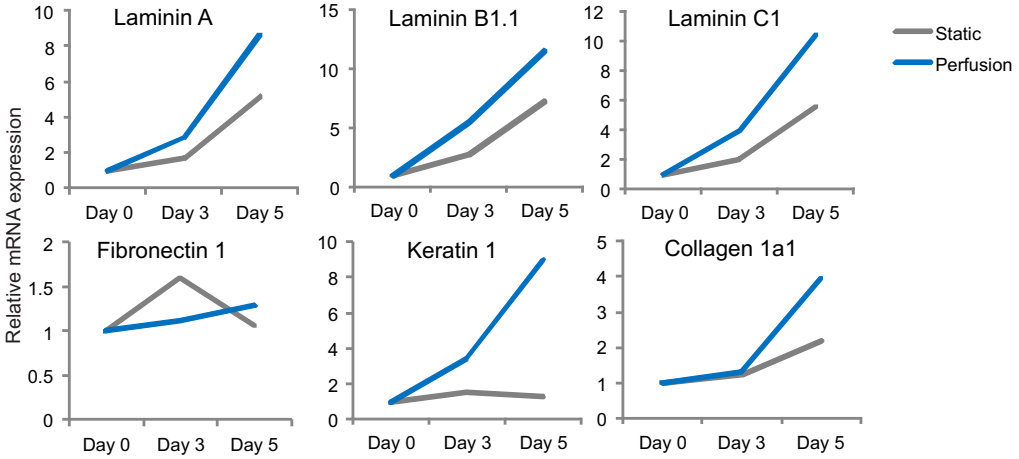

Figure 4-3 mRNA expression levels of structural ECM genes over five days in static or perfusion. Data are obtained from Table 2-1.

4.3 Contributions of soluble versus ECM-based signals

We next sought to gain a more complete understanding of how disrupting heparan sulfate proteoglycan binding functionally affects mESCs. From experiments involving blocking either soluble signaling (perfusion), ECM-based signaling (sodium chlorate or collagenase), or both, we observed that cell-secreted signals emanating from different sources can have drastically different effects on cells. However, all these studies included exogenously added LIF and BMP4. To determine how these modes of signaling function in the absence of exogenously added signals, we assessed the contribution of soluble versus ECM-based signals in serum-free N2B27 media alone.

We analyzed expression of markers indicative of early differentiation towards the ectoderm (FGF5), endoderm (Gata4), or mesoderm (Brachyury) lineages in cells grown for five days without LIF or BMP4. In static cultures, cells grown in the presence of sodium chlorate have increased levels of Gata4 compared to those without sodium chlorate (Figure 4-4). Conversely, cells grown under perfusion show very different expression patterns for ectoderm and mesoderm

markers depending on whether they are grown in the presence or absence of sodium chlorate (Figure 4-4). These results are consistent with a situation in which, when soluble cell-secreted signals are dominant over ECM-based signals (static culture with sodium chlorate), cells tend towards endoderm differentiation, whereas the dominance of ECM-based signals over soluble signals (perfusion culture without sodium chlorate) causes cells to differentiate towards mesoderm and ectoderm. However, this data only includes monitoring expression of one marker per differentiation lineage at a single timepoint, while any conclusive claims about differentiation trajectories would require assessing expression levels and dynamics of many additional lineage markers.

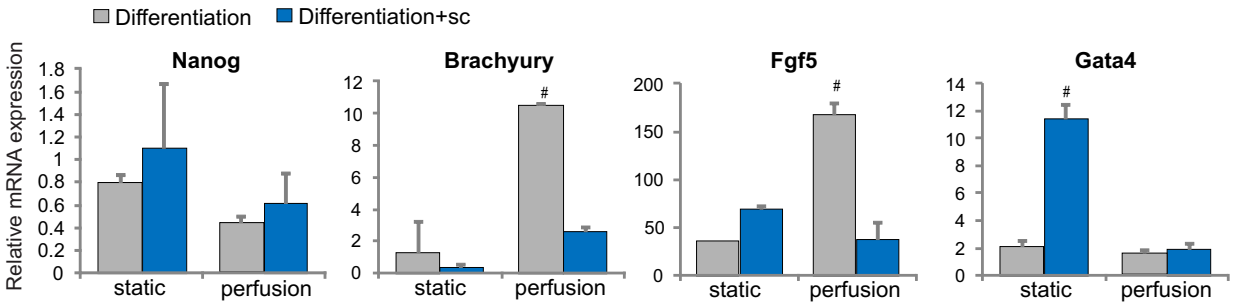

Figure 4-4 mRNA expression levels of a self-renewal marker (Nanog) and early differentiation markers indicative of the three somatic lineages, mesoderm (Brachyury), ectoderm (FGF5), and endoderm (Gata4), after five days in the indicated conditions in the absence of LIF and BMP4.

Because of these drastic changes in marker expression upon exposure of mESCs to different types of cell-secreted signals, we wanted to assess the potential of cells grown under these conditions to self-renew and to remain pluripotent. To assess self-renewal, we replated cells after growth in static or perfusion in media containing LIF and BMP4 in the presence or absence of sodium chlorate and found that the only cells that were able to replate and grow were those grown in normal static conditions (Figure 4-5). However, the inability of cells grown in sodium chlorate to successfully be cultured further could be because they were not able to properly attach to the culture surface due to the effects of residual sodium chlorate. Because the ability to self-renew implies maintenance of pluripotentiality, we further explored self-renewal ability by assessing this characteristic.

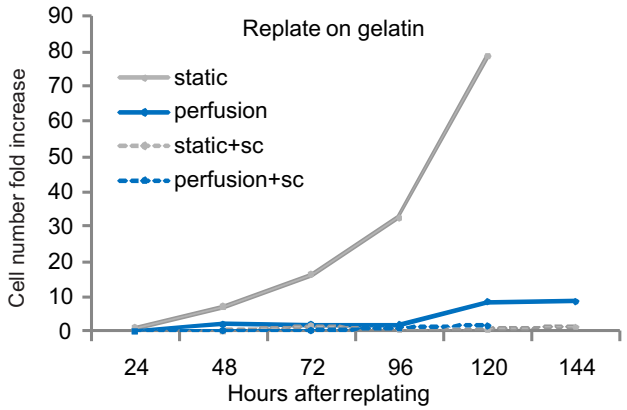

Figure 4-5 Fold increase in growth of cells that were replated into static self-renewal media from growth in static or perfusion in the presence or absence of sodium chlorate.

To determine whether mESCs grown in static or perfusion in the presence or absence of sodium chlorate were able to differentiate and maintain the full range of pluripotent potential, we formed embryoid bodies and checked morphology and expression of differentiation markers. We noticed that mESCs grown in the presence of sodium chlorate, which expressed self-renewal markers (Figure 4-1c), had greatly diminished embryoid body forming efficiency, and formed bulbous, uncompact embryoid bodies (Figure 4-6a), indicating that the ability of these cells to remain fully poised for differentiation was compromised. To further assess pluripotentiality, we compared histology sections from embryoid bodies formed from cells that had been grown in N2B27+LIF+BMP4 media in perfusion and static cultures in the presence or absence of sodium chlorate. As expected, we found that the largest and most complex-looking EBs were formed in the presence of both soluble and ECM-based cell-secreted signals (Figure 4-6b). We also analyzed marker expression from these EBs and found that removing soluble signals using perfusion seems to bias cells toward mesodermal differentiation and away from endoderm or ectoderm, while removing ECM-based signals with sodium chlorate biased cells toward an endoderm fate and away from mesoderm (Figure 4-6c). The very low number and small size of EBs formed from cells grown in perfusion in the presence of sodium chlorate prohibited characterization of this condition in terms of marker expression. The differentiation biases seen from cells grown under perfusion or in the presence of sodium chlorate are consistent with the results seen above (Figure 4-4), whereby soluble cell-secreted signals bias mESCs towards endoderm, while ECM-based signals provide a bias towards mesoderm differentiation.

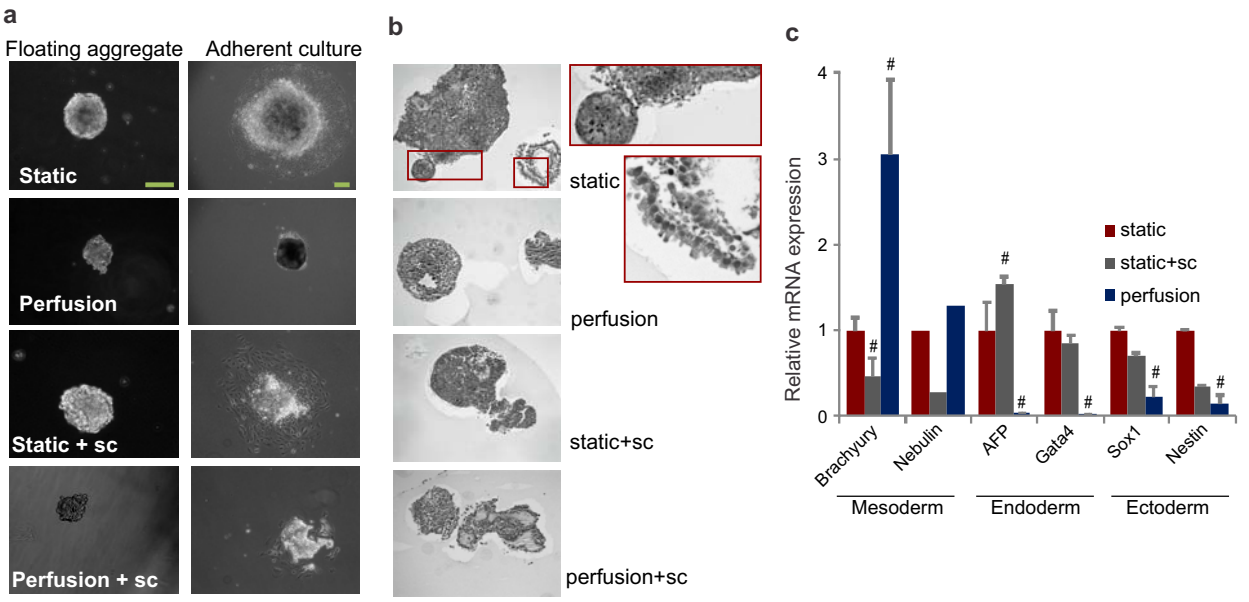

Figure 4-6 Embryoid body differentiation after manipulation of exogenous signaling. (a) Representative morphology of embryoid bodies growing in differentiation media after five days of exposure to the indicated conditions. (b) Histology sections of day 10 embryoid bodies from the same conditions as those in (a). Red boxes indicate regions of complex substructure including defined membrane edges and invagination. (c) Marker expression on day 9 of markers representing differentiation toward the three germ layers. # = $p<0.05$ for all pairwise comparisons.

Our initial studies with microfluidic perfusion indicated that in the absence of diffusible autocrine signaling, mESCs lose self-renewal characteristics and acquire early ectoderm and mesoderm differentiation characteristics on a population-wide level. Here, this trend was further supported using media without exogenous LIF and BMP4, with results also indicating that depletion of ECM-based autocrine signaling causes endoderm markers to increase (Figure 4-4). Finally, when both diffusible and ECM-based cell-secreted signals are inhibited by growing cells under perfusion with sodium chlorate, the cells have markers indicative of self-renewing cells, while they in fact do not retain the ability to differentiate properly (Figure 4-6). It is possible that mESCs in conventional static culture are able to stably regulate these distinct signals to maintain their balance between the naïve and poised states, thus allowing them to effectively retain their self-renewal and pluripotency characteristics.

4.4 Removal of endogenous matrix remodeling proteins affects ESC self-renewal

So far in this chapter, we have shown that blocking ECM-based signals is able to block the transition to a primed epiblast-like state that is normally induced by removing soluble cell-secreted proteins. However, the precise nature of the proteins involved in inducing this transition

is unclear. To determine whether there was a direct link between removing secreted signals and matrix remodeling, we looked towards endogenously secreted molecules responsible for remodeling and curating the ECM, the MMP family of proteins (Matrisian, 1990). MMPs are known to be secreted by mESCs (Guo et al., 2006b), so we analyzed expression of various members of the MMP family in self-renewing cultures and found that, while MMPs are expressed at low levels upon initial mESC plating, after five days in culture, MMP expression levels increase significantly, and tend to be higher in self-renewing cultures compared to differentiation cultures (serum+retinioic acid) (Figure 4-7). It is thus possible that ECM breakdown is functionally significant in the maintenance of self-renewal.

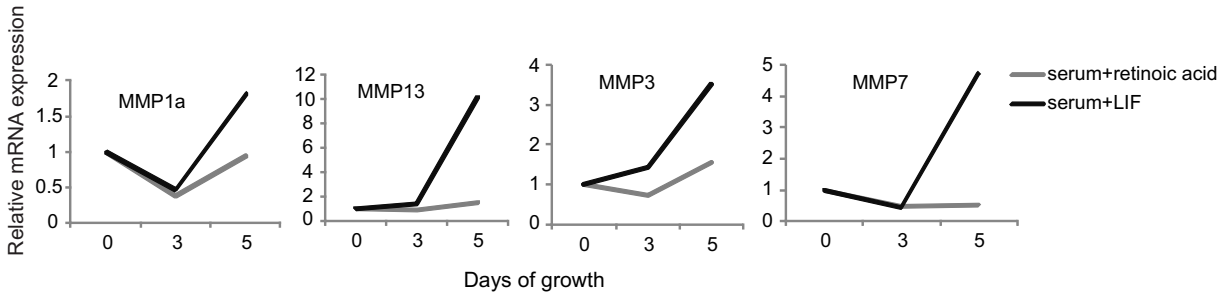

Figure 4-7 mRNA expression levels of MMPs during growth in static cultures under self-renewing (serum+LIF) or differentiation (serum+retinoic acid) conditions.

Because the exit from the ESC state seen under perfusion is related to the presence of the intact ECM, it is possible that a removal of MMPs under perfusion is responsible. MMPs are highly regulated at the transcriptional level by feedback mechanisms, they require proteolytic cleavage to become active, and they act at the level of a single molecule instead of activating a signaling cascade. For these reasons, their removal by perfusion could quickly and completely block their functionality. We show that we are able to recover MMP2 from perfused cells (Figure 4-8a), illustrating that it is being removed by flow. Levels of MMP2 protein were lower from cells under perfusion compared to those in static, which was also the case for transcript levels (Figure 4-8b), as would be expected if positive transcriptional feedback regulation mechanisms were being affected. Similarly, levels of MMP9 expression are lower in perfusion cultures as compared to static, a trend that is not affected by disrupting the matrix exogenously (Figure 4-8c). Thus, endogenous matrix remodeling proteins are being removed under perfusion, and as we have already shown that levels of matrix structural proteins increases under perfusion (Figure

4-3), we hypothesize that the inability of mESCs to properly regulate their matrix under perfusion may be responsible for the resulting phenotype.

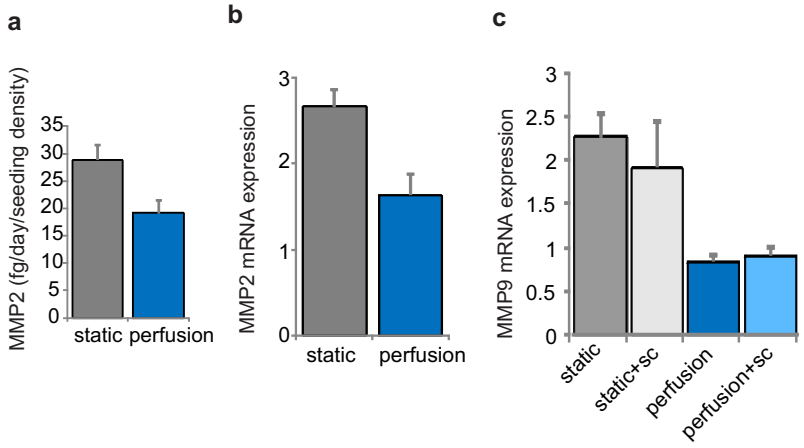

Figure 4-8 MMP production and secretion. (a) Secreted protein levels of MMP2 in static and perfusion culture over five days, analyzed by ELISA. (b) Relative levels of MMP2 mRNA expression in static and perfusion cultures. (c) Relative levels of MMP9 mRNA expression in static and perfusion cultures in the presence or absence of sodium chlorate.

To determine whether mESC-secreted MMPs are functional in terms of self-renewal, we blocked these endogenous remodeling proteins in static culture and assessed the resulting phenotype. We found that adding the MMP inhibitor Batimastat caused an increase in FGF5 and a decrease in Klf4 and Nanog levels, trends that were also seen under perfusion (Figure 4-9a). We also found that ESCs cannot be cultured for multiple passages in conditions where MMPs are inhibited by the presence of the small molecule MMP inhibitor, Ro32-3555. After two passages in the presence of this inhibitor, cells grew poorly and differentiated (Figure 4-9b), and were no longer viable by passage 3. Cells that were seeded in self-renewal media, switched to self-renewal media+Ro32-3555 after a 24 hour attachment period, and grown in this media for five additional days showed a decrease in Nanog expression levels (Figure 4-9c), indicating that the inhibitor is not merely causing an exit from self-renewal by altering attachment or growth. Together, these results indicate that matrix remodeling is critical in maintaining the mESC state and that removal of cell-secreted factors means that matrix remodeling cannot occur properly, thus inducing exit from the self-renewing state.

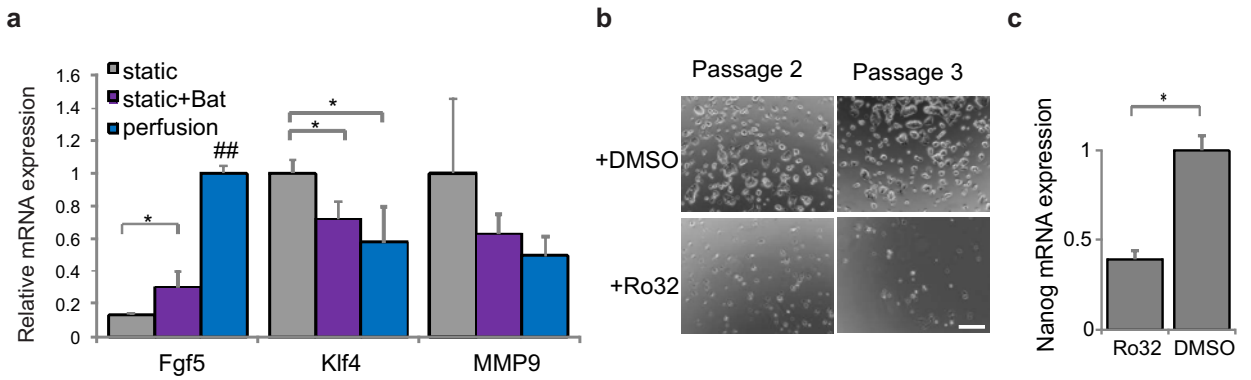

Figure 4-9 MMPs are functional in mESC cultures. (a) Relative mRNA expression levels of cells grown in the indicated conditions, Bat = Batimastat, an MMP inhibitor. (b) Cells grown with or without MMP inhibitor Ro32-3555 for multiple passages, scale bar = 400 µm. (c) Relative Nanog mRNA expression levels of cells grown for five days in Ro32-3555 or DMSO. * =p<0.05.

4.5 Discussion

The extracellular matrix significantly contributes, directly or indirectly, to the cell-secreted microenvironment of adherent cells. Here we show that, in addition to the known pro-self renewal LIF/BMP4 signals and the pro-differentiation FGF4-ERK autocrine stimulus, there also exist ECM-bound factors that control the exit from mESC self-renewal. In normal cultures, matrix remodeling is constantly occurring to modulate levels of or access to these factors. However, under perfusion, the secreted factors that are responsible for remodeling are removed such that ECM turnover does not occur and mESCs exit their naïve self-renewing state (Figure 4-10).

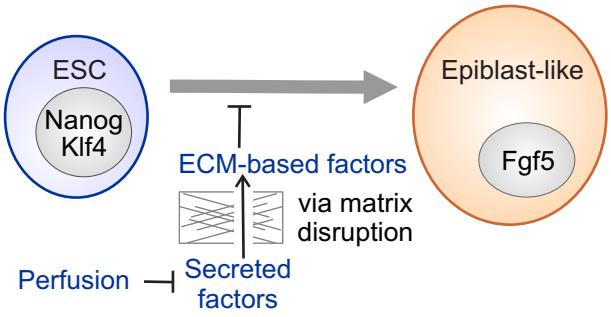

Figure 4-10 Model depicting the normal function of ECM-based and secreted endogenous factors in the exit from the self-renewing ESC state, and how perfusion disrupts these signals.

The cell-secreted extracellular environment can be broadly separated into soluble and ECM-based signals. Here, we show that we can manipulate both modes of signaling individually or in

parallel, resulting in mESC populations with vastly different differentiation potentials. This ability can be useful when trying to determine the influence of soluble or ECM-based signaling on specific processes, including directed differentiation or maintenance of self-renewal. These results also show that it is crucial to consider these multiple modes of signaling when discussing the contributions of cell-secreted signals, as soluble versus tethered ligands can act in very different ways, which will be discussed further in chapter 6.

Here, we show that the ECM contributes to spontaneous differentiation in mESC cultures, thus implicating matrix remodeling as a crucially important process in controlling presentation of proteins from the ESC microenvironment to maintain self-renewal, and we show that the presence of LIF and BMP4 and a matrix remodeler is sufficient for this maintenance. An important class of endogenous cell-secreted ECM remodelers is the MMP family, and we show that their inhibition in static culture causes mESC differentiation. While various components of the ECM have been shown to play a role in enhancing or inhibiting ESC self-renewal (Chowdhury et al., 2010; Domogatskaya et al., 2008; Hayashi et al., 2007; Lanner et al., 2010), this is the first demonstration of the importance of ECM remodeling on maintenance of mESC self-renewal.

By showing that removal of soluble cell-secreted proteins causes mESCs to exit their self-renewing state, that MMPs are removed under perfusion and are functional in mESC cultures, and that matrix remodeling under perfusion causes mESCs to remain self-renewing, we can indirectly implicate the removal of MMPs in the phenotype resulting from perfusion. A model then emerges in which MMPs normally act in mESC cultures to curate the matrix, either by removing proteins that normally inhibit self-renewal, or by releasing trapped pro-self-renewal ligands and allowing them to signal. Under perfusion, this system is disrupted and cells exit their self-renewing state unless exogenously provided with matrix remodeling proteins.

These results further emphasize the power of microfluidic perfusion in uncovering previously unknown roles for cell-secreted signals. This robust method can be broadly applied to other cell types to test hypotheses based on the effects of cell-secreted signals or the roles and contributions of ECM-based signals. Once we uncovered the importance of endogenous MMPs in maintaining mESC self-renewal, we went on to further characterize this novel role and

determine the mechanism by which MMPs act to aid in the maintenance of self-renewal, the results of which are described in chapter 5.

4.6 Methods

For information regarding cell lines, culture additions, and qPCR protocols, refer to Appendix 1. For information regarding perfusion culture, flow cytometry, or embryoid body formation, refer to the methods in chapter 2.8.

Immunofluorescence

For HepSS staining, cells were blocked with endogenous biotin blocking kit (Invitrogen) and incubated overnight with HepSS antibody at 1:100 (Lifespan Biosciences) and secondary antibody (TMR NeutrAvidin, Invitrogen) was added at 1:500 for one hour. Cells were counterstained with 1:100000 Hoechst (Sigma).

ELISA

Enzyme-linked immunosorbent assay was performed on samples from static conditioned medium, or from the medium collected from the perfusion output. Because of the discrepancy in volume between these two types of samples, perfusion output medium was spun down using an Amicon 3 kD cutoff filter spin column and reconstituted to the same volume as the static conditioned medium. MMP2 ELISA was purchased from RayBioTech, and assay was performed according to manufacturer's instructions.

Cell replating

Cells grown for five days in static or perfusion culture were trypsinized and replated at the same density as the original seeding density in static self-renewal conditions in 96-well plates. Three wells of cells in each condition were recovered and counted daily using a Coulter counter.

Embryoid body histology

Embryoid bodies were transferred to a 1.5 ml tube and allowed to settle by gravity. Media was removed and liquified HistoGel was added, then tube was transferred to ice to allow HistoGel to solidify. The resulting specimen was wrapped in lens paper and placed in a histology cassette,

then incubated in formalin overnight. The next day, cassettes were transferred to 70% ethanol and sectioned and H&E stained in the histology facility.

Chapter 5 Matrix remodeling maintains ESC self-renewal in static cultures

5.1 Introduction

After showing that extracellular matrix remodeling is necessary to retain mESC self-renewal in the absence of soluble autocrine cues, we further probed the role of the matrix in contributing to cell phenotype to determine whether remodeling alone is sufficient to maintain self-renewal. The mechanisms behind how extracellular matrices affect ESC fate are largely unexplored, so we sought to further investigate this important aspect of the ESC extracellular microenvironment.

Routine culture of mESCs generally involves a feeder layer composed of mitotically inactivated mouse embryonic fibroblasts (MEFs) coupled with exogenous addition of LIF (Tremml et al., 2008). These conditions have also been used to reprogram somatic cells to pluripotency after ectopic expression of defined factors (Takahashi and Yamanaka, 2006; Okita et al., 2007; Wernig et al., 2007; Maherali et al., 2007). MEFs are known to contribute to mESC self-renewal by the secretion of LIF (Smith et al., 1988; Williams et al., 1988), but many mESC lines grow better in the presence versus the absence of feeders even with exogenous LIF, indicating that the contribution from MEFs extends beyond LIF secretion.

Several novel mechanisms have recently been described that allow for the maintenance of mESC self-renewal in the absence of LIF, including simultaneous inhibition of ERK and GSK3 (Ying et al., 2008), inhibition of NF-κB signaling (Dutta et al., 2011), inhibition of Src signaling (Li et al., 2011), and induction of Smad signaling (Soncin et al., 2009). These studies indicate that inhibition of many signaling pathways can not only aid in self-renewal but can actually be sufficient for its maintenance. Our results from chapter 2 and chapter 4 show that LIF is not sufficient for mESC maintenance, even with the addition of BMP4 in serum-free conditions. Thus, other pathways are clearly important in maintaining self-renewal, and based on the fact that matrix remodeling is necessary for self-renewal, it is possible that signals upstream of these other pathways lie within the matrix. Matrix remodeling may be causing matrix-based signals to be removed from the matrix surface during remodeling and thus not signal normally, or it may be

allowing signals from within the matrix to be presented to the cells, thus providing additional extracellular signals.

In chapter 4, we forced remodeling of the matrix by adding sodium chlorate or collagenase, and showed that this affected cells differently than did depleting endogenous soluble signals. Now, we show that we can remodel the matrix in a more controlled way by adding MMP1, and find that this addition is sufficient to maintain long-term LIF-independent mESC self-renewal. We go on to further characterize the system, describing a novel system for LIF-independent mESC self-renewal that relies on an endogenously secreted factor. The work described in this chapter is currently being prepared for publication.

5.2 Feeder cells secrete MMPs that functionally influence ESC self-renewal

Because endogenous ECM remodeling proteins are necessary for mESC self-renewal (Figure 4-9), we investigated whether one of the roles of feeder layers beyond LIF secretion involves enhancing matrix remodeling. We found that, consistent with the role of MEFs in providing a supportive self-renewal environment for mESCs, MEFs secrete high levels of MMPs as compared to mESCs (Figure 5-1a). To see whether mESCs are able to induce MMP secretion by MEFs, we grew mESCs on a transwell insert above a MEF culture and compared expression from these MEFs to that of MEFs grown alone (Figure 5-1b). We found that MEFs grown in the presence of mESC-secreted signals had higher levels of MMP expression, indicating a paracrine-mediated effect (Figure 5-1c). However, mESCs grown in the presence of MEF-secreted signals did not have higher expression levels of MMPs (Figure 5-1d), indicating that this paracrine upregulation is not universal.

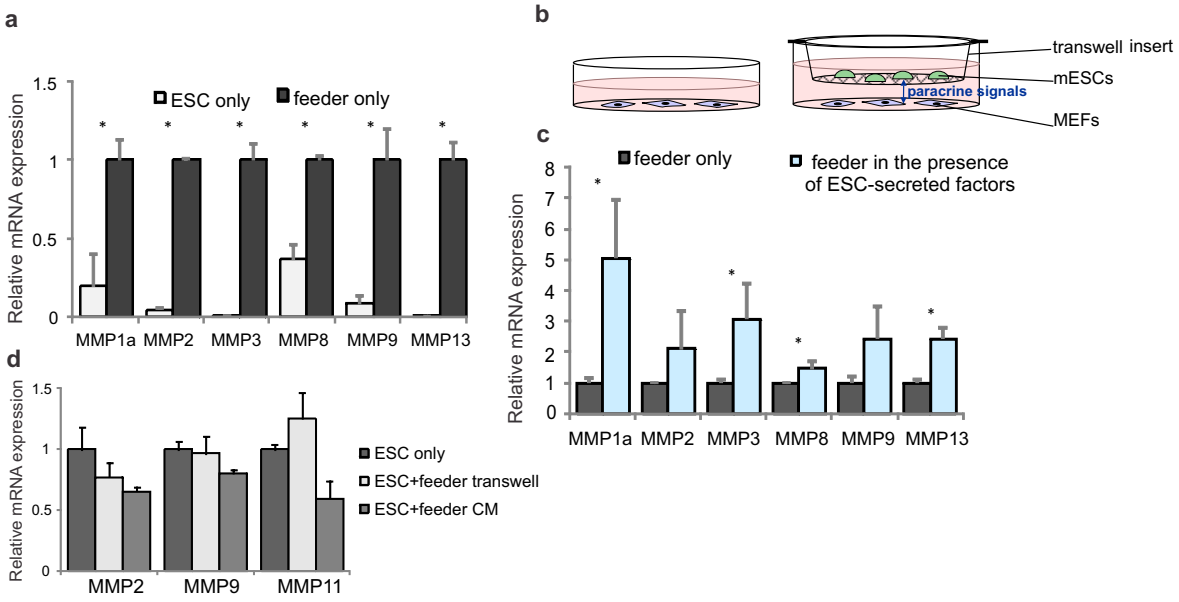

Figure 5-1 MMP secretion by feeder cells. (a) mRNA expression levels of MMPs in ESCs or feeders. (b) Diagram showing setup for generating MEF expression levels show in (c). (c) mRNA expression levels of MMPs in feeders or in feeders above which ESCs were growing on a transwell insert. (d) mRNA expression levels of selected MMPs in ESCs alone, in the presence of feeders on a transwell, or in the presence of feeder-conditioned medium (CM).

To test the functionality of the MMPs secreted by MEFs in maintaining mESC self-renewal, we added the small molecule MMP inhibitor Ro32-3555 to a culture of mESCs and MEFs, and found that it did not affect MEF survival, but did inhibit mESC growth (Figure 5-2a). This effect was quantified using two separate mESC reporter cell lines with GFP linked to histones H2A or H2B to count the relative number of ESCs versus feeders in the resulting co-cultures, and there was significantly more mESC survival in the presence of MMPs (Figure 5-2b).

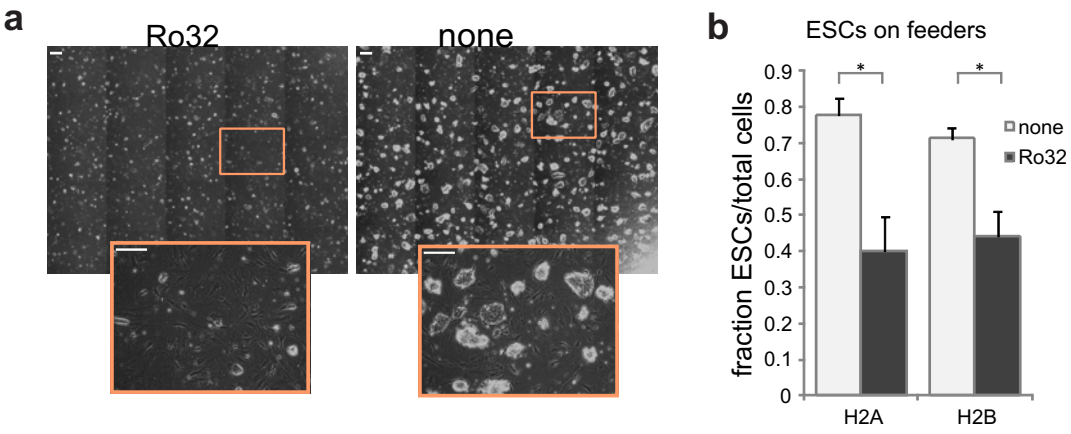

Figure 5-2 Functionality of MMPs secreted by feeders. (a) Images of ESCs growing on feeders for two days in the presence or absence of the MMP inhibitor Ro32-3555. Enlarged image shows the presence of an intact feeder layer in both cases. All scale bars = 400µm. (b) Fraction of ESCs in the total cell population after two days of growth on a

feeder layer in the presence or absence of Ro32. Data was obtained using two separate ESC cell lines with GFP fused to histone H2A or H2B. *=$p<0.05$ for pairwise comparisons.

Together, these results indicate that MEFs secrete matrix remodeling proteins, and that inhibition of such proteins affects mESC self-renewal. The effects of MEFs on maintenance of ESC self-renewal are known to act beyond secretion of LIF, and here we provide evidence for a novel role that MEFs play by acting to remodel the extracellular matrix.

5.3 MMP1/collagenase maintain ESC self-renewal

Because MMP1a is the most highly expressed metalloproteinase in the mESC-MEF paracrine system (Figure 5-1c), we added exogenous MMP1 to pure ESC cultures to assess the effect of matrix remodeling on self-renewal in the absence of feeders. Remarkably, we found that addition of MMP1 was able to maintain mESC colony morphology in serum-based media in the absence of LIF after four days of growth (Figure 5-3a), with relatively high expression of self-renewal markers Nanog and Rex1 and low expression of early differentiation markers FGF5 and Dnmt3b (Figure 5-3b). MMP1 is also known as interstitial collagenase, and acts by cleaving collagen type I, II, and III. To ensure that the maintenance of mESC self-renewal was a functional effect of MMP1 activity, we also added type I crude collagenase to mESC cultures in the absence of LIF and found a similar upregulation of self-renewal markers and downregulation of early differentiation markers (Figure 5-3b).

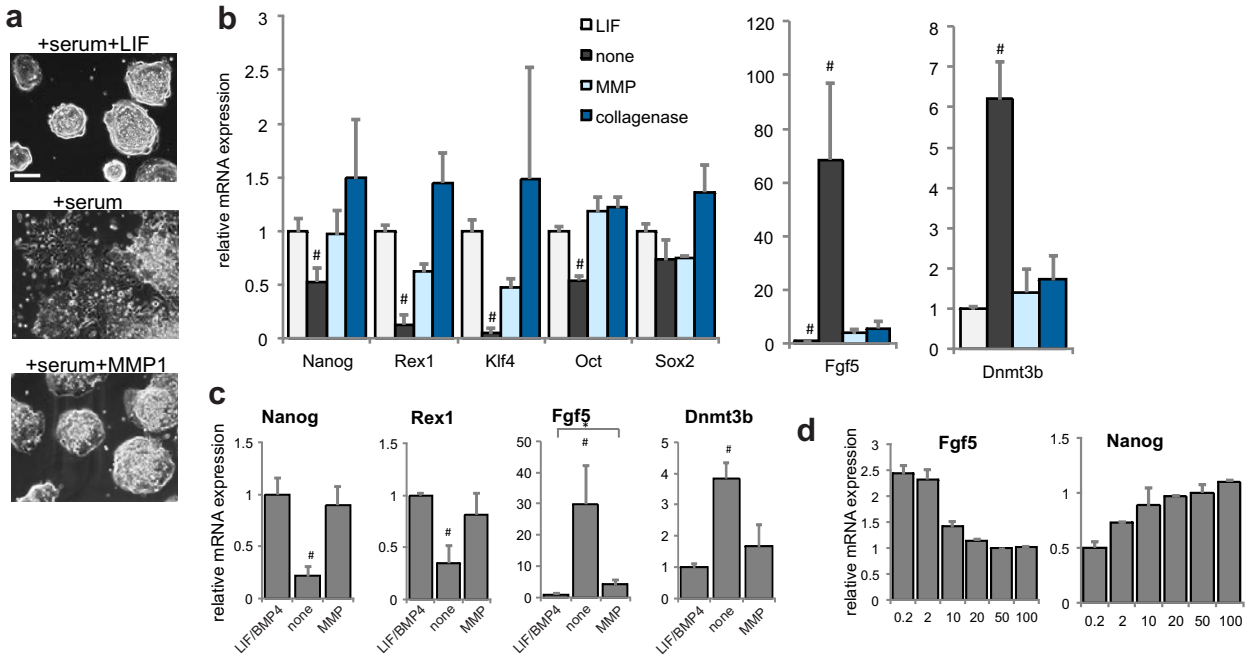

Figure 5-3 Acute effects of collagenase addition. (a) Representative images of mESCs after four days of growth in the indicated conditions. Scale bar = 200µm. (b) mRNA expression levels of self-renewal and differentiation markers after four days in the indicated conditions in the presence of serum. (c) mRNA expression levels of self-renewal and differentiation markers after four days in the indicated conditions in serum-free media. (d) mRNA expression levels of FGF5 and Nanog; x-axis numbers indicate the MMP1 concentration added in ng/ml. **=p<0.001, * =p<0.05; #=p<0.05 for all pairwise comparisons, all data represents averages of at least three independent experiments and error bars represent SD.

A similar result was observed in serum-free N2B27 media, where cells with MMP1 added for five days had a similar expression pattern to cells with added LIF and BMP4, which was distinct from the pattern seen in N2B27 media alone, where levels of self-renewal markers decrease while levels of differentiation markers increase (Figure 5-3c), an effect that was found to be dose-dependent (Figure 5-3d).

To determine whether other MMPs have the same effect, we added a gelatinase (MMP2) and a stromelysin (MMP3), and found that they were not able to halt differentiation (Figure 5-4), while addition of collagenase is able to maintain self-renewal (Figure 5-3b), indicating that cleavage of collagen is an integral event in MMP1-mediated self-renewal.

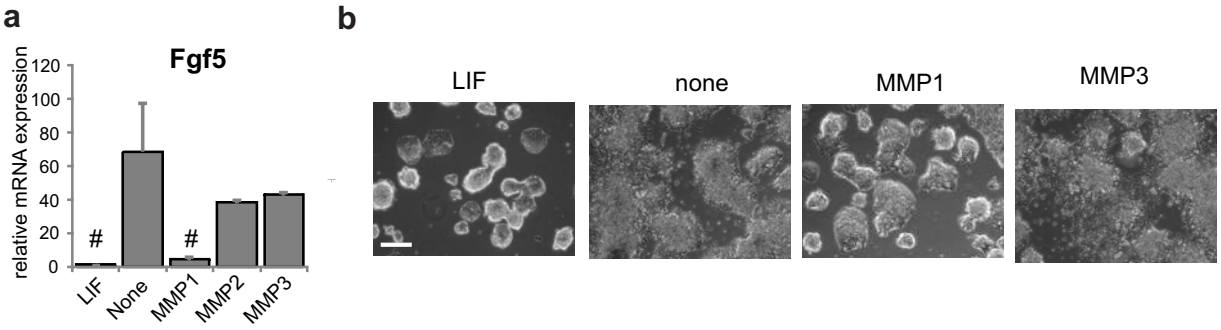

Figure 5-4 Contributions of other MMPs. (a) FGF5 mRNA expression from cells grown in the presence of other recombinant MMPs. (b) Representative images from mESCs grown for three days in the indicated conditions in the presence of serum. Scale bar = 200μm.

To look more closely at the expression pattern that emerges in the presence of MMP, we performed high-throughput RNA sequencing analysis on mESCs grown in serum-free media in the presence or absence of LIF and BMP4 with or without added MMP. We found that the correlation between the MMP and LIF/BMP4 conditions was higher than that between the MMP and no addition conditions (Figure 5-5a,b). Further analysis of genes whose expression increased significantly (greater than 9-fold) in the presence of MMP in the presence or absence of LIF/BMP4 generated a list of seven genes that went up in the presence of MMP under any conditions (Figure 5-5c). Closer analysis of the genes that were specifically up- or down-regulated in the presence of MMP compared to its absence yielded a list of selected genes of interest (Figure 5-5d). The genes that decrease in the presence of MMP include several collagen genes, which would be expected if a negative feedback loop existed whereby the presence of MMP caused a downregulation of MMP target proteins. Other genes on this list include genes implicated in differentiation and fate specification, including many genes from the FGF, Hox, and Sox families. Conversely, genes that go up in the presence of MMP include self-renewal genes such as Esrrb, genes in the Dppa family, Nanog, Pou5f1 and Zfp42, as well as other MMP family genes. Finally, performing pathway analysis on genes altered in the presence versus the absence of MMP showed several pathways affected by the presence of MMP, the most significant being genes related to stem cell pluripotency, as expected (Figure 5-5e). These data indicate that MMP addition causes broad-scale changes in mESCs that activate pathways associated with self-renewal.

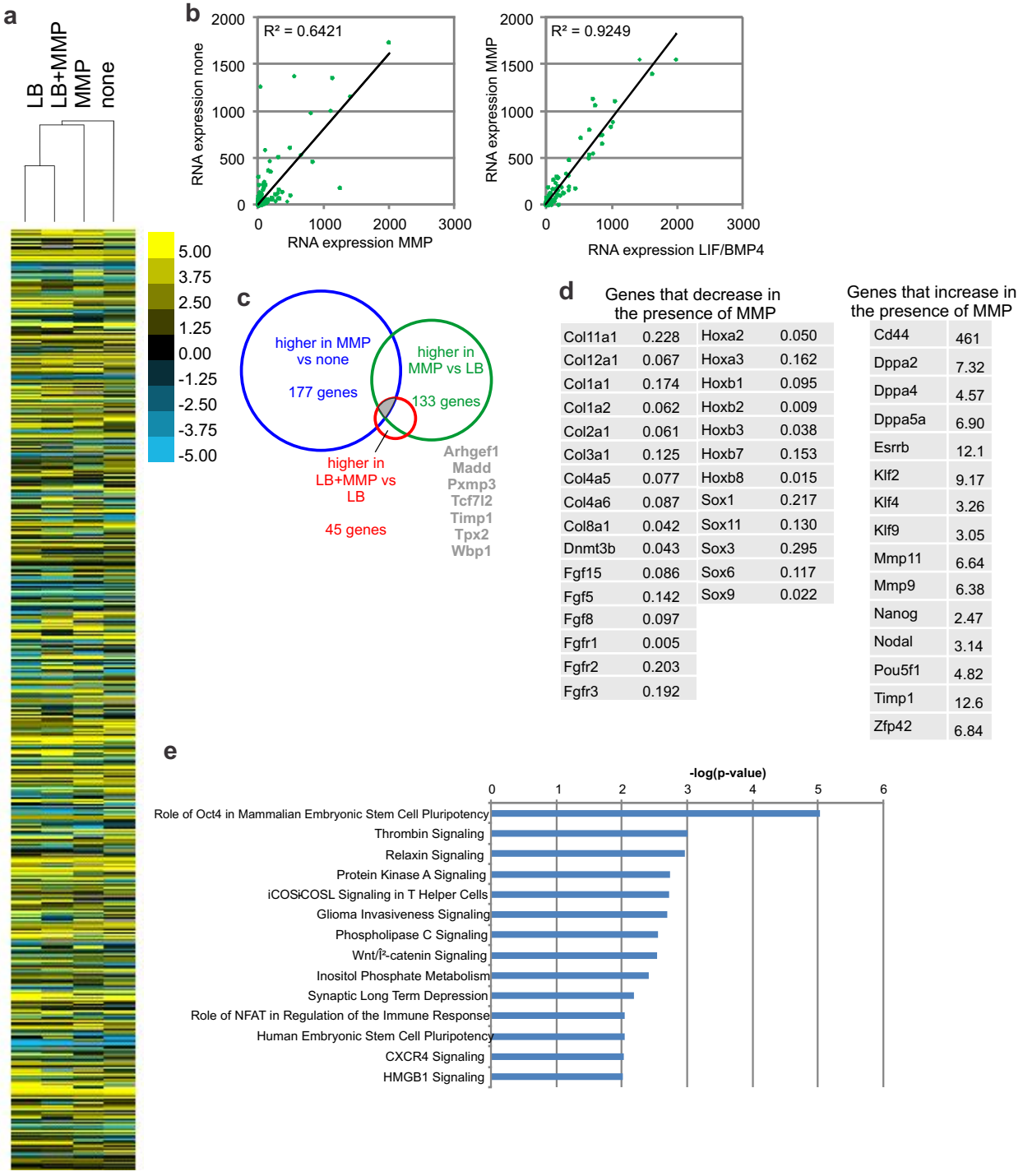

Figure 5-5 High-throughput RNA-sequencing data. (a) Heatmap comparing RNA-seq data from cultures of cells grown with LIF/BMP4 (LB), MMP1, neither, or both, clustered hierarchically using an average linkage after $\log_2$ transformation. (b) Correlation between all genes expressed in the RNA-seq dataset in the indicated conditions. (c) Representation of genes that increase in expression by more than 9-fold after addition of MMP. Grey gene names indicate the 7 genes that are present in all three datasets. (d) Tables showing representative genes that increase or decrease due to the presence of MMP in serum-free cultures. (e) Pathway analysis showing the most significantly upregulated pathways in the presence of MMP versus its absence, generated using RNA-seq data.

In an attempt to create a tool with which to study MMP1-mediated phenomena, we established a doxycycline-inducible MMP1a-GFP mESC line that successfully upregulated mRNA expression levels of MMP1a upon doxycycline stimulation in a dose-dependent manner (Figure 5-6a). However, MMP1a expression was only mildly effective at promoting mESC self-renewal (Figure 5-6b). We suspect that this is due in part to the fact that MMPs require significant post-translational modification and processing to become active, and the presence of the GFP moiety may have hindered these processes. It is also possible that mESCs do not possess the machinery required to process this protein at high efficiency. Finally, doxycycline has an inhibitory effect against MMPs, and MMP1 in particular (Smith Jr. et al., 1999), so overexpressing MMP1 in a constitutive system would likely be more effective than using this doxycyline-inducible system.

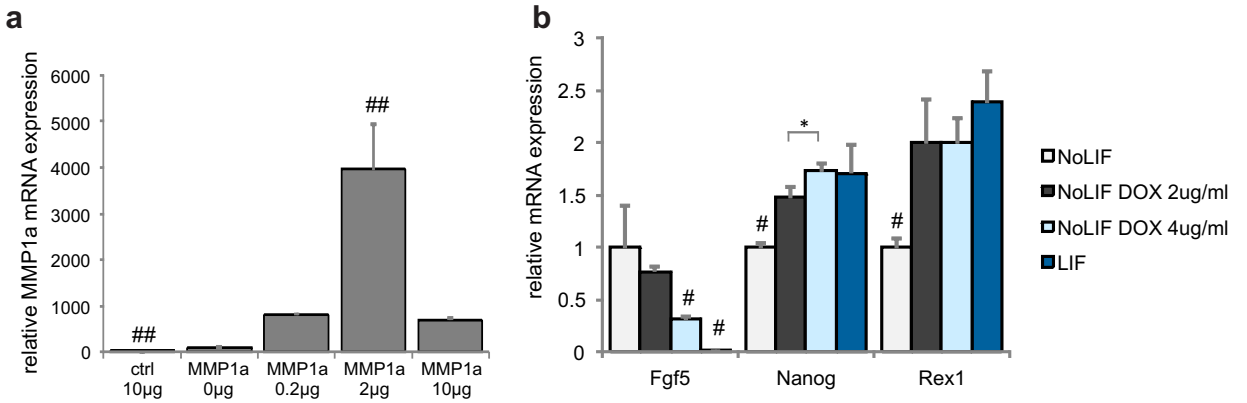

Figure 5-6 Inducible MMP1a-overexpressing cell line. (a) Relative MMP1a mRNA expression levels in control cells or the MMP1a-inducible line. Numbers represent concentration of added doxycycline in µg/ml. (b) Relative mRNA expression levels of the indicated genes in the MMP1a-inducible cell line grown for four days in the indicated conditions.

5.4 Long term LIF-independent culture of ESCs is possible in the presence of MMP1

The maintenance of self-renewal marker expression in the presence of MMP1 or collagenase over five days is interesting, but does not show that MMP is functional in terms of affecting mESC self-renewal or pluripotency. To address this, we cultured mESCs for several passages in the complete absence of LIF but presence of MMP1 in serum-containing media, and found that these cells had indistinguishable morphology (Figure 5-7a) and similar growth kinetics (Figure 5-7b) and protein levels (Figure 5-7c) to cells grown in the presence of LIF. At twenty passages, we found very similar gene expression patterns (Figure 5-7d), with the exception of a modest increase in FGF5. However, FGF5 is a very sensitive early differentiation marker that increases

up to 60-fold after 5 days in media with no LIF or MMP1 (Figure 5-3b), so a slight upregulation after 20 passages does not indicate significant differentiation.

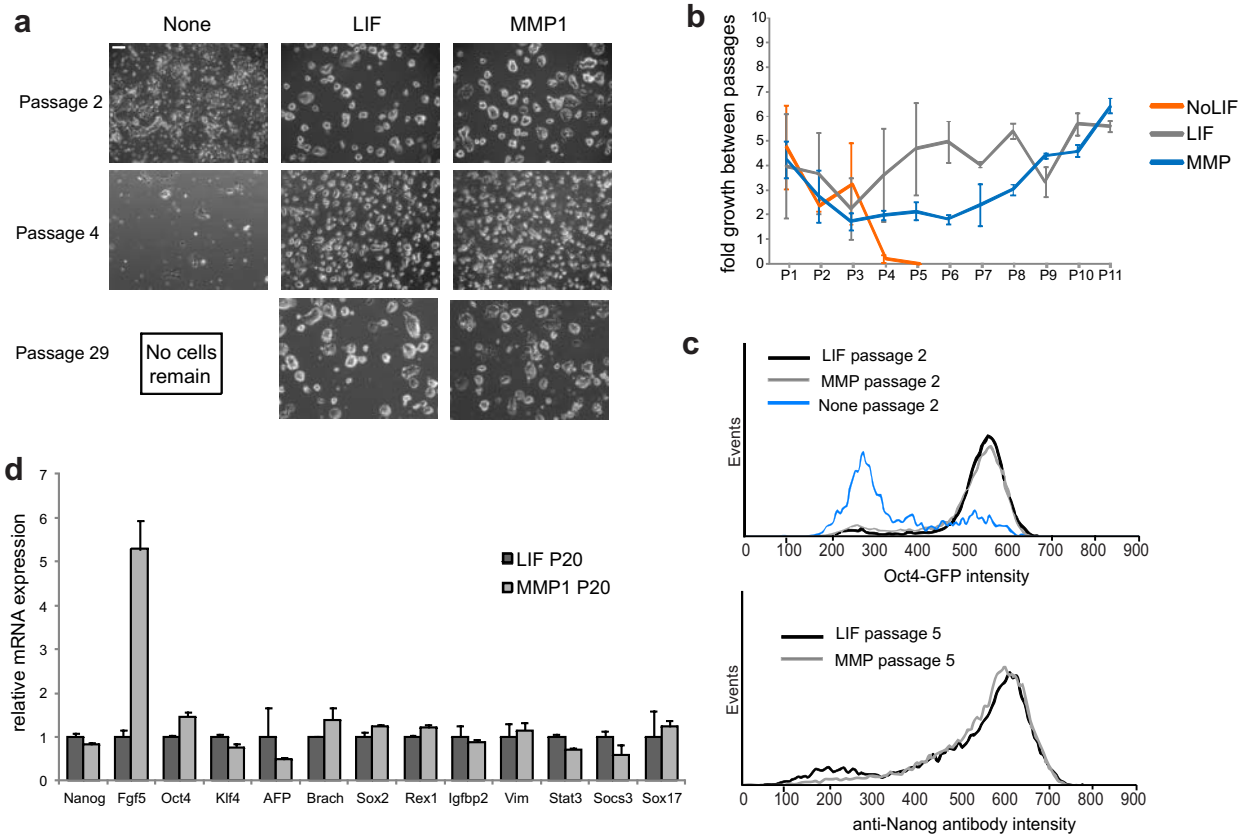

Figure 5-7 Long-term maintenance of self-renewal by MMP1 addition. (a) Representative images of cells grown under the indicated conditions for the indicated number of passages. Scale bar = 200μm (b) Fold growth of cells during each passage over the course of 11 passages in the indicated conditions. (c) Flow cytometry histograms of Oct4-GFP reporter mESCs after two passages with indicated additions (top) and of Nanog immunofluorescent staining intensity after five passages with indicated additions (bottom). (d) mRNA expression levels of a broad marker panel after 20 passages in serum-containing media with added LIF or MMP1. All error bars represent SD.

For mESCs to be truly self-renewing, they must also be able to retain their pluripotency. To assess pluripotency, we made embryoid bodies from mESCs cultured for five passages in the presence of MMP1 and absence of LIF, and found normal embryoid body formation as well as normal expression patterns of differentiation markers (Figure 5-8).

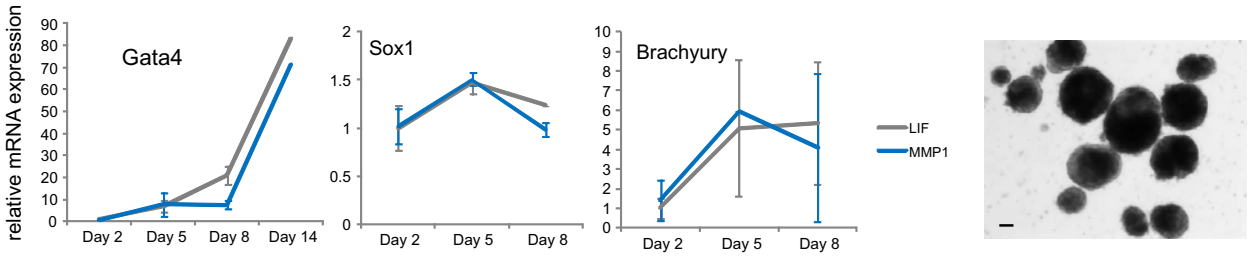

Figure 5-8 Embryoid body mRNA expression level timecourse after EB growth for the indicated number of days with no LIF or MMP1, after five passages in media supplemented with either LIF or MMP1. Image shows representative embryoid bodies from MMP1 condition on day 5. Scale bar = 400μm.

5.5 Pathways not implicated in MMP-mediated self-renewal

To identify the mechanism behind MMP-mediated mESC self-renewal, we first looked toward pathways that have been previously implicated in LIF-independent maintenance of mESC self-renewal, described in chapter 5.1. We found that MMP1 addition does not inhibit ERK signaling, as assessed by the presence of active ERK (Figure 5-9a), nor does it inhibit expression of downstream NF-κB targets (Figure 5-9b), indicating that MMP1 does not act through either of these signaling pathways. Self-renewal is also not being maintained through the action of Smads, as Smad inhibition actually enhances MMP1-mediated self-renewal (Figure 5-9c). This result also indicates that the cells have not transitioned to a more epiblast stem cell-like state, in which self-renewal is mediated through Smad2/3 instead of Stat3 (Figure 1-1).

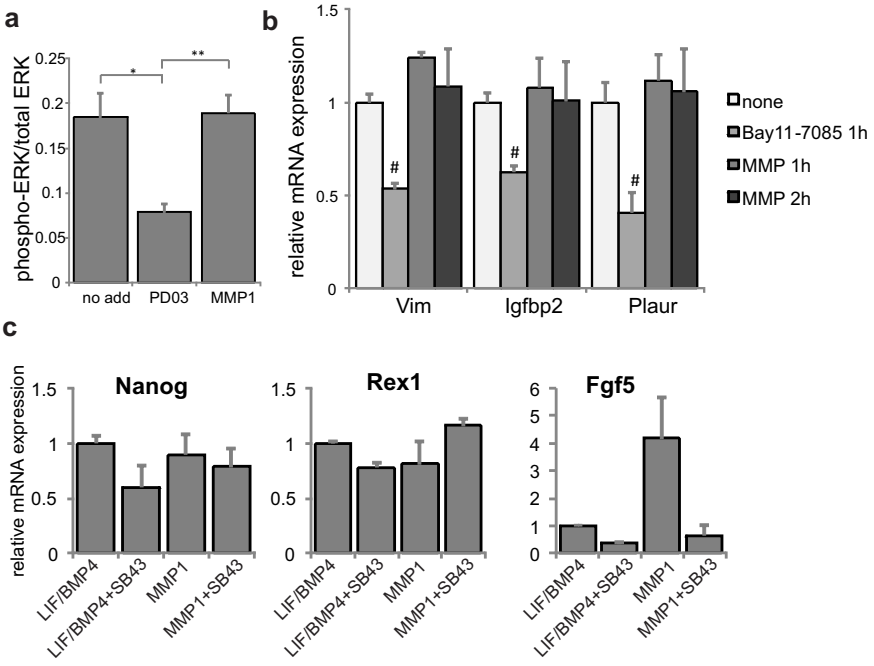

Figure 5-9 Signaling pathways not involved in MMP-mediated self-renewal. (a) Phosphorylated ERK levels with the indicated additions, analyzed by ELISA (PD03 = PD0325901, ERK inhibitor). (b) mRNA expression levels of NF-κB downstream target genes after addition of the NF-κB inhibitor Bay11-7085, or of MMP1 for the indicated number of hours. (c) mRNA expression of differentiation and self-renewal markers in the presence or absence of SB431542, an Alk4/5/7 inhibitor of Activin/Nodal signaling.

Endogenous Wnt signaling has recently been shown to be important for mESC self-renewal (ten Berge et al., 2011), and Wnt has also been shown to bind to the extracellular matrix and heparan sulphate proteoglycans (Schryver et al., 1996; Fuerer et al., 2010). It thus represented an attractive candidate for contributing to MMP1-mediated self-renewal. However, we found that inhibition of extracellular Wnt or inhibition of the export of Wnt to the extracellular domain, by the protein Dkk1 (Berendsen et al., 2011) or by the small molecule inhibitor IWP2, respectively (Figure 5-10a), caused neither a drastic reduction in levels of self-renewal markers nor a significant increase in levels of differentiation markers in the presence of MMP (Figure 5-10b). We also found that TCF-eGFP reporter mESCs (ten Berge et al., 2008) that report on Wnt pathway activation were not activated in the presence of MMP1 (Figure 5-10c,d), nor were canonical downstream Wnt targets upregulated after short-term stimulation with MMP1 (Figure 5-10e). Thus, it is unlikely that the primary signaling pathway involved in MMP-mediated self-renewal uses endogenous Wnt signals.

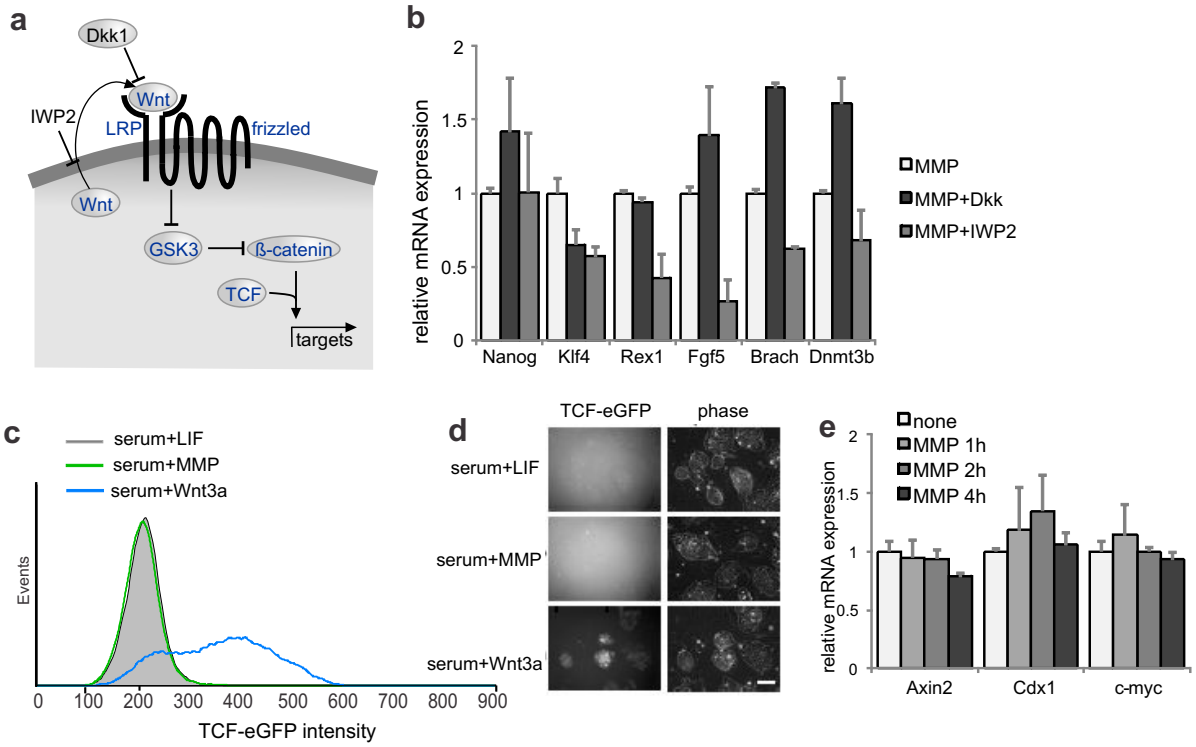

Figure 5-10 Wnt signaling is not involved in MMP-mediated self-renewal. (a) Model indicating relevant Wnt inhibitor mechanisms of action and downstream signaling activities. (b) mRNA expression levels of self-renewal and differentiation markers in the presence of Wnt pathway inhibitors. (c) Flow cytometry histogram of Wnt reporter activation after two days of the indicated additions to mESCs grown on feeders. (d) Representative fluorescent and phase images of cells analyzed in (c). Scale bar = 200µm. (e) mRNA expression levels of Wnt downstream target genes after short-term addition of MMP for the indicated number of hours.

5.6 MMP acts by releasing a gp130 ligand that signals through Stat3

The most well-studied and first-described mechanism of maintaining mESC self-renewal involves signaling of LIF (Smith et al., 1988) through the homodimeric gp130-LIFR receptor complex to activate JAK. We thus assessed whether MMP1 was causing a similar signaling pathway to be activated, perhaps by allowing an endogenous ligand to be released from the extracellular matrix to initiate the pathway. We found that gp130, a common receptor subunit for many extracellular LIF-family signaling proteins (Heinrich et al., 2003), is required for MMP1-mediated self-renewal, as its knockdown shifted transcription patterns toward those seen in a more differentiated state (Figure 5-11a). Likewise, signaling through JAK is essential for this phenotype, as its inhibition by small molecule causes rapid differentiation in the presence of either MMP1 or LIF (Figure 5-11b).

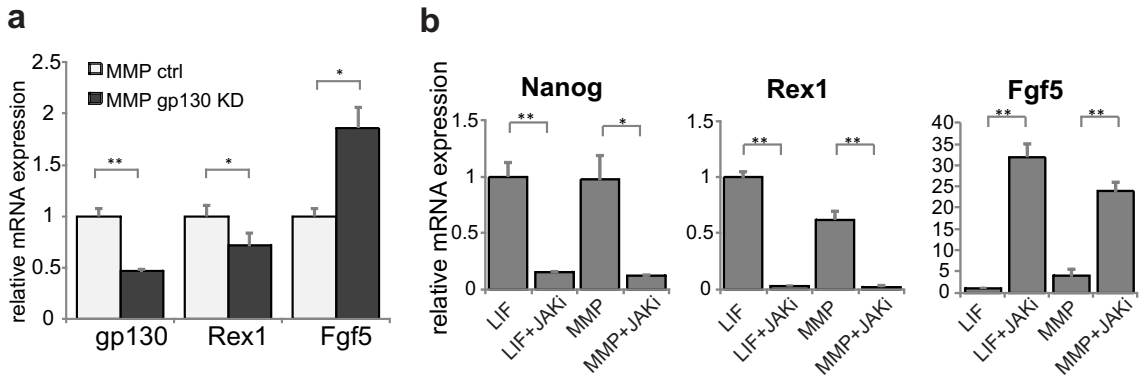

Figure 5-11 Signals directly downstream of LIF are active in MMP-mediated self-renewal. (a) mRNA expression levels after shRNA-mediated gp130 knockdown in the presence of MMP compared to levels using a control shRNA vector. (b) mRNA expression levels of self-renewal markers after addition of a JAK inhibitor.

The primary transcription factor that acts downstream of gp130 and JAK to maintain LIF-mediated self-renewal is Stat3 (Hirai et al., 2011), which activates a number of genes involved in maintenance of self-renewal (Chen et al., 2008). We thus asked whether Stat3 was active in the presence of MMP1, and found that the addition of MMP1 induced Stat3 phosphorylation (Figure 5-12a,b), whereas this was not the case with the addition of MMP3 (Figure 5-12b). The activation of Stat3 is known to rapidly cause transcriptional changes of several downstream targets, including Socs3, Klf4, and Stat3 itself (Bourillot et al., 2009). We find that, as soon as 1 hour after stimulation with either LIF or MMP1, transcription levels of all three genes increase significantly (Figure 5-12c), further indicating that Stat3 is being activated in both cases.

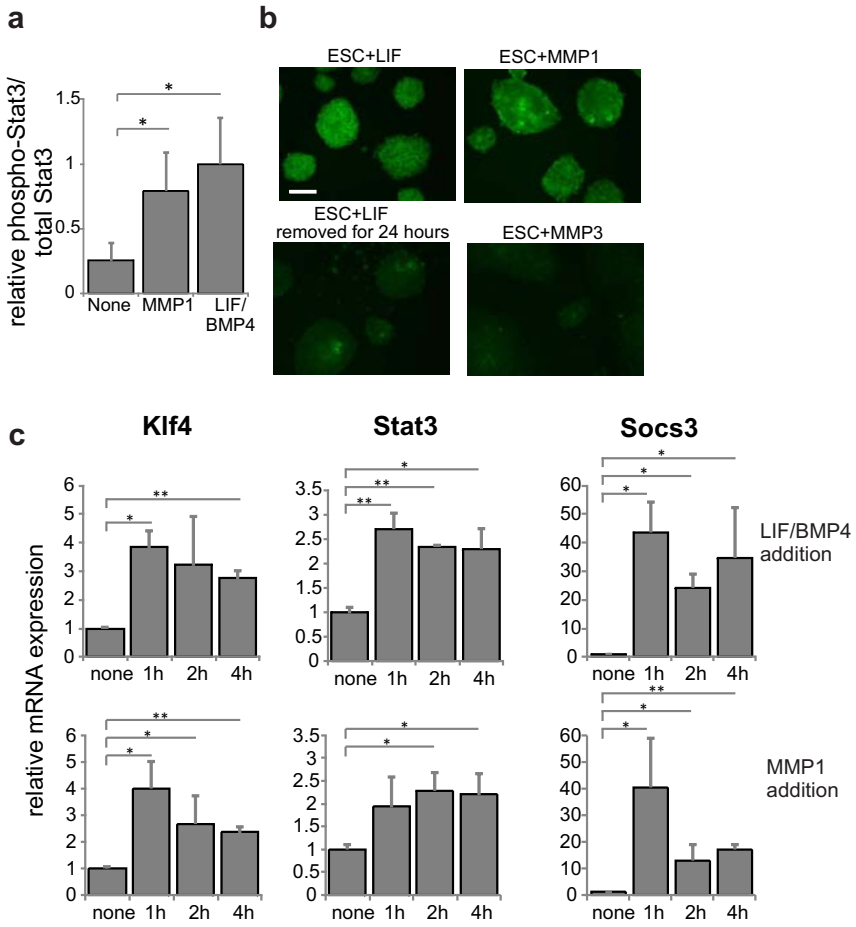

Figure 5-12 Stat3 is activated with addition of MMP. (a) Phosphorylated (T705) Stat3 levels with the indicated additions, analyzed by ELISA. (b) Immunofluorescence staining for phosphorylated (T705) Stat3 in cells grown in the indicated conditions. Scale bar = 200μm. (c) mRNA expression levels of Stat3 downstream targets after short-term addition of LIF/BMP4 or MMP1. *=$p<0.05$ for pairwise comparisons.

The functional significance of Stat3 activation in the presence of MMP was tested using shRNA knockdowns. Knockdown of Stat3 causes rapid differentiation in the presence of LIF (Figure 5-13), and we found that this also held true in the presence of MMP, as assessed via morphology (Figure 5-13a) and gene expression (Figure 5-13b). This result was confirmed using a separate hairpin to target Stat3, to ensure that the effect of the knockdown was specific to this molecule (Figure 5-13c). Thus, addition of MMP triggers a signaling cascade that acts through the gp130-JAK-Stat3 pathway, with similar sensitivity to inhibition and activation kinetics as the pathway stimulated by exogenous LIF addition.

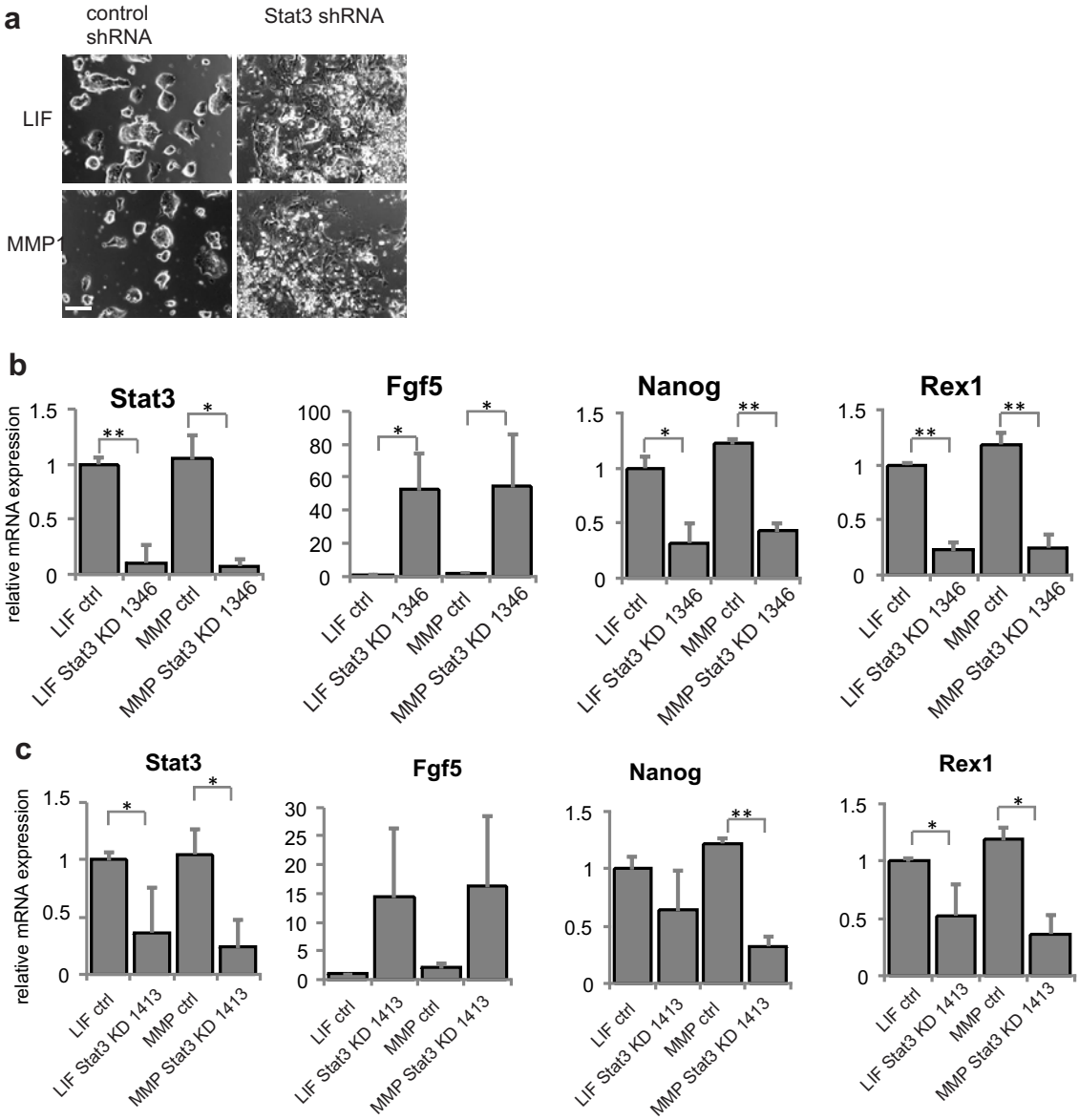

Figure 5-13 Stat3 signaling is required for MMP-mediated self-renewal. (a) Representative images of cells after two passages with added LIF or MMP1 with a control shRNA construct or Stat3 shRNA, construct 1346. Scale bar = 200µm. (b) mRNA expression levels of self-renewal and differentiation markers in cells grown in indicated conditions with a control shRNA or Stat3 shRNA, construct 1346. (c) mRNA expression levels of self-renewal and differentiation markers in cells grown in indicated conditions with a control shRNA or Stat3 shRNA, construct 1413. **=p<0.001, *=p<0.05 for pairwise comparisons.

Knowing that gp130, JAK, and Stat3 are all involved in MMP-mediated self-renewal, we went on to see whether we could identify the upstream ligand responsible for activating this signaling pathway. Because inhibition of essential components of the LIF-mediated self-renewal pathway are able to inhibit MMP1-mediated self-renewal, and the fact that LIF is known to be secreted and detected by mESCs in an autocrine manner (Davey et al., 2007; Zandstra et al., 2000), it is

possible that endogenous LIF itself is responsible for the MMP1-mediated phenotype. To check this, we added a blocking antibody to LIF and found that the antibody was able to successfully block LIF-mediated self-renewal, but interestingly, it did not affect MMP1-mediated self-renewal (Figure 5-14a). It is unlikely that MMP is acting as a direct signal due to the fact that the inhibition of its enzymatic function affects ESC self-renewal (Figure 5-2), so we looked toward other candidate ligands that could be released from the matrix by MMP. Other ligands in the LIF family that use the gp130 receptor and are both secreted by mESCs and have the appropriate receptors expressed include IL-11, oncostatin M (OSM), ciliary neurotrophic factor (CNTF), cardiotrophin-1 (CT-1), and cardiotrophin-like cytokine factor 1 (CLCF1) (Heinrich et al., 2003) (Figure 5-14b).

Referring to our RNA-sequencing data, we found a very strong upregulation of the IL11 receptor in the presence of MMP, indicating a possible feedback mechanism that could be acting to allow mESC sensitivity to IL11 for activation of the gp130-Stat3 pathway. Knocking down IL11 did not affect LIF-mediated self-renewal, as expected, but it also did not affect MMP-mediated self-renewal (Figure 5-14c). Of the other ligands mentioned above, OSM (Yoshida et al., 1994), CNTF (Conover et al., 1993), and CT-1 (Pennica et al., 1995) have been shown to be able to maintain ESC self-renewal. These three proteins were all also able to activate Stat3, as the Stat3 downstream target Socs3 showed significant upregulation after 1 hour in the presence of any of these ligands, and blocking the ligands using blocking antibodies inhibited this activity (Figure 5-14d). However, blocking the ligands in the presence of MMP did not block Stat3 transcriptional activity to baseline levels, alone or together (Figure 5-14e), indicating that the ligand activating the gp130-JAK-Stat3 pathway upon addition of MMP is not a ligand that has been previously implicated in maintaining mESC self-renewal.

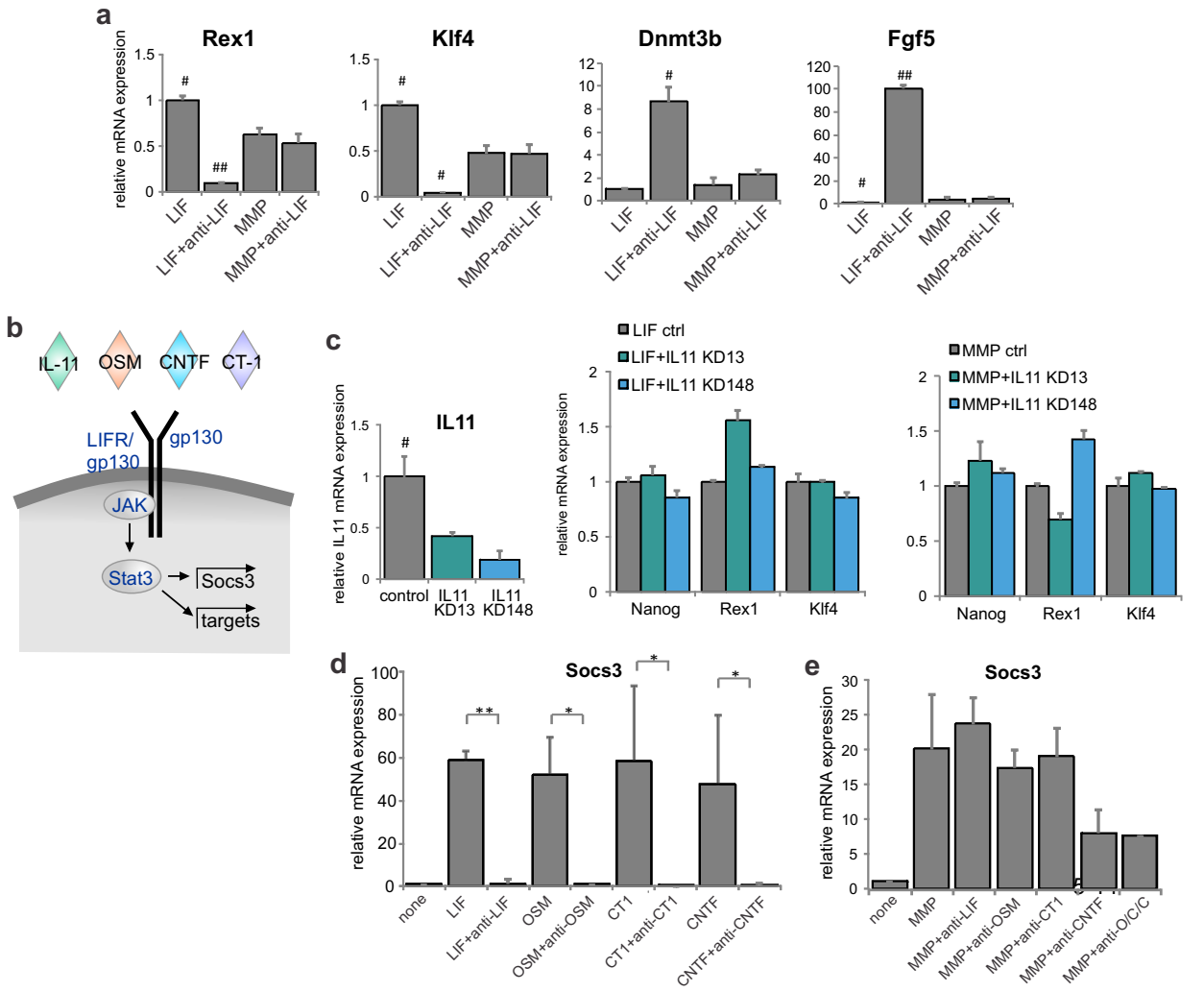

Figure 5-14 Upstream ligand is not a known gp130 ligand. (a) mRNA expression levels of self-renewal and differentiation markers after addition of a LIF-blocking antibody to cells with added LIF or added MMP1. (b) Model depicting other ligands that act through the gp130 receptor to activate JAK and Stat3 and downstream targets. (c) mRNA expression of self-renewal and differentiation markers after IL11 knockdown in the presence of LIF or MMP. (d) mRNA expression levels of a Stat3 target gene after 1 hour of indicated additions. (e) mRNA expression levels of a Stat3 target gene after 1 hour of indicated additions. O/C/C indicates blocking the three ligands OSM, CT1, and CNTF. ##=p<0.001, #=p<0.05 for pairwise comparisons.

5.7 Discussion

Regulation of cell signaling at the level of the ECM has been shown to occur in many contexts. Embryonic stem cells have been shown to maintain self-renewal on softer substrates approaching the stiffness of the cells themselves (Chowdhury et al., 2010), and substrate stiffness has been shown to affect neuronal stem cell differentiation (Keung et al., 2011) and the availability of autocrine signals (Wells and Discher, 2008). Reducing the sulfation of heparan sulfate proteoglycans in the ECM has been shown to help maintain self-renewal of mESCs by reducing

signaling from autocrine FGF4 ligands (Lanner et al., 2010). Here, we find that the ECM also harbors mESC-secreted self-renewal-promoting factors that can be released or activated to signal through the gp130-JAK-Stat3 pathway, thus providing the first evidence for an endogenously secreted factor that is produced at sufficient levels to maintain ESC self-renewal (Figure 5-15).

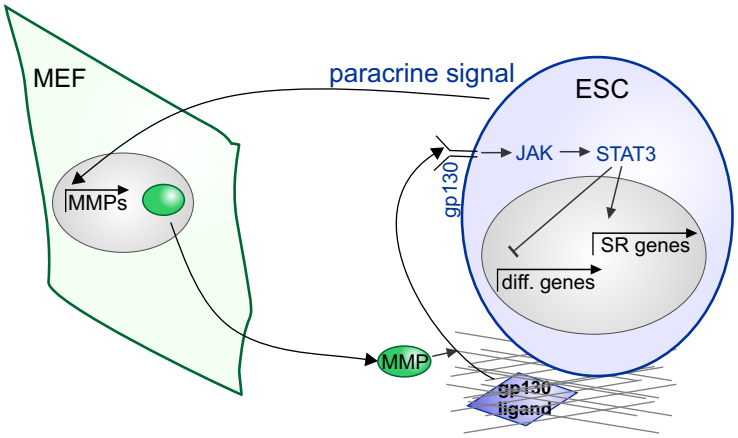

Figure 5-15 Model depicting the effect of matrix remodelling on mESCs.

The actions of ECM-based signals require dynamic regulation of the ECM, which is performed endogenously by matrix metalloproteinases, both in vitro and in vivo during development (Vu and Werb, 2000). For mESCs, though endogenous secretion levels of MMPs are low, we show that co-culture with MEFs that secrete high levels of MMPs enhances mESC self-renewal. The ability of MEFs to maintain self-renewal was partly clarified by isolation of LIF as a diffusible factor produced by stromal cells (Smith et al., 1988), but the fact that many mESC lines self-renew better with feeders than with just serum+LIF suggests that MEFs have other roles besides secreting LIF. Here we find a novel role for MEFs in their secretion of MMPs, a mechanism that could be important in other co-culture systems to release cell-type-specific secreted factors from the extracellular matrix.

The identification of a stem-cell-secreted factor produced at levels sufficient to maintain ESC self-renewal indicates the importance of autocrine signals present in any cell's extracellular matrix. Autocrine ligands have been identified that contribute to mESC self-renewal, including LIF (Zandstra et al., 2000) and Wnt3a (ten Berge et al., 2008). However, autocrine levels of LIF are not high enough to maintain self-renewal, and autocrine Wnt, while necessary for maintenance of self-renewal, is not sufficient to maintain self-renewal in the absence of LIF. We

find that blocking CNTF appears to decrease Stat3 transcriptional activity, though it does not decrease Stat3 activity to baseline levels. This indicates that CNTF may be acting in part to cause the signaling through Stat3 required to maintain self-renewal in the presence of MMP1, but it does not account for full activation of the signal. It is possible that matrix-based ligands are acting through other mechanisms such as by activation of integrins, as integrin activation has been shown to activate Stat3 in other specific systems (Guo et al., 2006a). The secretion and sequestering of functional autocrine-acting ligands likely extends beyond those that act on ESCs, and the specific mechanisms by which they can be removed and activated may vary in different systems. This study shows that the extracellular matrix is an often-overlooked but major source of signaling molecules, and opens up the possibility for further studies on the diverse effects of extracellular matrix remodeling on maintaining and directing stem cell fate.

5.8 Methods

For information regarding cell lines, culture additions, and qPCR protocols, refer to Appendix 1. For information regarding flow cytometry or embryoid body formation, refer to the methods in chapter 2.8.

Cell culture

Mouse embryonic fibroblasts were cultured in DMEM supplemented with 3% fetal bovine serum (Hyclone), 4 mM L-glutamine and 1X penicillin-streptomycin. Transwell assays were performed in 6-well plates using 3.0 μm polyester membrane 24 mm inserts (Corning).

RNA-sequencing

mRNA libraries were prepared from total RNA isolated with Trizol (Invitrogen) and purified with Dynabeads mRNA purification kit (Invitrogen). RNA was fragmented using Ambion RNA Fragmentation Reagents (Invitrogen), first strand cDNA was prepared using SuperScript III Reverse Transcriptase (Invitrogen), and second strand cDNA was prepared using Second Strand Buffer (Invitrogen) and DNA Polymerase I (New England Biolabs). Whole transcriptome mRNA sequencing of barcoded samples was performed on an Illumina GAIIx and data was processed according to the Illumina pipeline – Firecrest as the image analysis module, Bustard as the base calling module, and Bowtie for sequence alignment. Reads were mapped to the mouse

reference genome and RPKM values were generated with help from the MIT BioMicro core facility and Fugen Li. Heat map was generated using the freely downloadable software Java Treeview and Cluster 3.0.

Inducible cell line construction

The doxycycline-inducible MMP1a-GFP cell line was made by cloning a purchased MMP1a cDNA (Source BioScience) into the pLV-TetO plasmid obtained from Laurie Boyer's lab. After confirming the presence of the desired insert by sequencing, the MMP1a-containing plasmid was transfected into 293 cells along with gag-pol (Delta8.2) and env (VSV G) lentiviral transfection plasmids using Fugene HD. The resulting filtered 293-conditioned media was used to infect mESCs 48 h later and cells were induced with doxycyline so GFP-positive cells could be sorted.

Short-term target inductions

To test for the rapid induction of transcriptional targets, cells were plated at approximately 5 x 10^4 cells/ml in a 12-well plate in LIF-containing media. The next day, media was replaced with no-LIF media. 24 hours later, media containing the desired activators and/or inhibitors was prepared and added for 1-4 hours. Cells were immediately washed with PBS and harvested by trypsin, then analyzed for target gene expression using qRT-PCR.

ELISA

Enzyme-linked immunosorbent assay was performed on media collected from wells in which cells were grown for 48 hours. Results were normalized by the average cell density (using an exponential growth model and the initial/final cell numbers) and duration to determine a secretion in grams/cell/hr under both conditions. Media was spun down using an Amicon 3 kD cutoff filter spin column. Phospho-ERK ELISA was purchased from R and D Systems, and assay was performed according to manufacturer's instructions. Phospho-Stat3 ELISA was purchased from RayBioTech, and assay was performed according to manufacturer's instructions.

Immunofluorescence

For activated Stat3, cells were incubated overnight with primary phospo-Stat3 antibody (Cell Signaling Technology) at 1:100 and secondary (anti-rabbit AF488, Invitrogen) was added for two hours at 2 μg/ml. Cells were counterstained with 1:100000 Hoechst (Sigma).

shRNA knockdown experiments

For shRNA knockdowns, candidate shRNA hairpins were cloned into a packaging vector for transfection into Phoenix cells and subsequent infection into mESCs. shRNA-containing cells were GFP sorted and immediately plated for knockdown verification or experimental use. shRNA constructs used are listed below.

Gene	Starting nt	shRNA sequence
Stat3	1346	TGCTGTTGACAGTGAGCGACTGAGTTGAATTATCAGCTTATAGTGAAGCCAC AGATGTATAAGCTGATAATTCAACTCAGGTGCCTACTGCCTCGGA
Stat3	1413	TGCTGTTGACAGTGAGCGCCAGAGGGTCTCGGAAATTTAATAGTGAAGCCA CAGATGTATTAAATTTCCGAGACCCTCTGATGCCTACTGCCTCGGA
gp130	909	TGCTGTTGACAGTGAGCGACACCATATAATTTATCAGTGATAGTGAAGCCAC AGATGTATCACTGATAAATTATATGGTGGTGCCTACTGCCTCGGA
IL11	1363	TGCTGTTGACAGTGAGCGCGAGGATTTAAATACATATCTATAGTGAAGCCA CAGATGTATAGATATGTATTTAAATCCTCTTGCCTACTGCCTCGGA
IL11	1481	TGCTGTTGACAGTGAGCGACAGAGCATCACCTTATAACTATAGTGAAGCCA CAGATGTATAGTTATAAGGTGATGCTCTGGTGCCTACTGCCTCGGA

Chapter 6 Manipulating ESC organization and signaling

6.1 Introduction

So far, we have described and implemented methods for controlling different types of mESC endogenous signaling. In this chapter, we describe a new method for probing how the accessibility of extracellular signals affects mESC phenotype, and implement an existing method to dissect the relationship between morphology and function in heterogeneous mESC cultures.

One prevalent method by which to manipulate and assess cell-cell signaling involves patterning cells in specific locations and monitoring their interactions. Many of these approaches involve creating regions of proteins on a surface to which cells can be added. For example, microscale cell patterns can be created by using substrates that include chemically modified regions to which cells can attach (Chen et al., 1997; Kane et al., 1999), or by physically constraining cell location (Folch et al., 2000; Flaim et al., 2005). Signaling proteins can also be patterned so that the differing effects of tethered versus soluble ligands can be determined (Fan et al., 2007). However, there are limitations to patterning cells, especially cells that grow in colonies or clumps, such as ESCs. If mESCs are patterned as single cells, significant time is required for colony formation, which may compromise the surface functionalization or cellular properties. Instead, patterning mESCs as large clumps may cause them to form abnormally structured colonies that do not accurately mimic the colonies formed in normal culture. Therefore, a method by which patterns can be formed around already-established ESC colonies growing in normal culture could aid in studies of intracolony signal propagation and local signal presentation. To this end, we use polyethylene glycol diacrylate (PEGDA) hydrogels onto which ligands can be tethered.

Polyethylene glycol diacrylate (PEGDA) is a biocompatible polymer that can form hydrogels in the presence of photoinitiator and UV light (Nguyen and West, 2002). Photopolymerizable PEG hydrogels have been used for a variety of tissue engineering applications due to their biocompatibility and mild polymerization conditions, including their use in drug delivery systems (Peppas et al., 1999), in cell encapsulation for transplantation (Cruise et al., 1999; Pathak et al., 1992), and as a scaffold for cartilage regeneration (Elisseeff et al., 1999). For these

and other purposes, it is often desirable to incorporate growth factors within PEG hydrogels for signaling or slow release, the most direct incorporation method being direct loading into the hydrogel during formation (Zhu, 2010). However, this approach gives a rapid burst release of protein, so other means of growth factor incorporation has included protein adsorption (Holland et al., 2005) or covalent tethering of acrylated growth factors (DeLong et al., 2005).

Because PEGDA remains in liquid form until activated by UV, it can be used to form hydrogels in specific patterns and locations. Here, we show a novel method for the incorporation of proteins in and on polymerized PEGDA hydrogels to provide signals to adherent cells in specific locations. Immobilization of ligands onto substrates can be functionally relevant from a signaling point of view, as many important cell signaling proteins are presented from within the extracellular matrix, both in vivo and in vitro. Immobilized ligands may act differently than soluble ligands, as they can have local concentration differences and gradients can be established (Saha and Schaffer, 2006), and activation of their downstream signaling pathways may be sustained due to the fact that ligands are not endocytosed by the cell (Kuhl and Griffith-Cima, 1996). For example, it was shown that LIF bound to thin films supported mESC pluripotency for two weeks in the absence of soluble LIF (Alberti et al., 2008), and LIF has been shown to exist naturally in both matrix-bound and soluble forms, with potentially distinct biological functions (Robertson et al., 1993). We can use the PEGDA hydrogel patterning system to specifically pattern signals around already-formed colonies with the ability to pattern two or more signals in any conformation around growing cells. This will allow for studies involving how signal presentation affects stem cell properties and how signals act together or in opposition in established mESC colonies.

PEGDA hydrogels have also been adapted for use in polymerization-activated cell sorting, a technique developed in our lab for selective photo-encapsulation of undesired cells growing in a culture dish, allowing for recovery of desired cells at high purity. Because this method is applied to adherent cells growing in a dish, it allows for selection and recovery of cells based on morphological characteristics or subcellular localization in a way that alternative sorting methods cannot achieve. Here, we have applied this method to sort mESCs based on morphology.

As described in chapter 2.4, mESCs exist as a heterogeneous population with an apparent correlation between morphology and the primed versus naïve state. In addition to population-wide heterogeneity, expression within a colony has been shown to be heterogeneous for the pluripotency markers pSTAT3, Nanog, and Oct4, with a radial organization caused by autocrine signaling between cells (Davey and Zandstra, 2006). While intracolony heterogeneity can be measured by immunofluorescence, it is often obvious morphologically. For example, in hESC cultures, it was found that cells at the outer edge of colonies are morphologically and biologically distinct from central cells in the absence of feeders, adopting a more feeder-like morphology, a phenomenon attributed to differences in local concentrations of intracolony paracrine signals (Moogk et al., 2010). Though such intracolony spatial heterogeneity is also seen in mESC populations, it is not known whether the cells on the outside of a colony are more differentiated than cells in the center, whether both types of cells can interconvert, or whether both types of cells are necessary to maintain a stable ESC population. Because most cellular separation methods rely on detaching cells from the substrate before assaying them, it has not previously been possible to separate mESCs based on morphology alone.

Our method of using hydrogels for sorting cells involves use of a transparency mask to shield cells meant to be collected, while other cells in the culture are exposed to UV light in the presence of PEGDA prepolymer such that they are selectively encapsulated and not recovered. A similar method also developed in our lab, termed radical-activated cell-sorting, uses UV light to create locally active reactive oxygen species that selectively kill unwanted cells growing in a dish such that desired cells can be monitored and collected. These techniques were both applied to mESC populations in an attempt to separate cells based on morphological phenotype. Such an approach could allow us to separate naïve and primed populations and assess their ability to interconvert, and it could also allow for separation of different sections of a colony to probe functional differences in cells at the center versus the outside of a single colony.

6.2 Patterning signals around existing ESC colonies

We implemented hydrogels made from photopolymerizable PEGDA as a method for patterning externally accessible proteins in specific locations around growing cell colonies. First, we showed that we could include proteins in the PEGDA prepolymer that polymerized into the

hydrogel, and that we could tether proteins to the hydrogen for external accessibility. To do this, we incorporated streptavidin linked to acrylamide within the prepolymer and showed that it was stable within the polymerized hydrogel for several days, as there was no functionally significant leaching from the hydrogel for three days and the small increase in streptavidin concentration seen was probably due to evaporation of the surrounding liquid (Figure 6-1a). We then biotinylated fluorescently labeled BSA and showed that it bound specifically to the structures in which streptavidin was incorporated (Figure 6-1b).

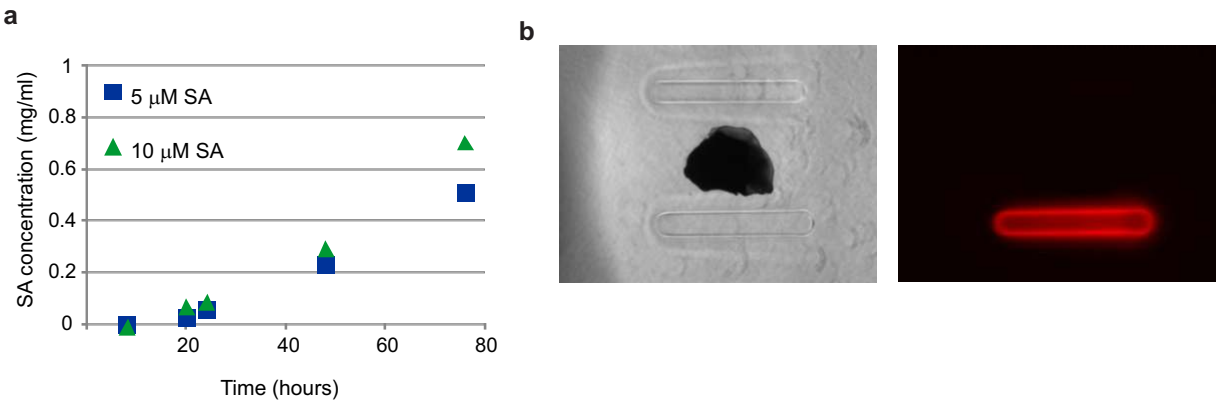

Figure 6-1 Selective tethering of proteins to hydrogels. (a) The change in streptavidin (SA) concentration in PBS in one well of a 96-well plate with several SA-containing PEGDA structures. (b) Phase (left) and fluorescence (right) images of PEGDA structures. The bottom structure contains SA while the top does not. Both structures were incubated with biotin-linked BSA conjugated with a texas red fluorophore. The central spot is for alignment.

Before implementation with cells, we optimized concentrations and binding times in an effort to use the least amount of reagents to achieve a reasonable signal. We used biotinylated BSA linked to a texas red fluorophore and measured fluorescent intensity to quantify binding of protein to the outside of the hydrogels. We found that little or no binding occurred at concentrations below 0.5 μM BSA (Figure 6-2a), while concentrations higher than 0.5 μM did not appreciably increase levels of bound protein (Figure 6-2b). Conversely, higher concentrations of streptavidin did increase bound protein levels (Figure 6-2b,c), and increasing incubation time of biotinylated BSA also increased signal at high concentrations of streptavidin (Figure 6-2c). Based on this data, we chose a streptavidin concentration of 10 μM, a biotinylated molecule concentration of 0.5 μM, and an incubation time of 10 minutes.

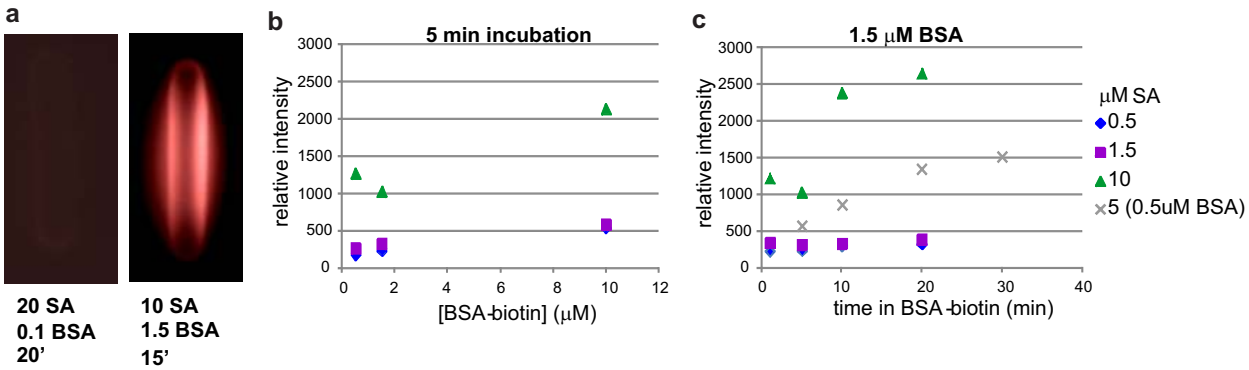

Figure 6-2 Optimization of concentrations and times for hydrogel preparation. (a) PEGDA structures with the indicated concentration of SA and BSA (in μM), with BSA incubated for the indicated number of minutes. (b) Fluorescent intensity of structures with biotin-linked BSA-texas red added for 5 minutes at the given concentrations with varying SA concentrations polymerized within the hydrogels. (c) Fluorescent intensity of structures with 1.5 μM biotin-linked BSA-texas red incubated for varying times with different SA concentrations.

Once we were able to consistently and stably pattern proteins on polystyrene, we generated a mask to polymerize structures around one half of an average-sized mESC colony. We then patterned LIF around established colonies to analyze how far this signal was able to propagate through the colony (Figure 6-3a). This procedure is very scalable, as polymerization only takes seconds, and we were able to pattern more than 100 structures in a 35 mm dish for a single experiment (Figure 6-3b). Hydrogels without streptavidin incorporated provided a control within the same dish, and we could pattern left-facing structures with streptavidin and right-facing structures without streptavidin for easy identification and quantification (Figure 6-3b).

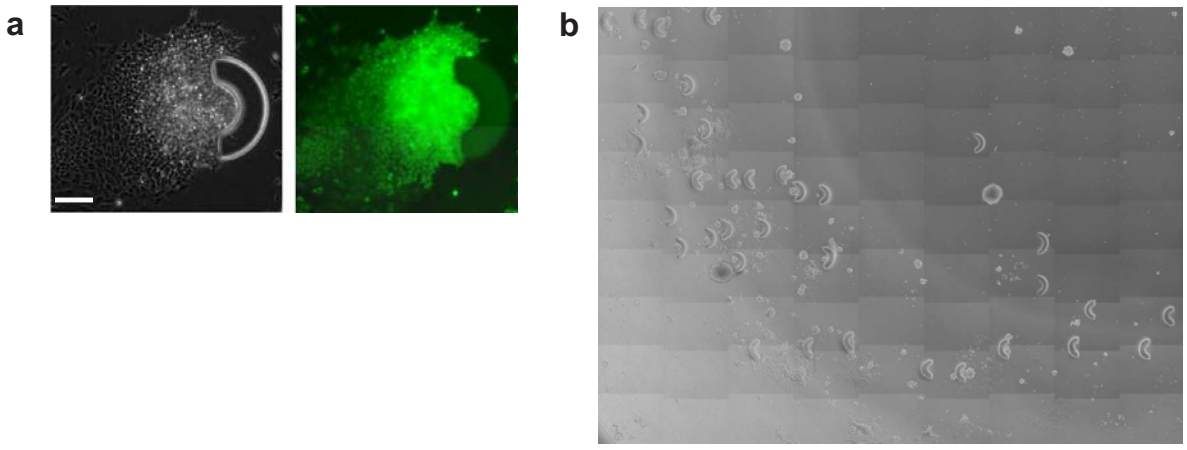

Figure 6-3 PEGDA structures around mESC colonies. (a) Image of a structure with tethered LIF at two days after structure formation and four days after mESC plating. mESCs are fixed and stained with an Oct4 antibody. Scale bar = 100 μm. (b) Composite image of the bottom left corner of a culture dish with multiple PEGDA structures formed around existing mESC colonies.

While this approach allowed for observation of striking morphological differences within the colony, we found quantification to be simpler when LIF was attached at a single point on the edge of a colony. For quantification, the colony was fixed and stained for expression of the pluripotency marker Oct4 after 2 days of exposure to the LIF-tethered PEGDA post, and the Oct4-GFP intensity was quantified after masking the cell image using information from the DAPI channel, which stains cell nuclei (Figure 6-4a). We found that cells growing near posts to which LIF was tethered generally had higher levels of Oct4 expression (Figure 6-4b), and this method could be adapted to quantify the relationship between distance from the post and Oct4 expression level.

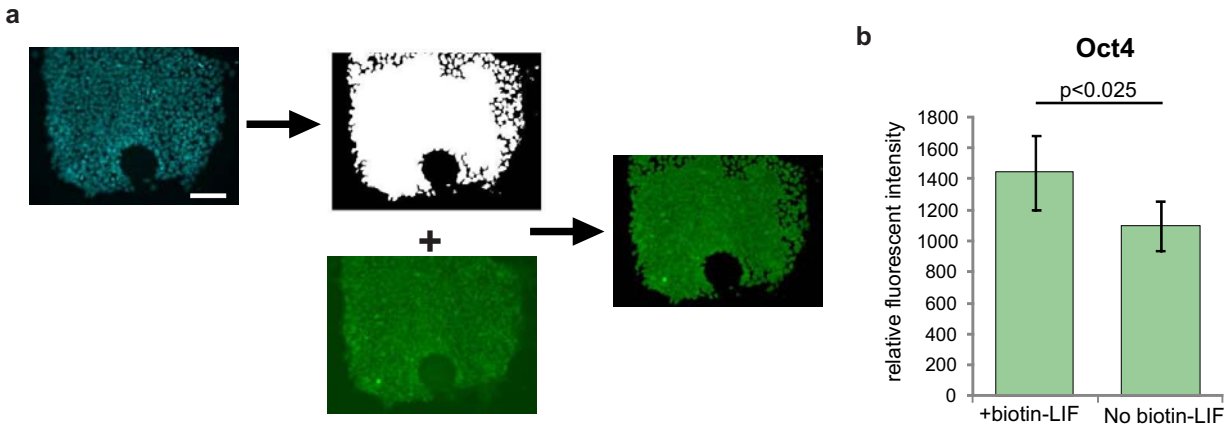

Figure 6-4 Quantification of Oct4 fluorescence in the presence or absence of tethered LIF. (a) Scheme for using DAPI images to mask the colony area around a PEGDA post for quantification. Scale bar = 100 μm. (b) Quantification results from cells near PEGDA structures that do or do not contain streptavidin after 3 days of growth after addition of biotinylated LIF. Data for each condition represent averages of six independent experiments.

Though this result showed that we could successfully pattern LIF adjacent to a growing ESC colony, we did not pursue this research any further because there were no clear questions to be addressed using this technology at the time of its development and optimization. However, now that we have delineated some roles of matrix-based versus soluble signals and we know more about how microenvironmental cues affect mESC fate, this technology could be applied in the future to compare the effects of soluble and matrix-bound cues, with more specific applications discussed in chapter 7.2.

6.3 Morphological assessment of cell fate

The most straightforward way to quickly assess the maintenance of self-renewal is by monitoring cell morphology. However, morphology is notoriously difficult to quantify and is instead used almost exclusively as a qualitative assessment. As explained in chapter 2.4, several days of culture generates heterogeneous mESC populations, but it is unclear the extent to which heterogeneous cultures contain multiple populations that are reversible. For example, mESC colonies tend to have a densely packed, three-dimensional center, whereas cells at the edges of the colonies are more spread out and single cells can be identified, more reminiscent of differentiated cells. However, it is not known whether the edge cells express lower levels of self-renewal markers or whether they can re-form healthy ESC colonies upon passage. To answer such questions, a method must be used in which cells can be sorted while alive and adherent on a culture dish, as removing them from the dish would disrupt their substrate attachments and therefore their morphology. For this, we applied two related techniques, radical-activated and polymerization-activated cell sorting, diagrammed in Figure 6-5.

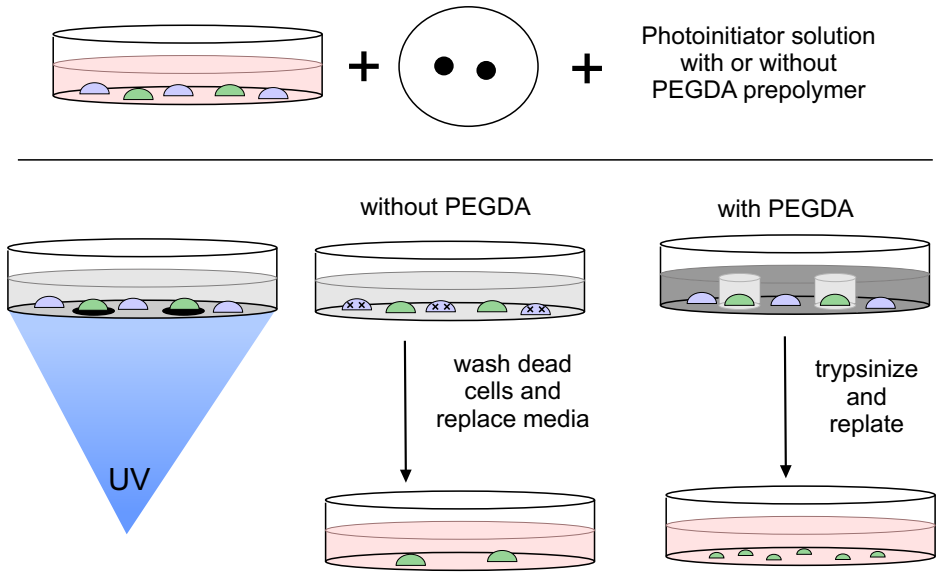

Figure 6-5 Techniques for sorting adherent cells by morphology. A mask is applied to cells growing in a dish to block desired cells (shown as green), and photointiator solution is added without PEGDA prepolymer for radical-activated cell sorting and with prepolymer for polymerization-activated cell sorting. UV is then applied to the entire dish. In radical-activated cell sorting, cells exposed to UV light die and can be removed from the dish by washing (bottom panel, center). In polymerization-activated cell sorting, the UV-exposed cells are bound in the hydrogel so desired cells can be removed by trypsinization and replated (bottom panel, right side).

As a method of sorting mESCs based on morphology, we first applied radical-activated cell sorting to populations of mESCs and showed that a mask could be applied to block targeted colonies from UV exposure such that they could survive, while non-targeted colonies died and lost fluorescence (Figure 6-6a). These dead cells could be washed away and the remaining cells would consist of the targeted population (Figure 6-6b).

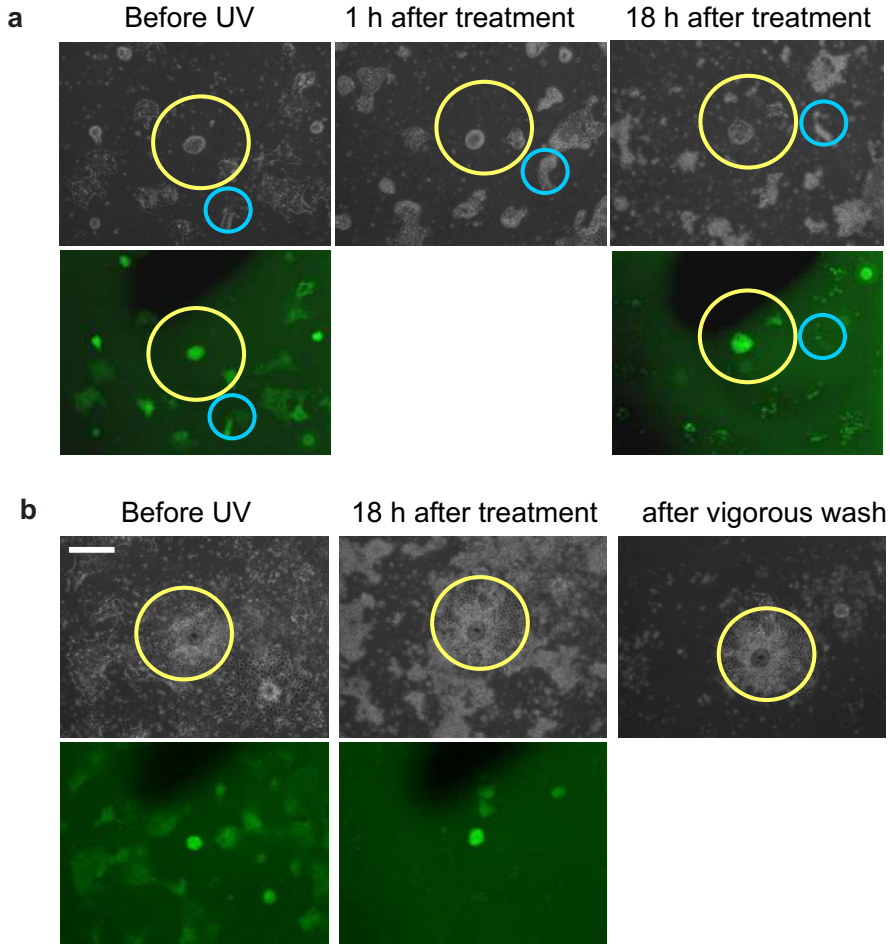

Figure 6-6 Radical-activated sorting of mESCs. (a) Phase and fluorescent images of Sox2-GFP reporter mESCs before and after masking center colony (yellow circle) and exposing the rest of the dish to UV. Blue circles show the same point in all three images, note fluorescence before treatment and removal of cells and lack of fluorescence after treatment. (b) Another example of sorting mESCs by masking the center cells (yellow circle) and exposing the rest to UV. The day following treatment, all cells that had been exposed to UV can be removed by washing the dish, leaving the desired cells. Scale bars = 100 μm.

While this approach allowed us to select and monitor specific populations, we wanted to be able to quickly remove and recover different subpopulations within a dish for downstream assays and for replating and monitoring growth or self-renewal of the separate subpopulations. To automate the sorting process, we implemented MATLAB scripts that were able to identify self-renewing

colonies within a dish (Figure 6-7a), which we could use to selectively mask these colonies or to create an inverse mask and selectively mask the non-self-renewing cells. With Eloise Shaw, a high-school student intern in the lab, polymerization-activated cell sorting was performed such that entire colonies that looked more or less self-renewing could be successfully isolated from identical cultures and compared using qRT-PCR (Figure 6-7b,c). We were able to quantify a difference in differentiation marker expression in colonies that appeared to be more self-renewing morphologically (Figure 6-7c), but further work will be required to functionally define these sorted populations of cells or to sort different populations within single colonies.

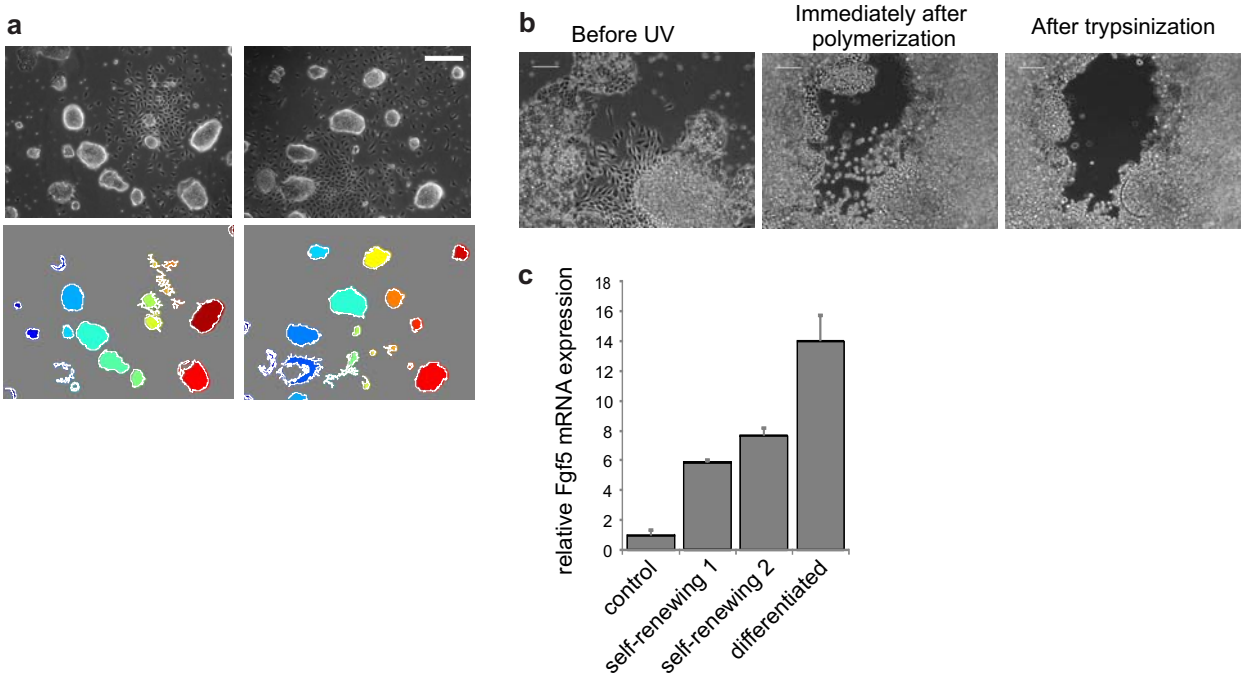

Figure 6-7 Polymerization-activated sorting of mESCs. (a) Images of cells growing in a dish and the associated mask produced using a MATLAB script that identifies self-renewing colonies. (b) Images of differentiated-looking mESCs targeted for sorting, before and after hydrogel polymerization and after trypsinizing and removing the desired cells. The center of the image was targeted for recovery. Scale bar = 100 µm. (c) Relative FGF5 mRNA expression in sorted populations of mESCs. Morphologically distinct differentiated cells on day 5 of culture in serum-free media with LIF and BMP4 were sorted and compared to colonies that appeared to be more self-renewing. The control is day 2 mESCs grown in the presence of serum and LIF.

6.4 Discussion

In this chapter, we describe methods for signal patterning and cell sorting that have potential for further studies regarding how established ESC colonies respond to and generate extracellular signals. Our novel method for presenting signals to existing mESC colonies at desired locations

can be adapted for many other applications. Multiple proteins could be patterned on a single dish simply by polymerizing streptavidin-containing structures sequentially and adding biotinylated proteins between polymerization steps. Thus, signaling proteins could be patterned asymmetrically to study how signals enhance or oppose one another within a single colony. Because this method can be applied to cells in any configuration at any time during their culture period, there is unlimited spatial and temporal control over signal presentation. This could allow for in-depth studies of how the signaling microenvironment affects cells in terms of tethered versus soluble signals. Moreover, any adherent cell type can be adapted for use with this system, as the size of the posts or shape of the polymerized structure can be immediately altered based on a given cell or colony morphology. However, it is important to consider that many other methods exist for patterning signals, some of which may be easier to implement or more appropriate to address particular questions.

One drawback of our signal patterning method is that its analysis relies on in situ cell position within a colony. This greatly limits the kinds of assays that can be pursued, as most downstream analysis techniques require harvesting cells in bulk for further preparation steps. To partially get around this limitation, we can combine patterning techiques with our ability to selectively sort populations of cells by position or morphology. After several days of localized signal presentation, separate regions of cells that were exposed or not exposed to a tethered signal could be isolated, allowing for more sophisticated analyses beyond immunofluorescent staining. However, this approach may still dilute out much of the positional information present in the dish and it does not allow for high-resolution analysis of signal propagation within a colony.

The ability to perform morphology-based sorting of mESCs that we demonstrated in this chapter could theoretically be used to selectively sort and analyze subpopulations or areas of colonies in normal culture. However, we have not yet successfully sorted sections of a single colony due to the fact that ESCs growing in colonies have very strong cell-cell bonds such that when one portion of the colony is targeted for polymerization-activated cell sorting, the majority of the colony ends up being trypsinized and recovered downstream. Further optimization could therefore go into making a stronger polymer for ensuring encapsulation or finding cell dissociation methods that are more efficient than trypsin at breaking up colonies. Alternatively, radical-activated cell sorting may be a better approach, as part of a colony could be selectively

killed and removed, leaving the remainder of the colony. However, we have seen aberrant cell death in the cells masked during this process, indicating that the free radicals intended to kill the unmasked cells may diffuse and damage the masked cells, making this method in its current state unreliable for delicate cells such as mESCs. Thus, instead of trying to sort out sections of colonies, these morphology-based methods may be best suited to sorting specific subpopulations within a heterogenous population of ESCs, for example, for sorting out cells within a differentiating population that are more or less amenable to differentiation toward a specific lineage.

The increasing sophistication of imaging technologies and the ability to monitor cells over long periods of time has allowed for a better understanding of the relationship between how cell morphology relates to function. For example, fibroblasts were tracked during reprogramming to induced pluripotent stem cells and their successful reprogramming potential was found to be related to expression of certain markers but not others, which did not always correlate with colony morphology (Chan et al., 2009). Morphological characteristics have also been identified that precede molecular marker activation during reprogramming (Smith et al., 2010). A similar approach could be used during directed differentiation by imaging and tracking ESCs over several days and quantifying the information encoded in their morphology, including parameters such as cell size, nucleus size, cell/colony shape, and colony edge properties. Once cells with different morphological characteristics are identified, they could then be sorted out and assayed for other phenotypic characteristics, including mRNA/protein expression levels and functional differentiation potential. In this way, cells that are more likely to adopt a particular differentiation lineage fate over another can be identified early in a label-free system and isolated to identify the molecular mechanisms behind their specific differentiation propensity.

6.5 Methods

PEGDA hydrogel preparation

Polyethylene glycol diacrylate (PEGDA) 1000 (Laysan Bio) solution was combined with 2.5% w/w catalase (Sigma) to prevent cells from free radical damage. Irgacure® 2959 photoinitiator (CIBA) was dissolved in 100% methanol (250 mg photoinitiator (PI) per 1 mL methanol) and

vortexed. Immediately prior to sorting, 6 μL of the PI solution was added to 1 mL of the PEGDA solution to constitute the final prepolymer, which was added to cells growing in the culture dish.

PEGDA signal patterning

For signal patterning, a transparency mask was inserted in the light path of the microscope with the desired shape and the microscope UV filter was applied to only cure the hydrogel at the desired location. A ten second UV exposure was sufficient to cure the hydrogel. This process could be automated by picking the desired locations for PEGDA structures before adding the hydrogel. 10 μM streptavidin (Sigma) was used for all experiments. Texas Red-linked BSA (Invitrogen) and LIF (esgro, Millipore) were used at 0.5 μM and were incubated with the PEGDA structures for 20 minutes in a humidified incubator at 37°C. Biotin was conjugated to these proteins in-house using the EZ-Link Micro Sulfo-NHS-Biotinylation Kit (Pierce), at a 50-fold molar excess. Specifically, 200 μl BSA at 1 mg/ml was incubated with 18.4 μl biotin, whereas 50 μl LIF at 0.1 mg/ml was incubated with 1.52 μl biotin.

Morphology-based cell sorting

For radical- or polymerization-activated cell sorting, the entire plate was masked using a specially-generated transparency mask that blocked the desired cells. A photoinitiator solution was added for radical-activated sorting (PEGDA solution minus PEGDA), while the PEGDA solution described above was used for polymerization-activated sorting. The entire dish was exposed to UV light for 12 minutes. After exposure, the excess photoinitiator solution or prepolymer was aspirated and cells were trypsinized if further analysis was required. A custom MATLAB script was used to identify self-renewing colonies.

Immunofluorescence

For Oct4 staining, cells were incubated overnight with primary Oct4 antibody (Abcam) at 5 μg/ml and secondary (anti-goat AF488, Abcam) was added for one hour at 1:250. Cells were counterstained with 1:100000 Hoechst (Sigma).

Chapter 7 Conclusions

7.1 Contributions

The primary objective of this thesis was to establish methods to manipulate the embryonic stem cell extracellular signaling environment, and to implement those methods to improve our understanding of how cell-secreted signals contribute to embryonic stem cell self-renewal and differentiation. The major contributions by which this goal was achieved are summarized below.

Demonstrating a requirement for mESC-secreted soluble factors

We successfully established the first conditions for multi-day culture of mESCs in serum-free media with decreased soluble signaling by growing cells under continuous microfluidic perfusion in N2B27 media with LIF and BMP4, and showed that cell-secreted factors are being removed and cells can survive. We then assessed the resulting cell phenotype after five days of continuous perfusion and found that the cells that started out as mESCs exited their self-renewing state. This result was unexpected and novel, as the media in which the cells were growing was previously thought to be sufficient for self-renewal. We went on to find that the cells growing for several days under perfusion exhibited a more primed epiblast-like phenotype, indicating that the default steady state of pluripotent stem cells in the absence of cell-secreted soluble signals is more primed than naïve. Together, these results establish a platform for assessing sufficiency of exogenous signals to produce a given phenotype and for determining the contributions of endogenously secreted soluble signals. Because this platform is suitable for several day culture of embryonic stem cells, it should be easily applicable to other stem cell systems and for cells such as cancer cells, whose growth and metastasis often depends on cell-secreted signals.

Revealing the necessity of mESC extracellular matrix remodeling

After finding that mESCs exit their self-renewing state under perfusion, we went on to determine the signals responsible for this exit. When thinking about the cell-secreted microenvironment as a whole, it became clear that some cell-secreted signals were not being affected under perfusion, including those that remained part of the extracellular matrix. We found that broadly disrupting the binding function or structural integrity of the ECM using sodium chlorate or collagenase,

respectively, caused cells growing under perfusion to maintain their self-renewing state, which was our initial indication of the importance of matrix remodeling on maintaining self-renewal. Based on this novel role for ECM-based signals, we sought a connection between removing soluble signals and affecting matrix remodeling. Matrix metalloproteinases normally act to remodel the matrix, and we show for the first time that this class of proteins is required to maintain mESC self-renewal. Thus, because MMPs are removed under perfusion, they are no longer able to perform their essential duties as matrix remodeling proteins, resulting in an exit from the stable self-renewing mESC state. The necessity of MMPs extends to paracrine culture as well, as we found that the high levels of MMPs secreted by feeder cells functionally aid in mESC self-renewal, a newly identified contribution that feeders provide to mESCs. This contribution is unique in that it acts at the level of the extracellular matrix, whereas previously identified contributions from feeder cells have involved either ligand secretion or contact-mediated signaling.

Establishing the sufficiency of MMP1 to maintain self-renewal

To more specifically examine the effects of matrix remodeling, we grew mESCs in the absence of LIF but the presence of MMP1 and, astonishingly, found that self-renewal was maintained with similar morphology, growth rates, mRNA and protein expression levels, and pluripotentiality for several passages. While mESCs grown in serum in the absence of LIF degenerate and die after 4-5 passages, we have been able to maintain mESC growth and proper morphology for 30 passages in serum+MMP1, and it is likely that this effect could be extended indefinitely. A similar effect is seen with addition of a crude collagenase cocktail but not with MMPs that have substrates other than collagen, indicating the specificity of the matrix proteins involved. MMP1 thus represents the first exogenously added non-LIF-family protein that has been identified with the ability to maintain LIF-independent ESC self-renewal.

Identifying a novel non-canonical autocrine system involved in mESC self-renewal

We found that MMP1 is not acting to maintain self-renewal by inhibiting pathways that have been previously implicated in opposing self-renewal, but that it is instead acting in what is likely to be an indirect manner through the gp130-JAK-Stat3 pathway. While more work is required to further characterize exactly how ECM remodeling is able to maintain mESC self-renewal in

terms of the signal upstream of gp130 and how collagenase causes this ligand to transition from a latent to an active state, the fact that the upstream effector of self-renewal is an endogenous signal is a novel concept that represents the first example of an mESC-secreted signal that is produced at amounts sufficient to maintain self-renewal. The mechanism by which exogenous or endogenous MMPs act at the level of the endogenous extracellular matrix to activate another cell-secreted signal represents a new kind of indirect autocrine system that will alter the general perception of how cell-secreted signals contribute to fundamental cellular processes and may enhance our understanding of how matrix remodeling contributes to development at early embryonic stages.

7.2 Future directions

Many of the results presented in this thesis are far from being complete works, and the results that do appear to complete a story actually leave many routes of questioning open to pursue. Here I describe several broad directions with specific starting points that future work could take to continue and enhance the research described above or to utilize and adapt techniques and preliminary results for new but related projects.

Using perfusion as a screening platform

We showed that growing mESCs under perfusion caused them to exit their self-renewing state, a fate that could be avoided by simultaneously disrupting the extracellular matrix. While these results show that LIF and BMP4 are not sufficient to maintain mESC self-renewal and that matrix-based components play a role, we still have not identified the full complement of soluble factors required to maintain self-renewal. To do so is difficult given our current perfusion setup because it would require high-throughput screening of different combinations of factors at different absolute and relative concentrations. However, the microfluidic perfusion device could be adapted for use as a screening platform by including many small chambers for growing mESCs with a simple readout that only requires a small number of cells and no removal of cells from the chip, such as using a reporter cell line or performing immunofluorescence staining. Perfusion systems can provide several advantages over traditional screens performed in multiwell plates, including the fact that cell loading and media changes can be automated, small

media volumes are typically used, and there is precise temporal control over when factors are added and removed.

Several design considerations need to be taken into account to design a useful perfusion platform with many independent culture chambers. Ideally, cells would be loaded into all chambers simultaneously, allowed to attach, and perfusion with different media formulations would begin after cell attachment. This would require that all chambers can be addressed both simultaneously and individually, a task that can be accomplished if cells are loaded through a common opening that is used as a cell output during perfusion culture. For a first generation device with separate media inputs, a medium-throughput device with between 10-20 chambers would be most practical to develop and test. Once cell loading and culture are optimized in this sort of system, more sophisticated systems with overlapping combinatorial inputs could be devised. The small chamber size inherent to microfluidic cultures allows for precise temporal control over factor addition, providing an additional screening parameter. For any high-throughput system, developing an automated input method for media addition is essential to ensure proper delivery of factors to the right places at the right times, and this work is ongoing in the lab.

Once the microfluidic perfusion device is adapted to become a high-throughput system, it could be used in a variety of ways, two of which are described in more detail below. As mentioned above, perfusion is a powerful means of assessing the sufficiency of signals to elicit a specific process or phenotype. Because soluble cell-secreted signals are being removed under perfusion, the media composition is more defined under perfusion than in static culture. Thus, if cell-secreted signals are important mediators of a particular response, this will likely become clear under perfusion. For mESCs, we can go beyond the finding that LIF and BMP4 are not sufficient to maintain self-renewal to determine what is in fact sufficient. Candidate molecules that have been shown to act extracellularly to aid in mESC self-renewal could be added to mESCs growing under perfusion, alone or in combination in the presence of LIF and BMP4, and a simple assay could be devised to assess the resulting phenotype. A simple assessment of the maintenance of self-renewal versus the transition to a more epiblast-like state that could be implemented in a high-throughput manner involves comparing FGF5 levels, as levels of FGF5 mRNA increase 7-fold under normal perfusion conditions (Figure 2-9a). An FGF5 reporter cell line would thus be very useful for this type of screen, as the relative fluorescence levels could be measured easily

and quickly. If promising candidates were found for addition that significantly decreased FGF5 reporter protein levels, these signals could be applied to mESCs growing in the larger scale perfusion device such that the cells could be removed and tested downstream in qPCR and flow cytometry assays for further verification of self-renewal characteristics.

Another application for a high-throughput screening platform was discussed in chapter 3, involving determining conditions for specific, high-efficiency directed differentiation. Perfusion is a good system with which to identify conditions for directed differentiation of mESCs for many reasons. First, it provides a neutral signaling background in which cell-secreted factors are not acting to enhance or block any exogenously added factors to be tested. Second, we have shown that mESCs are already primed for differentiation in the absence of cell-secreted signals, which means they may be more easily convinced to differentiate in one way or another given the correct signals. Third, perfusion culture can be scaled up given the appropriate output assay, as mentioned above, so multiple conditions could be assessed at once and an optimized differentiation cocktail could be devised. We have already shown that rapid and specific differentiation towards the mesoderm lineage is possible under perfusion (Figure 3-2). Because growth of ESCs under perfusion predisposes them to a meso- or ectodermal fate (Figure 4-4), another system that could utilize such technology is the derivation of excitatory cortical neurons from pluripotent stem cells.

In vitro derivation of excitatory neurons has been performed using neural stem cells, but these neurons may not have the ability to generate all types of cortical neurons in vivo (Hansen et al., 2011). Pluripotent stem cells may therefore be a better starting cell type for this process, and induced pluripotent stem cells can be created from cells with neuronal disease backgrounds. Many such diseases target only one type or group of neurons, so to determine the specific disease mechanisms, it is necessary to have protocols in place for generating specific and functional neurons of all types. Given an appropriate marker for the desired type of neuron to be generated, a screen could be performed in a specially designed perfusion device, as in the above example, to add in candidate factors and assess fluorescent intensity levels. Though the cell yield from the screening platform would likely be too low to perform functional studies on the resulting cells, promising candidates from the screen could be applied to scaled-up cultures such that cells could be harvested and tested functionally, making this platform more of a discovery platform than an

actual method for large-scale differentiation. The applications described in this section could be applied to other types of differentiation and for screens of other multipotent stem cells, as could the use of this type of platform for screening for sufficient self-renewal conditions. Thus, the production and implementation of such a system is a promising new direction for perfusion research now that conditions and protocols for pluripotent stem cell growth under perfusion have been established and the resulting phenotype has been characterized.

Monitoring and quantifying changes in secretome profile during self-renewal and differentiation

Perfusion can be used as a tool to more efficiently differentiate cells, and its small cell-to-media volume ratio and its temporal control also make it an ideal platform for assessing subtle changes in how the protein secretion profile changes during a differentiation protocol. The information obtained regarding such changes could be used to more precisely recreate differentiation progression in vitro by identifying and adding back in relevant factors at appropriate stages of differentiation. To more fully understand what is secreted and when, we also need to be able to create testable models of protein secretion under perfusion, which could then be combined with downstream assays for verification. To achieve these goals, another area in which our system could be improved is by integration of our microdevice with other microsystems for downstream analysis of small media volumes or small cell numbers.

As ESCs differentiate toward a particular lineage, they downregulate secretion of molecules whose functions involve maintaining pluripotency while upregulating secretion of lineage-specific factors (Farina et al., 2011). However, studies to date have analyzed secreted proteins in large-scale cultures at a few discrete time points over the course of differentiation, and thus do not provide a complete picture of how the secretion profile changes over time. Perfusion could feasibly be used to perform this type of analysis, one problem being that small cell numbers in large perfusion volumes may mean that any cell-secreted proteins, particularly those secreted at low levels, are obscured by proteins in the media, which is a problem we ran into in a previous attempt to submit perfusion samples for mass spectrometry analysis. To get around this, we could use the small media volume of the perfusion chambers to our advantage by collecting the chamber media at several timepoints per day after allowing cell-secreted proteins to accumulate

in the chambers, and combine this with methods to remove the most prevalent background media protein, BSA, from the media prior to analysis. The resulting cell-conditioned media could then be analyzed by mass spectrometry with the advantage that it is already concentrated in a way that cell-secreted proteins should dominate over proteins present in the media.

Using mass spectrometry to analyze secretion profiles gets at which proteins are secreted and when, but to quantify levels of secretion and secretion patterns within a population, more sophisticated modeling techniques need to be employed. We introduced a simple model in chapter 3.3 for removal of a cell-secreted ligand at different flow rates and cell densities. However, this model was never tested experimentally and is likely to be missing important parameters. Thus, further work could go in to refining this model, perhaps starting with an engineered cell secretion system that can be easily monitored. For example, an inducible overexpression system could be generated and calibrated such that addition of the inducer (e.g., doxycyline) at a specific level is known to trigger secretion of a certain amount of protein per cell. Then, the inducer could be added to cells growing under perfusion at different flow rates and densities and the outflow media could be collected and analyzed by ELISA. This system could be put in place for many different ligands, each with their own overexpression cell line, such that the effects of ligand diffusivity and receptor densities can be accounted for. With all the resulting data demonstrating how flow rate relates to ligand removal at different cell densities, a more thorough model can be developed and used to describe the secretion rates and binding characteristics of diverse endogenous ligands.

Both the preceding examples for using information gleaned from microscale perfusion involve collecting the media from the device and applying it to a macroscale assay, either mass spectrometry or ELISA. Many other desirable downstream applications for the media from perfusion or the cells themselves are also best performed with large numbers of cells, especially for stem cells as they are, by definition, functionally defined, and this limits our ability to design and perform assays. The screening experiments described in the prior example were designed to use fluorescence markers or immunostaining, but this approach only provides information about one or a few parameters. To enhance the downstream analytical ability and thus the utility of the perfusion device, integration of the device with other microsystems that have been optimized to perform biological assays on small scales would be immensely useful. Microscale devices have

been designed to perform mass spectrometry (Song et al., 2010) and protein quantification (Kellner et al., 2011; Dixit and Kaushik, 2012), among other biological assays, and though implementation with our existing device or with a more high-throughput version would require significant time and effort, it would enable the investigation of much more sophisticated questions involving secretion profiles and cell phenotype resulting from manipulations of endogenous signals.

Assessing specificity and universality of matrix remodeling proteins

We found that addition of MMP1 allows for long-term LIF-independent maintenance of mESC self-renewal. However, the extent to which this phenomenon holds true for other cell systems or with other MMPs is completely unknown. We showed that neither MMP2 nor MMP3 are able to maintain mESC self-renewal (Figure 5-4a), and we also have results indicating that MMP production from feeder cells is not necessary for mEpiSC self-renewal (Figure 7-1). These results bring up many new research directions, including determination of why MMP1 and collagenase work as functionally significant mESC matrix remodelers, while other classes of MMP molecules don't; finding whether other MMPs have the same effect as MMP1 in ESCs or other stem cell systems; and identifying a corresponding in vivo role for MMP autocrine or paracrine signals in the developing embryo.

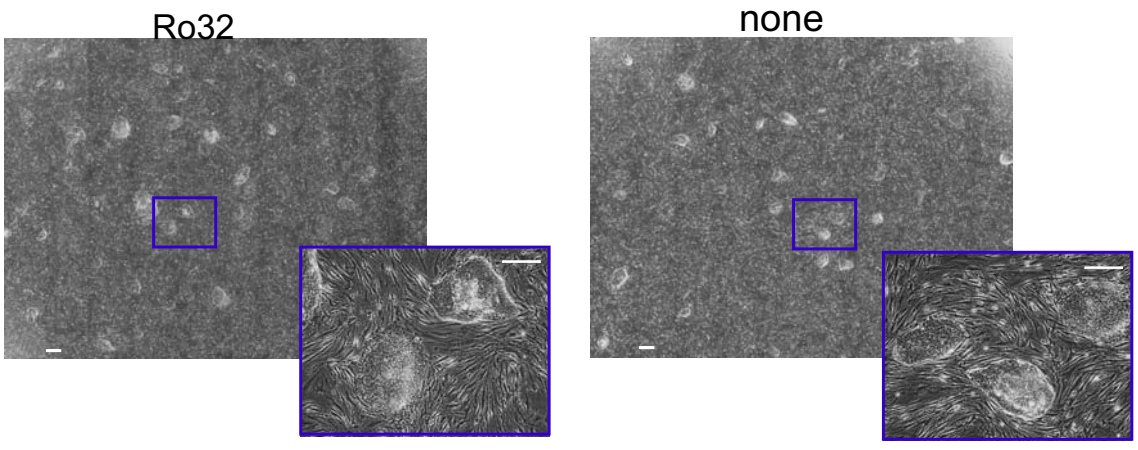

Figure 7-1 Images of EpiSCs growing on feeders after two passages in the presence or absence of the collagenase-specific MMP inhibitor Ro32-3555. Scale bars = 400 μm.

There are 23 MMPs in mice, 16 of which are secreted (Nuttall et al., 2004), all with unique cleavage substrates and tissue expression patterns. Of these, MMP1a, 1b, 8, and 13 cleave triple-

helicar fibrillar collagens specifically, while the others cleave gelatin (partially hydrolyzed collagen) or other extracellular matrix proteins. While it would be simple to add in other MMPs to ESC cultures and test their ability to maintain self-renewal or activate Stat3, the more interesting study would involve finding what factors are released upon addition of different MMPs, as it is possible that specific cell-secreted proteins are bound in the matrix by different structural ECM molecules or activated upon cleavage by specific MMPs. To find these putative ECM-bound factors, addition of MMP could be combined with perfusion to immediately remove and identify factors released from the matrix, using methods described in the preceding section. This approach could potentially be used to definitively identify the ligand responsible for MMP1-mediated self-renewal and to identify other endogenously secreted ligands that are normally trapped within the ECM in ESC cultures.

Based on our result indicating that mEpiSCs are not affected by MMP inhibition to the extent that mESCs are (Figure 7-1, compare to Figure 5-2), we might assume that this phenomenon is specific to the mESC system, which makes sense considering that the ligand involved in MMP1-mediated ESC self-renewal acts through a pathway that is not relevant to mEpiSC maintenance. However, the MMP inhibitor used in these co-culture experiments is specific to collagenases, so it remains possible that other MMP-family proteins are required to maintain EpiSC self-renewal, which could easily be tested by employing other inhibitors. It would also be interesting to determine the effect of exogenous MMP1 or other MMPs on EpiSC self-renewal in the absence of other exogenously added factors. EpiSCs require FGF2 and exogenous or endogenous Activin for self-renewal, but it is possible that these or related molecules are being produced by the cells and getting trapped in the ECM, as is the case with ESCs. Perhaps MMP1 would not cleave the appropriate matrix molecule to allow the EpiSC signal to escape, but a different MMP would. These sorts of questions can extend beyond pluripotent stem cells to more committed stem cell systems and addition of the right kind of matrix remodeling proteins could allow for a more realistic recapitulation of the in vivo niche.

The fact that ESCs rapidly produce a complex endogenous ECM when grown in vitro is not so surprising given the importance of cell-cell adhesions and basement membrane formation in the developing embryo. When tissue-specific expression of MMPs in mouse was assessed, it was found that almost all MMPs are present in the uterus or placenta at some point during embryonic

development, and that MMP1a and 1b are found exclusively in the uterus and testis and no other organs (Nuttall et al., 2004). Thus, the paracrine role played by feeder cells in supplying MMPs to ESCs could also be present in the early embryo, which receives paracrine signals from the uterus (Figure 1-3). In another study, MMP expression was monitored in the implanting blastocyst and only MMP1a, 1b, 2, and 9 were detected (Chen et al., 2007), indicating possible autocrine roles for these proteins as well. Knocking out any individual MMP does not cause embryonic lethality, but this is likely due to the fact that enough MMPs are present to take over necessary functions in the absence of one. Thus, testing the in vivo functionality of specific MMPs may require overexpressing the protein and checking for misregulation, or knocking out more than one closely related MMP, like both MMP1a and 1b. While these sorts of studies are not trivial, the mechanisms involved in the progression from pre- to post-implantation blastocyst require significant cell movement and complex signaling patterns, all actions that can involve MMPs, and the fact that MMPs function so significantly in mESCs provides further evidence that they may have an important role in embryonic development.

Developing and implementing methods for further characterizing endogenous ECM properties

Exogenously remodeling the ECM has allowed us to uncover a fascinating new mechanism by which mESCs can maintain their self-renewal. However, endogenous matrix remodeling proteins are constantly at work in normal cultures, and their roles are almost completely uncharacterized in in vitro stem cell systems. Recent work has identified ECM structural properties as strongly contributing to stem cell fate in many systems (Engler et al., 2006; Saha et al., 2008; Chowdhury et al., 2010) and tools have been developed for measuring ECM structural properties. More work is also going in to creating synthetic matrices to mimic those that are found in in vivo niches (Keung et al., 2010), and understanding how these matrices compare to and interact with endogenous ECM will be crucial to generating reliable, defined in vitro tissue engineering systems. The relevance and functions of cell-secreted signals can vary widely depending on the signals' extracellular location, whether they are bound at the membrane surface, secreted in the bulk media, or bound to or within the ECM. Future work could therefore also go into characterizing and quantifying the differences in how soluble versus tethered signals act, using the ability to localize patterns of specific signals around stem cell colonies.

Current methods for measuring ECM structural properties mostly rely on atomic force microscopy (AFM) (Ludwig et al., 2007). The sensitivity of AFM allows it to take force measurements of single cells by assessing their deformability, a property that has been found to vary greatly between different cell types (Chowdhury et al., 2008). However, the elastic modulus, essentially a quantification of deformability, of endogenous ECMs has not been assessed. Beyond its ability to activate or remove ECM-bound signaling proteins, matrix remodeling also has the ability to broadly alter ECM structural properties. While adding collagenase to mESC cultures at low concentrations allows cells to maintain self-renewal in the absence of LIF (Figure 5-3b), adding it at high concentrations actually causes the cells to be removed from their substrate and form spheroid cultures, a phenomenon that is most apparent in serum-free cultures. This indicates that collagenase is broadly altering the structural properties of the endogenous ECM and is likely performing this function to some extent at low concentrations. Because it has been shown that mESCs self-renew in the absence of LIF on soft substrates (Chowdhury et al., 2010), it is possible that the ECM structural changes caused by collagenase contribute to the LIF-independent self-renewal phenotype we describe, a question that could be addressed by devising a way to measure endogenous matrix stiffness.

Conversely, it is possible that the ability of soft substrates to enhance self-renewal is due to the fact that cell-secreted proteins that are normally bound in the matrix are more accessible in a more porous matrix. For stem cell maintenance and tissue engineering applications, many types of artificial matrices have been described, but the mechanisms that make them more or less appropriate for specific applications are largely unknown. The contribution of the endogenously secreted matrix is also not often taken into account, so better methods for assessing endogenous ECM makeup and determining how secreted signaling proteins interact with and bind to structural matrix proteins could aid in the production of more relevant in vitro models for stem cell maintenance and differentiation in embryonic and adult stem cell systems.

The endogenous ECM contains many proteins that have both soluble and matrix-bound forms. These forms can have functionally different consequences (Robertson et al., 1993; Saha and Schaffer, 2006), so determining which secreted proteins exist in these different forms and what their functional differences are is important when describing the cell-secreted microenvironment. Proteins bound in the ECM may signal for longer than soluble proteins due to their inability to

diffuse from the receptor, and they may be bound in concentrated pockets in the ECM with other proteins, such that the simultaneous signaling of two or more proteins elicits a different signaling result than signals acting alone through any single pathway. The actions of exogenous signals are generally assessed by adding in soluble forms of the proteins of interest, but it is becoming increasingly apparent that ECM-bound signals also contribute to cell phenotype in a major way. Thus, studies using our tethered protein presentation system could be combined with studies using identical soluble cues to distinguish the contributions of each type of signal and could be broadly applied to further uncover methods by which ECM-bound proteins act in contrast to their soluble counterparts.

All the methods described in this section have the added benefit that they can be implemented using any stem cell system, or even more generally with any adherent cells. Applying and combining the techniques and approaches described in this chapter to study and manipulate exogenous signals could therefore be used for defining optimal culture systems and addressing a wide range of questions involving the contributions or limitations of extracellular signals, allowing for further discoveries regarding how the cell-secreted microenvironment affects cell phenotype.

References

Alberti, K., R.E. Davey, K. Onishi, S. George, K. Salchert, F.P. Seib, M. Bornhäuser, T. Pompe, A. Nagy, C. Werner, and P.W. Zandstra. 2008. Functional immobilization of signaling proteins enables control of stem cell fate. *Nat. Methods*. 5:645–650.

Alexander, C.M., E.J. Hansell, O. Behrendtsen, M.L. Flannery, N.S. Kishnani, S.P. Hawkes, and Z. Werb. 1996. Expression and function of matrix metalloproteinases and their inhibitors at the maternal-embryonic boundary during mouse embryo implantation. *Development*. 122:1723–1736.

Baeuerle, P.A., and W.B. Huttner. 1986. Chlorate -- a potent inhibitor of protein sulfation in intact cells. *Biochem Biophys Res Commun*. 141:870–877.

Banerjee, I., N. Sharma, and M. Yarmush. 2011. Impact of co-culture on pancreatic differentiation of embryonic stem cells. *Journal of Tissue Engineering and Regenerative Medicine*. 5:313–323.

Bao, S., F. Tang, X. Li, K. Hayashi, A. Gillich, K. Lao, and M.A. Surani. 2009. Epigenetic reversion of post-implantation epiblast to pluripotent embryonic stem cells. *Nature*. 461:1292–1295.

Becker, K.A., J.L. Stein, J.B. Lian, A.J. van Wijnen, and G.S. Stein. 2010. Human embryonic stem cells are pre-mitotically committed to self-renewal and acquire a lengthened G1 phase upon lineage programming. *J. Cell. Physiol.* 222:103–110.

Bendall, S.C., M.H. Stewart, P. Menendez, D. George, K. Vijayaragavan, T. Werbowetski-Ogilvie, V. Ramos-Mejia, A. Rouleau, J. Yang, M. Bosse, G. Lajoie, and M. Bhatia. 2007. IGF and FGF cooperatively establish the regulatory stem cell niche of pluripotent human cells in vitro. *Nature*. 448:1015–1021.

Berendsen, A.D., L.W. Fisher, T.M. Kilts, R.T. Owens, P.G. Robey, J.S. Gutkind, and M.F. Young. 2011. Modulation of canonical Wnt signaling by the extracellular matrix component biglycan. *Proceedings of the National Academy of Sciences*.

ten Berge, D., W. Koole, C. Fuerer, M. Fish, E. Eroglu, and R. Nusse. 2008. Wnt Signaling Mediates Self-Organization and Axis Formation in Embryoid Bodies. *Cell Stem Cell*. 3:508–518.

ten Berge, D., D. Kurek, T. Blauwkamp, W. Koole, A. Maas, E. Eroglu, R.K. Siu, and R. Nusse. 2011. Embryonic stem cells require Wnt proteins to prevent differentiation to epiblast stem cells. *Nat. Cell Biol.* 13:1070–1075.

Bernfield, M., M. Götte, P.W. Park, O. Reizes, M.L. Fitzgerald, J. Lincecum, and M. Zako. 1999. Functions of cell surface heparan sulfate proteoglycans. *Annu. Rev. Biochem.* 68:729–777.

Bertocchini, F., and C.D. Stern. 2002. The Hypoblast of the Chick Embryo Positions the Primitive Streak by Antagonizing Nodal Signaling. *Developmental Cell*. 3:735–744.

Blagovic, K., L.Y. Kim, and J. Voldman. 2011. Microfluidic Perfusion for Regulating Diffusible Signaling in Stem Cells. *PLoS ONE*. 6:e22892.

Bökel, C., and N.H. Brown. 2002. Integrins in development: moving on, responding to, and sticking to the extracellular matrix. *Dev. Cell*. 3:311–321.

Bortvin, A., M. Goodheart, M. Liao, and D.C. Page. 2004. Dppa3 / Pgc7 / stella is a maternal factor and is not required for germ cell specification in mice. *BMC Dev. Biol*. 4:2.

Bourillot, P., I. Aksoy, V. Schreiber, F. Wianny, H. Schulz, O. Hummel, N. Hubner, and P. Savatier. 2009. Novel STAT3 Target Genes Exert Distinct Roles in the Inhibition of Mesoderm and Endoderm Differentiation in Cooperation with Nanog. *STEM CELLS*. 27:1760–1771.

Boyer, L.A., T.I. Lee, M.F. Cole, S.E. Johnstone, S.S. Levine, J.P. Zucker, M.G. Guenther, R.M. Kumar, H.L. Murray, R.G. Jenner, D.K. Gifford, D.A. Melton, R. Jaenisch, and R.A. Young. 2005. Core Transcriptional Regulatory Circuitry in Human Embryonic Stem Cells. *Cell*. 122:947–956.

Braam, S.R., L. Zeinstra, S. Litjens, D. Ward-van Oostwaard, S. van den Brink, L. van Laake, F. Lebrin, P. Kats, R. Hochstenbach, R. Passier, A. Sonnenberg, and C.L. Mummery. 2008. Recombinant vitronectin is a functionally defined substrate that supports human embryonic stem cell self-renewal via alphavbeta5 integrin. *Stem Cells*. 26:2257–2265.

Brons, I.G.M., L.E. Smithers, M.W.B. Trotter, P. Rugg-Gunn, B. Sun, S.M. Chuva de Sousa Lopes, S.K. Howlett, A. Clarkson, L. Ahrlund-Richter, R.A. Pedersen, and L. Vallier. 2007. Derivation of pluripotent epiblast stem cells from mammalian embryos. *Nature*. 448:191–195.

Brown, N.H. 2011. Extracellular matrix in development: insights from mechanisms conserved between invertebrates and vertebrates. *Cold Spring Harb Perspect Biol*. 3.

Burdon, T., C. Stracey, I. Chambers, J. Nichols, and A. Smith. 1999. Suppression of SHP-2 and ERK Signalling Promotes Self-Renewal of Mouse Embryonic Stem Cells. *Dev Biol*. 210:30–43.

Campbell, K.P. 1995. Three muscular dystrophies: loss of cytoskeleton-extracellular matrix linkage. *Cell*. 80:675–679.

Canham, M.A., A.A. Sharov, M.S.H. Ko, and J.M. Brickman. 2010. Functional Heterogeneity of Embryonic Stem Cells Revealed through Translational Amplification of an Early Endodermal Transcript. *PLoS Biol*. 8:e1000379.

Chambers, I., J. Silva, D. Colby, J. Nichols, B. Nijmeijer, M. Robertson, J. Vrana, K. Jones, L. Grotewold, and A. Smith. 2007. Nanog safeguards pluripotency and mediates germline development. *Nature*. 450:1230–1234.

Chan, E.M., S. Ratanasirintrawoot, I.-H. Park, P.D. Manos, Y.-H. Loh, H. Huo, J.D. Miller, O. Hartung, J. Rho, T.A. Ince, G.Q. Daley, and T.M. Schlaeger. 2009. Live cell imaging distinguishes bona fide human iPS cells from partially reprogrammed cells. *Nat. Biotechnol.* 27:1033–1037.

Chen, C.S., M. Mrksich, S. Huang, G.M. Whitesides, and D.E. Ingber. 1997. Geometric control of cell life and death. *Science*. 276:1425–1428.

Chen, L., M. Nakai, R.J. Belton Jr, and R.A. Nowak. 2007. Expression of extracellular matrix metalloproteinase inducer and matrix metalloproteinases during mouse embryonic development. *Reproduction*. 133:405–414.

Chen, X., H. Xu, P. Yuan, F. Fang, M. Huss, V.B. Vega, E. Wong, Y.L. Orlov, W. Zhang, J. Jiang, Y.-H. Loh, H.C. Yeo, Z.X. Yeo, V. Narang, K.R. Govindarajan, B. Leong, A. Shahab, Y. Ruan, G. Bourque, W.-K. Sung, N.D. Clarke, C.-L. Wei, and H.-H. Ng. 2008. Integration of External Signaling Pathways with the Core Transcriptional Network in Embryonic Stem Cells. *Cell*. 133:1106–1117.

Chou, Y.-F., H.-H. Chen, M. Eijpe, A. Yabuuchi, J.G. Chenoweth, P. Tesar, J. Lu, R.D.G. McKay, and N. Geijsen. 2008. The Growth Factor Environment Defines Distinct Pluripotent Ground States in Novel Blastocyst-Derived Stem Cells. *Cell*. 135:449–461.

Chowdhury, F., Y. Li, Y.-C. Poh, T. Yokohama-Tamaki, N. Wang, and T.S. Tanaka. 2010. Soft Substrates Promote Homogeneous Self-Renewal of Embryonic Stem Cells via Downregulating Cell-Matrix Tractions. *PLoS ONE*. 5:e15655.

Chowdhury, F., S. Na, O. Collin, B. Tay, F. Li, T. Tanaka, D.E. Leckband, and N. Wang. 2008. Is cell rheology governed by nonequilibrium-to-equilibrium transition of noncovalent bonds? *Biophys. J.* 95:5719–5727.

Cimetta, E., E. Figallo, C. Cannizzaro, N. Elvassore, and G. Vunjak-Novakovic. 2009. Micro-bioreactor arrays for controlling cellular environments: Design principles for human embryonic stem cell applications. *Methods*. 47:81–89.

Conover, J.C., N.Y. Ip, W.T. Poueymirou, B. Bates, M.P. Goldfarb, T.M. DeChiara, and G.D. Yancopoulos. 1993. Ciliary neurotrophic factor maintains the pluripotentiality of embryonic stem cells. *Development*. 119:559–565.

Conti, M.A., S. Even-Ram, C. Liu, K.M. Yamada, and R.S. Adelstein. 2004. Defects in cell adhesion and the visceral endoderm following ablation of nonmuscle myosin heavy chain II-A in mice. *J. Biol. Chem.* 279:41263–41266.

Cormier, J.T., N.I.Z. Nieden, D.E. Rancourt, and M.S. Kallos. 2006. Expansion of Undifferentiated Murine Embryonic Stem Cells as Aggregates in Suspension Culture Bioreactors. *Tissue Eng*. 12:3233–3245.

Coyle, R.C., A. Latimer, and J.R. Jessen. 2008. Membrane-type 1 matrix metalloproteinase regulates cell migration during zebrafish gastrulation: Evidence for an interaction with non-canonical Wnt signaling. *Experimental Cell Research*. 314:2150–2162.

Crouch, C.F., H.W. Fowler, and R.E. Spier. 1985. The adhesion of animal cells to surfaces: The measurement of critical surface shear stress permitting attachment or causing detachment. *Journal of Chemical Technology and Biotechnology. Biotechnology*. 35:273–281.

Cruise, G.M., O.D. Hegre, F.V. Lamberti, S.R. Hager, R. Hill, D.S. Scharp, and J.A. Hubbell. 1999. In vitro and in vivo performance of porcine islets encapsulated in interfacially photopolymerized poly(ethylene glycol) diacrylate membranes. *Cell Transplantation*. 8:293–306.

Darnell, J.E. 1997. STATs and Gene Regulation. *Science*. 277:1630–1635.

Das, S.K., S. Yano, J. Wang, D.R. Edwards, H. Nagase, and S.K. Dey. 1997. Expression of matrix metalloproteinases and tissue inhibitors of metalloproteinases in the mouse uterus during the peri-implantation period. *Developmental Genetics*. 21:44–54.

Davey, R.E., K. Onishi, A. Mahdavi, and P.W. Zandstra. 2007. LIF-mediated control of embryonic stem cell self-renewal emerges due to an autoregulatory loop. *FASEB J.* 21:2020–2032.

Davey, R.E., and P.W. Zandstra. 2006. Spatial Organization of Embryonic Stem Cell Responsiveness to Autocrine Gp130 Ligands Reveals an Autoregulatory Stem Cell Niche. *Stem Cells*. 24:2538–2548.

DeLong, S.A., J.J. Moon, and J.L. West. 2005. Covalently immobilized gradients of bFGF on hydrogel scaffolds for directed cell migration. *Biomaterials*. 26:3227–3234.

Deng, C.X., A. Wynshaw-Boris, M.M. Shen, C. Daugherty, D.M. Ornitz, and P. Leder. 1994. Murine FGFR-1 is required for early postimplantation growth and axial organization. *Genes Dev.* 8:3045–3057.

Desai, S.P., D.M. Freeman, and J. Voldman. 2009. Plastic masters-rigid templates for soft lithography. *Lab Chip*. 9:1631–1637.

Dewey, C.F., Jr, S.R. Bussolari, M.A. Gimbrone Jr, and P.F. Davies. 1981. The dynamic response of vascular endothelial cells to fluid shear stress. *J Biomech Eng*. 103:177–185.

DeWitt, A.E., J.Y. Dong, H.S. Wiley, and D.A. Lauffenburger. 2001. Quantitative analysis of the EGF receptor autocrine system reveals cryptic regulation of cell response by ligand capture. *J Cell Sci*. 114:2301–2313.

Dixit, C.K., and A. Kaushik. 2012. Nano-structured arrays for multiplex analyses and Lab-on-a-Chip applications. *Biochem. Biophys. Res. Commun.* 419:316–320.

Dollery, C.M., J.R. McEwan, and A.M. Henney. 1995. Matrix metalloproteinases and cardiovascular disease. *Circ. Res.* 77:863–868.

Domogatskaya, A., S. Rodin, A. Boutaud, and K. Tryggvason. 2008. Laminin-511 but Not -332, -111, or -411 Enables Mouse Embryonic Stem Cell Self-Renewal In Vitro. *Stem Cells*. 26:2800–2809.

Dutta, D., S. Ray, P. Home, M. Larson, M.W. Wolfe, and S. Paul. 2011. Self-Renewal Versus Lineage Commitment of Embryonic Stem Cells: Protein Kinase C Signaling Shifts the Balance. *STEM CELLS*. 29:618–628.

Egorova, A.D., K. Van der Heiden, S. Van de Pas, P. Vennemann, C. Poelma, M.C. DeRuiter, M.T.H. Goumans, A.C. Gittenberger-de Groot, P. ten Dijke, R.E. Poelmann, and B.P. Hierck. 2011. Tgfβ/Alk5 signaling is required for shear stress induced klf2 expression in embryonic endothelial cells. *Developmental Dynamics*. 240:1670–1680.

Eiselleova, L., K. Matulka, V. Kriz, M. Kunova, Z. Schmidtova, J. Neradil, B. Tichy, D. Dvorakova, S. Pospisilova, A. Hampl, and P. Dvorak. 2009. A Complex Role for FGF-2 in Self-Renewal, Survival, and Adhesion of Human Embryonic Stem Cells. *STEM CELLS*. 27:1847–1857.

Elisseeff, J., K. Anseth, D. Sims, W. Mcintosh, M. Randolph, and R. Langer. 1999. Transdermal photopolymerization for minimally invasive implantation. *Proceedings of the National Academy of Sciences of the United States of America*. 96:3104–3107.

Engler, A.J., S. Sen, H.L. Sweeney, and D.E. Discher. 2006. Matrix Elasticity Directs Stem Cell Lineage Specification. *Cell*. 126:677–689.

Enver, T., M. Pera, C. Peterson, and P.W. Andrews. 2009. Stem Cell States, Fates, and the Rules of Attraction. *Cell Stem Cell*. 4:387–397.

Evans, M.J., and M.H. Kaufman. 1981. Establishment in culture of pluripotential cells from mouse embryos. *Nature*. 292:154–156.

Fan, V.H., K. Tamama, A. Au, R. Littrell, L.B. Richardson, J.W. Wright, A. Wells, and L.G. Griffith. 2007. Tethered epidermal growth factor provides a survival advantage to mesenchymal stem cells. *Stem Cells*. 25:1241–1251.

Farina, A., C. D'Aniello, V. Severino, D.F. Hochstrasser, A. Parente, G. Minchiotti, and A. Chambery. 2011. Temporal proteomic profiling of embryonic stem cell secretome during cardiac and neural differentiation. *PROTEOMICS*. 11:3972–3982.

Fehling, H.J., G. Lacaud, A. Kubo, M. Kennedy, S. Robertson, G. Keller, and V. Kouskoff. 2003. Tracking mesoderm induction and its specification to the hemangioblast during embryonic stem cell differentiation. *Development*. 130:4217–4227.

Feldman, B., W. Poueymirou, V.E. Papaioannou, T.M. DeChiara, and M. Goldfarb. 1995. Requirement of FGF-4 for postimplantation mouse development. *Science*. 267:246–249.

Flaim, C.J., S. Chien, and S.N. Bhatia. 2005. An extracellular matrix microarray for probing cellular differentiation. *Nat Meth*. 2:119–125.

Fok, E.Y.L., and P.W. Zandstra. 2005. Shear-Controlled Single-Step Mouse Embryonic Stem Cell Expansion and Embryoid Body-Based Differentiation. *Stem Cells*. 23:1333–1342.

Folch, A., B.H. Jo, O. Hurtado, D.J. Beebe, and M. Toner. 2000. Microfabricated elastomeric stencils for micropatterning cell cultures. *J. Biomed. Mater. Res.* 52:346–353.

Foudi, A., K. Hochedlinger, D. Van Buren, J.W. Schindler, R. Jaenisch, V. Carey, and H. Hock. 2009. Analysis of histone 2B-GFP retention reveals slowly cycling hematopoietic stem cells. *Nat. Biotechnol.* 27:84–90.

Fuerer, C., S.J. Habib, and R. Nusse. 2010. A study on the interactions between heparan sulfate proteoglycans and Wnt proteins. *Developmental Dynamics*. 239:184–190.

Gaver III, D.P., and S.M. Kute. 1998. A Theoretical Model Study of the Influence of Fluid Stresses on a Cell Adhering to a Microchannel Wall. *Biophys J*. 75:721–733.

Gearing, D.P., M.R. Comeau, D.J. Friend, S.D. Gimpel, C.J. Thut, J. McGourty, K.K. Brasher, J.A. King, S. Gillis, and B. Mosley. 1992. The IL-6 signal transducer, gp130: an oncostatin M receptor and affinity converter for the LIF receptor. *Science*. 255:1434–1437.

Grabowski, E., and F. Lam. 1995. Endothelial cell function, including tissue factor expression, under flow conditions. *Thromb Haemost.* 74:6.

Greber, B., G. Wu, C. Bernemann, J.Y. Joo, D.W. Han, K. Ko, N. Tapia, D. Sabour, J. Sterneckert, P. Tesar, and H.R. Schöler. 2010. Conserved and Divergent Roles of FGF Signaling in Mouse Epiblast Stem Cells and Human Embryonic Stem Cells. *Cell Stem Cell*. 6:215–226.

Greenbaum, D., N.M. Luscombe, R. Jansen, J. Qian, and M. Gerstein. 2001. Interrelating different types of genomic data, from proteome to secretome: 'oming in on function. *Genome Res.* 11:1463–1468.

Guo, G., J. Yang, J. Nichols, J.S. Hall, I. Eyres, W. Mansfield, and A. Smith. 2009. Klf4 reverts developmentally programmed restriction of ground state pluripotency. *Development*. 136:1063–1069.

Guo, W., Y. Pylayeva, A. Pepe, T. Yoshioka, W.J. Muller, G. Inghirami, and F.G. Giancotti. 2006a. Beta 4 integrin amplifies ErbB2 signaling to promote mammary tumorigenesis. *Cell*. 126:489–502.

Guo, Y., B. Graham-Evans, and H.E. Broxmeyer. 2006b. Murine embryonic stem cells secrete cytokines/growth modulators that enhance cell survival/anti-apoptosis and stimulate colony formation of murine hematopoietic progenitor cells. *Stem Cells*. 24:850–856.

Hall, V.J., J.V. Jacobsen, M.A. Rasmussen, and P. Hyttel. 2010. Ultrastructural and molecular distinctions between the porcine inner cell mass and epiblast reveal unique pluripotent cell states. *Developmental Dynamics*. 239:2911–2920.

Hamazaki, T., S.M. Kehoe, T. Nakano, and N. Terada. 2006. The Grb2/Mek Pathway Represses Nanog in Murine Embryonic Stem Cells. 26:7539–7549.

Hammerschmidt, M., and D. Wedlich. 2008. Regulated adhesion as a driving force of gastrulation movements. *Development*. 135:3625–3641.

Hanna, J., A.W. Cheng, K. Saha, J. Kim, C.J. Lengner, F. Soldner, J.P. Cassady, J. Muffat, B.W. Carey, and R. Jaenisch. 2010. Human embryonic stem cells with biological and epigenetic characteristics similar to those of mouse ESCs. *Proc. Natl. Acad. Sci. U.S.A.* 107:9222–9227.

Hansen, D.V., J.L.R. Rubenstein, and A.R. Kriegstein. 2011. Deriving Excitatory Neurons of the Neocortex from Pluripotent Stem Cells. *Neuron*. 70:645–660.

Hayashi, K., S.M.C. de S. Lopes, F. Tang, and M.A. Surani. 2008. Dynamic Equilibrium and Heterogeneity of Mouse Pluripotent Stem Cells with Distinct Functional and Epigenetic States. *Cell Stem Cell*. 3:391–401.

Hayashi, Y., M.K. Furue, T. Okamoto, K. Ohnuma, Y. Myoishi, Y. Fukuhara, T. Abe, J.D. Sato, R.-I. Hata, and M. Asashima. 2007. Integrins Regulate Mouse Embryonic Stem Cell Self-Renewal. *Stem Cells*. 25:3005–3015.

Hayes, B., S.R. Fagerlie, A. Ramakrishnan, S. Baran, M. Harkey, L. Graf, M. Bar, A. Bendoraite, M. Tewari, and B. Torok-Storb. 2008. Derivation, Characterization, and In Vitro Differentiation of Canine Embryonic Stem Cells. *STEM CELLS*. 26:465–473.

Heinrich, P.C., I. Behrmann, S. Haan, H.M. Hermanns, G. MüLler-Newen, and F. Schaper. 2003. Principles of interleukin (IL)-6-type cytokine signalling and its regulation. *Biochemical Journal*. 374:1.

Hilton, D.J., N.A. Nicola, N.M. Gough, and D. Metcalf. 1988. Resolution and purification of three distinct factors produced by Krebs ascites cells which have differentiation-inducing activity on murine myeloid leukemic cell lines. *J. Biol. Chem.* 263:9238–9243.

Hirai, H., P. Karian, and N. Kikyo. 2011. Regulation of embryonic stem cell self-renewal and pluripotency by leukaemia inhibitory factor. *Biochemical Journal*. 438:11–23.

Ho, J.E., E.H. Chung, S. Wall, D.V. Schaffer, and K.E. Healy. 2007. Immobilized sonic hedgehog N-terminal signaling domain enhances differentiation of bone marrow-derived mesenchymal stem cells. *J Biomed Mater Res A*. 83:1200–1208.

Holland, T.A., Y. Tabata, and A.G. Mikos. 2005. Dual growth factor delivery from degradable oligo(poly(ethylene glycol) fumarate) hydrogel scaffolds for cartilage tissue engineering. *Journal of Controlled Release*. 101:111–125.

Huang, H.-Y. 2006. The cytokine network during embryo implantation. *Chang Gung Med J*. 29:25–36.

Huang, X., C. Gottstein, R.A. Brekken, and P.E. Thorpe. 1998. Expression of soluble VEGF receptor 2 and characterization of its binding by surface plasmon resonance. *Biochem. Biophys. Res. Commun.* 252:643–648.

Hui, E.E., and S.N. Bhatia. 2007. Micromechanical control of cell-cell interactions. *Proc. Natl. Acad. Sci. U.S.A.* 104:5722–5726.

Humphries, D.E., and J.E. Silbert. 1988. Chlorate: A reversible inhibitor of proteoglycan sulfation. *Biochem Biophys Res Commun*. 154:365–371.

Hynes, R.O. 2009. The Extracellular Matrix: Not Just Pretty Fibrils. *Science*. 326:1216 –1219.

Iannaccone, P.M., G.U. Taborn, R.L. Garton, M.D. Caplice, and D.R. Brenin. 1994. Pluripotent Embryonic Stem Cells from the Rat Are Capable of Producing Chimeras. *Developmental Biology*. 163:288–292.

Ip, N.Y., S.H. Nye, T.G. Boulton, S. Davis, T. Taga, Y. Li, S.J. Birren, K. Yasukawa, T. Kishimoto, and D.J. Anderson. 1992. CNTF and LIF act on neuronal cells via shared signaling pathways that involve the IL-6 signal transducing receptor component gp130. *Cell*. 69:1121–1132.

Jackson, S.A., J. Schiesser, E.G. Stanley, and A.G. Elefanty. 2010. Differentiating Embryonic Stem Cells Pass through "Temporal Windows" That Mark Responsiveness to Exogenous and Paracrine Mesendoderm Inducing Signals. *PLoS ONE*. 5:e10706.

Jenniskens, G.J., A. Oosterhof, R. Brandwijk, J.H. Veerkamp, and T.H. van Kuppevelt. 2000. Heparan sulfate heterogeneity in skeletal muscle basal lamina: demonstration by phage display-derived antibodies. *J. Neurosci.* 20:4099–4111.

Jiang, J., Y.-S. Chan, Y.-H. Loh, J. Cai, G.-Q. Tong, C.-A. Lim, P. Robson, S. Zhong, and H.-H. Ng. 2008. A core Klf circuitry regulates self-renewal of embryonic stem cells. *Nat Cell Biol*. 10:353–360.

Joslin, E.J., L.K. Opresko, A. Wells, H.S. Wiley, and D.A. Lauffenburger. 2007. EGF-receptor-mediated mammary epithelial cell migration is driven by sustained ERK signaling from autocrine stimulation. *J. Cell. Sci*. 120:3688–3699.

Kalimi, G.H., and C.W. Lo. 1988. Communication compartments in the gastrulating mouse embryo. *J. Cell Biol.* 107:241–255.

Kalmar, T., C. Lim, P. Hayward, S. Muñoz-Descalzo, J. Nichols, J. Garcia-Ojalvo, and A. Martinez Arias. 2009. Regulated Fluctuations in Nanog Expression Mediate Cell Fate Decisions in Embryonic Stem Cells. *PLoS Biol*. 7:e1000149.

Kamei, K., S. Guo, Z.T.F. Yu, H. Takahashi, E. Gschweng, C. Suh, X. Wang, J. Tang, J. McLaughlin, O.N. Witte, K.-B. Lee, and H.-R. Tseng. 2009. An integrated microfluidic culture device for quantitative analysis of human embryonic stem cells. *Lab on a Chip*. 9:555.

Kane, R.S., S. Takayama, E. Ostuni, D.E. Ingber, and G.M. Whitesides. 1999. Patterning proteins and cells using soft lithography. *Biomaterials*. 20:2363–2376.

Kang, J.H., Y.C. Kim, and J.-K. Park. 2008. Analysis of pressure-driven air bubble elimination in a microfluidic device. *Lab on a Chip*. 8:176.

Kawasaki, H., K. Mizuseki, S. Nishikawa, S. Kaneko, Y. Kuwana, S. Nakanishi, S.-I. Nishikawa, and Y. Sasai. 2000. Induction of Midbrain Dopaminergic Neurons from ES Cells by Stromal Cell-Derived Inducing Activity. *Neuron*. 28:31–40.

Kellner, C., M.L. Botero, D. Latta, K. Drese, A. Fragoso, and C.K. O'Sullivan. 2011. Automated microsystem for electrochemical detection of cancer markers. *Electrophoresis*. 32:926–930.

Keung, A.J., E.M. de Juan-Pardo, D.V. Schaffer, and S. Kumar. 2011. Rho GTPases mediate the mechanosensitive lineage commitment of neural stem cells. *Stem Cells*. 29:1886–1897.

Keung, A.J., S. Kumar, and D.V. Schaffer. 2010. Presentation counts: microenvironmental regulation of stem cells by biophysical and material cues. *Annu. Rev. Cell Dev. Biol.* 26:533–556.

Kim, L., M.D. Vahey, H.-Y. Lee, and J. Voldman. 2006. Microfluidic arrays for logarithmically perfused embryonic stem cell culture. *Lab Chip*. 6:394.

King, K.R., S. Wang, D. Irimia, A. Jayaraman, M. Toner, and M.L. Yarmush. 2007. A high-throughput microfluidic real-time gene expression living cell array. *Lab on a Chip*. 7:77.

Kishimoto, T. 2005. INTERLEUKIN-6: From Basic Science to Medicine—40 Years in Immunology. *Annual Review of Immunology*. 23:1–21.

Korin, N., A. Bransky, U. Dinnar, and S. Levenberg. 2008. Periodic "flow-stop" perfusion microchannel bioreactors for mammalian and human embryonic stem cell long-term culture. *Biomedical Microdevices*. 11:87–94.

Kouskoff, V., G. Lacaud, S. Schwantz, H.J. Fehling, and G. Keller. 2005. Sequential development of hematopoietic and cardiac mesoderm during embryonic stem cell differentiation. *Proceedings of the National Academy of Sciences of the United States of America*. 102:13170 – 13175.

Kubo, A., K. Shinozaki, J.M. Shannon, V. Kouskoff, M. Kennedy, S. Woo, H.J. Fehling, and G. Keller. 2004. Development of definitive endoderm from embryonic stem cells in culture. *Development*. 131:1651–1662.

Kühl, M., S. Finnemann, O. Binder, and D. Wedlich. 1996. Dominant negative expression of a cytoplasmically deleted mutant of XB/U-cadherin disturbs mesoderm migration during gastrulation in Xenopus laevis. *Mechanisms of Development*. 54:71–82.

Kuhl, P.R., and L.G. Griffith-Cima. 1996. Tethered epidermal growth factor as a paradigm for growth factor-induced stimulation from the solid phase. *Nat. Med.* 2:1022–1027.

Kunath, T., M.K. Saba-El-Leil, M. Almousailleakh, J. Wray, S. Meloche, and A. Smith. 2007. FGF stimulation of the Erk1/2 signalling cascade triggers transition of pluripotent embryonic stem cells from self-renewal to lineage commitment. *Development*. 134:2895 –2902.

Lam, M.L., S.I. Hashem, and W.C. Claycomb. 2010. Embryonic stem cell-derived cardiomyocytes harbor a subpopulation of niche-forming Sca-1+ progenitor cells. *Mol Cell Biochem*. 349:69–76.

Lanner, F., K.L. Lee, M. Sohl, K. Holmborn, H. Yang, J. Wilbertz, L. Poellinger, J. Rossant, and F. Farnebo. 2010. Heparan Sulfation–Dependent Fibroblast Growth Factor Signaling Maintains Embryonic Stem Cells Primed for Differentiation in a Heterogeneous State. *STEM CELLS*. 28:191–200.

Lanner, F., and J. Rossant. 2010. The role of FGF/Erk signaling in pluripotent cells. *Development*. 137:3351 –3360.

Lauffenburger, D., and C. Cozens. 1989. Regulation of mammalian cell growth by autocrine growth factors: analysis of consequences for inoculum cell density effects. *Biotechnol. Bioeng.* 33:1365–1378.

Lauffenburger, D.A., G.T. Oehrtman, L. Walker, and H.S. Wiley. 1998. Real-time quantitative measurement of autocrine ligand binding indicates that autocrine loops are spatially localized. *Proc Natl Acad Sci USA*. 95:15368 –15373.

Lee, C.H., and B.M. Gumbiner. 1995. Disruption of gastrulation movements in Xenopus by a dominant-negative mutant for C-cadherin. *Dev. Biol.* 171:363–373.

Levenberg, S., B.Z. Katz, K.M. Yamada, and B. Geiger. 1998. Long-range and selective autoregulation of cell-cell or cell-matrix adhesions by cadherin or integrin ligands. *J. Cell. Sci.* 111 (Pt 3):347–357.

Levine, A.J., and A.H. Brivanlou. 2006. GDF3, a BMP inhibitor, regulates cell fate in stem cells and early embryos. *Development*. 133:209 –216.

Levine, A.J., Z.J. Levine, and A.H. Brivanlou. 2009. GDF3 is a BMP inhibitor that can activate Nodal signaling only at very high doses. *Developmental Biology*. 325:43–48.

Li, S., D. Harrison, S. Carbonetto, R. Fassler, N. Smyth, D. Edgar, and P.D. Yurchenco. 2002. Matrix assembly, regulation, and survival functions of laminin and its receptors in embryonic stem cell differentiation. *J. Cell Biol.* 157:1279–1290.

Li, X., L. Zhu, A. Yang, J. Lin, F. Tang, S. Jin, Z. Wei, J. Li, and Y. Jin. 2011. Calcineurin-NFAT Signaling Critically Regulates Early Lineage Specification in Mouse Embryonic Stem Cells and Embryos. *Cell Stem Cell*. 8:46–58.

Lo, C.W., and N.B. Gilula. 1979. Gap junctional communication in the preimplantation mouse embryo. *Cell*. 18:399–409.

Lu, P., K. Takai, V.M. Weaver, and Z. Werb. 2011. Extracellular matrix degradation and remodeling in development and disease. *Cold Spring Harb Perspect Biol*. 3.

Ludwig, T., R. Kirmse, K. Poole, and U.S. Schwarz. 2007. Probing cellular microenvironments and tissue remodeling by atomic force microscopy. *Pflügers Archiv - European Journal of Physiology*. 456:29–49.

Maherali, N., R. Sridharan, W. Xie, J. Utikal, S. Eminli, K. Arnold, M. Stadtfeld, R. Yachechko, J. Tchieu, R. Jaenisch, K. Plath, and K. Hochedlinger. 2007. Directly reprogrammed fibroblasts show global epigenetic remodeling and widespread tissue contribution. *Cell Stem Cell*. 1:55–70.

Martin, G.R. 1981. Isolation of a pluripotent cell line from early mouse embryos cultured in medium conditioned by teratocarcinoma stem cells. *Proc Natl Acad Sci USA*. 78:7634–7638.

Matrisian, L.M. 1990. Metalloproteinases and their inhibitors in matrix remodeling. *Trends in Genetics*. 6:121–125.

Mehta, K., and J.J. Linderman. 2006. Model-based analysis and design of a microchannel reactor for tissue engineering. *Biotechnol. Bioeng.* 94:596–609.

Mesnard, D., M. Donnison, C. Fuerer, P.L. Pfeffer, and D.B. Constam. 2011. The microenvironment patterns the pluripotent mouse epiblast through paracrine Furin and Pace4 proteolytic activities. *Genes & Development*. 25:1871 –1880.

Meyvantsson, I., and D.J. Beebe. 2008. Cell Culture Models in Microfluidic Systems. *Annu Rev Anal Chem*. 1:423–449.

Mitsui, K., Y. Tokuzawa, H. Itoh, K. Segawa, M. Murakami, K. Takahashi, M. Maruyama, M. Maeda, and S. Yamanaka. 2003. The Homeoprotein Nanog Is Required for Maintenance of Pluripotency in Mouse Epiblast and ES Cells. *Cell*. 113:631–642.

Mittal, N., and J. Voldman. 2011. Nonmitogenic survival-enhancing autocrine factors including cyclophilin A contribute to density-dependent mouse embryonic stem cell growth. *Stem Cell Research*. 6:168–176.

Moledina, F., G. Clarke, A. Oskooei, K. Onishi, A. Günther, and P.W. Zandstra. 2012. Predictive microfluidic control of regulatory ligand trajectories in individual pluripotent cells. *Proc. Natl. Acad. Sci. U.S.A.* 109:3264–3269.

Moogk, D., M. Stewart, D. Gamble, M. Bhatia, and E. Jervis. 2010. Human ESC colony formation is dependent on interplay between self-renewing hESCs and unique precursors responsible for niche generation. *Cytometry Part A*. 77A:321–327.

Murohashi, M., T. Nakamura, S. Tanaka, T. Ichise, N. Yoshida, T. Yamamoto, M. Shibuya, J. Schlessinger, and N. Gotoh. 2010. An FGF4-FRS2α-Cdx2 Axis in Trophoblast Stem Cells Induces Bmp4 to Regulate Proper Growth of Early Mouse Embryos. *STEM CELLS*. 28:113–121.

Murray, P., and D. Edgar. 2000. Regulation of programmed cell death by basement membranes in embryonic development. *J. Cell Biol.* 150:1215–1221.

Murry, C.E., and G. Keller. 2008. Differentiation of Embryonic Stem Cells to Clinically Relevant Populations: Lessons from Embryonic Development. *Cell*. 132:661–680.

Nakajima, M., T. Ishimuro, K. Kato, I.-K. Ko, I. Hirata, Y. Arima, and H. Iwata. 2007. Combinatorial protein display for the cell-based screening of biomaterials that direct neural stem cell differentiation. *Biomaterials*. 28:1048–1060.

Nguyen, K.T., and J.L. West. 2002. Photopolymerizable hydrogels for tissue engineering applications. *Biomaterials*. 23:4307–4314.

Nichols, J., E.P. Evans, and A.G. Smith. 1990. Establishment of germ-line-competent embryonic stem (ES) cells using differentiation inhibiting activity. *Development*. 110:1341 –1348.

Nikmanesh, M., Z. Shi, and J.M. Tarbell. Heparan sulfate proteoglycan mediates shear stress-induced endothelial gene expression in mouse embryonic stem cell-derived endothelial cells. *Biotechnology and Bioengineering*.

Niwa, H., K. Ogawa, D. Shimosato, and K. Adachi. 2009. A parallel circuit of LIF signalling pathways maintains pluripotency of mouse ES cells. *Nature*. 460:118–122.

Nuttall, R.K., C.L. Sampieri, C.J. Pennington, S.E. Gill, G.A. Schultz, and D.R. Edwards. 2004. Expression analysis of the entire MMP and TIMP gene families during mouse tissue development. *FEBS Letters*. 563:129–134.

Ogawa, K., A. Saito, H. Matsui, H. Suzuki, S. Ohtsuka, D. Shimosato, Y. Morishita, T. Watabe, H. Niwa, and K. Miyazono. 2007. Activin-Nodal signaling is involved in propagation of mouse embryonic stem cells. *Journal of Cell Science*. 120:55 –65.

Oka, M., K. Tagoku, T.L. Russell, Y. Nakano, T. Hamazaki, E.M. Meyer, T. Yokota, and N. Terada. 2002. CD9 Is Associated with Leukemia Inhibitory Factor-mediated Maintenance of Embryonic Stem Cells. *Mol. Biol. Cell*. 13:1274–1281.

Okita, K., T. Ichisaka, and S. Yamanaka. 2007. Generation of germline-competent induced pluripotent stem cells. *Nature*. 448:313–317.

Pathak, C.P., A.S. Sawhney, and J.A. Hubbell. 1992. Rapid photopolymerization of immunoprotective gels in contact with cells and tissue. *J. Am. Chem. Soc.* 114:8311–8312.

Peerani, R., K. Onishi, A. Mahdavi, E. Kumacheva, and P.W. Zandstra. 2009. Manipulation of Signaling Thresholds in "Engineered Stem Cell Niches" Identifies Design Criteria for Pluripotent Stem Cell Screens. *PLoS ONE*. 4:e6438.

Peerani, R., B.M. Rao, C. Bauwens, T. Yin, G.A. Wood, A. Nagy, E. Kumacheva, and P.W. Zandstra. 2007. Niche-mediated control of human embryonic stem cell self-renewal and differentiation. *EMBO J*. 26:4744–4755.

Pennica, D., K.J. Shaw, T.A. Swanson, M.W. Moore, D.L. Shelton, K.A. Zioncheck, A. Rosenthal, T. Taga, N.F. Paoni, and W.I. Wood. 1995. Cardiotrophin-1. Biological activities and binding to the leukemia inhibitory factor receptor/gp130 signaling complex. *J. Biol. Chem.* 270:10915–10922.

Peppas, N.A., K.B. Keys, M. Torres-Lugo, and A.M. Lowman. 1999. Poly(ethylene glycol)-containing hydrogels in drug delivery. *J Control Release*. 62:81–87.

Peracchia, C., and A.F. Dulhunty. 1976. Low resistance junctions in crayfish. Structural changes with functional uncoupling. *J. Cell Biol.* 70:419–439.

Perea-Gomez, A., F.D.J. Vella, W. Shawlot, M. Oulad-Abdelghani, C. Chazaud, C. Meno, V. Pfister, L. Chen, E. Robertson, H. Hamada, R.R. Behringer, and S.-L. Ang. 2002. Nodal Antagonists in the Anterior Visceral Endoderm Prevent the Formation of Multiple Primitive Streaks. *Developmental Cell*. 3:745–756.

Perris, R., and D. Perissinotto. 2000. Role of the extracellular matrix during neural crest cell migration. *Mechanisms of Development*. 95:3–21.

Pons, S., and E. Martí. 2000. Sonic hedgehog synergizes with the extracellular matrix protein vitronectin to induce spinal motor neuron differentiation. *Development*. 127:333–342.

Przybyla, L., and J. Voldman. 2012a. Probing Embryonic Stem Cell Autocrine and Paracrine Signaling Using Microfluidics. *Annual Review of Analytical Chemistry*. 5:null.

Przybyla, L.M., and J. Voldman. 2012b. Attenuation of extrinsic signaling reveals the importance of matrix remodeling on maintenance of embryonic stem cell self-renewal. *Proc. Natl. Acad. Sci. U.S.A.* 109:835–840.

Purpura, K.A., J. Morin, and P.W. Zandstra. 2008. Analysis of the temporal and concentration-dependent effects of BMP-4, VEGF, and TPO on development of embryonic stem cell-derived mesoderm and blood progenitors in a defined, serum-free media. *Experimental Hematology*. 36:1186–1198.

Rathjen, J., J.A. Lake, M.D. Bettess, J.M. Washington, G. Chapman, and P.D. Rathjen. 1999. Formation of a primitive ectoderm like cell population, EPL cells, from ES cells in response to biologically derived factors. *J Cell Sci*. 112:601–612.

Ringvall, M., J. Ledin, K. Holmborn, T. van Kuppevelt, F. Ellin, I. Eriksson, A.M. Olofsson, L. Kjellen, and E. Forsberg. 2000. Defective heparan sulfate biosynthesis and neonatal lethality in mice lacking N-deacetylase/N-sulfotransferase-1. *J. Biol. Chem.* 275:25926–25930.

Robertson, M., I. Chambers, P. Rathjen, J. Nichols, and A. Smith. 1993. Expression of alternative forms of differentiation inhibiting activity (DIA/LIF) during murine embryogenesis and in neonatal and adult tissues. *Dev. Genet.* 14:165–173.

Roovers, K., and R.K. Assoian. 2000. Integrating the MAP kinase signal into the G1 phase cell cycle machinery. *BioEssays*. 22:818–826.

Rosen, S.D., and H. Lemjabbar-Alaoui. 2010. Sulf-2: an extracellular modulator of cell signaling and a cancer target candidate. *Expert Opin. Ther. Targets*. 14:935–949.

Rosenthal, A., A. Macdonald, and J. Voldman. 2007. Cell patterning chip for controlling the stem cell microenvironment. *Biomaterials*. 28:3208–3216.

Saha, K., A.J. Keung, E.F. Irwin, Y. Li, L. Little, D.V. Schaffer, and K.E. Healy. 2008. Substrate modulus directs neural stem cell behavior. *Biophys. J.* 95:4426–4438.

Saha, K., and D.V. Schaffer. 2006. Signal dynamics in Sonic hedgehog tissue patterning. *Development*. 133:889–900.

Sanes, J.R., E. Engvall, R. Butkowski, and D.D. Hunter. 1990. Molecular heterogeneity of basal laminae: isoforms of laminin and collagen IV at the neuromuscular junction and elsewhere. *J. Cell Biol.* 111:1685–1699.

Schneider, M.R., H. Adler, J. Braun, B. Kienzle, E. Wolf, and H. Kolb. 2007. Canine Embryo-Derived Stem Cells—Toward Clinically Relevant Animal Models for Evaluating Efficacy and Safety of Cell Therapies. *STEM CELLS*. 25:1850–1851.

Schroeter, E.H., J.A. Kisslinger, and R. Kopan. 1998. Notch-1 signalling requires ligand-induced proteolytic release of intracellular domain. *Nature*. 393:382–386.

Schryver, B., L. Hinck, and J. Papkoff. 1996. Properties of Wnt-1 protein that enable cell surface association. *Oncogene*. 13:333–342.

Silvennoinen, O., B.A. Witthuhn, F.W. Quelle, J.L. Cleveland, T. Yi, and J.N. Ihle. 1993. Structure of the murine Jak2 protein-tyrosine kinase and its role in interleukin 3 signal transduction. *Proc. Natl. Acad. Sci. U.S.A.* 90:8429–8433.

Singh, A.M., T. Hamazaki, K.E. Hankowski, and N. Terada. 2007. A heterogeneous expression pattern for Nanog in embryonic stem cells. *Stem Cells*. 25:2534–2542.

Smith, A.G., J.K. Heath, D.D. Donaldson, G.G. Wong, J. Moreau, M. Stahl, and D. Rogers. 1988. Inhibition of pluripotential embryonic stem cell differentiation by purified polypeptides. *Nature*. 336:688–690.

Smith Jr., G.N., E.A. Mickler, K.A. Hasty, and K.D. Brandt. 1999. Specificity of inhibition of matrix metalloproteinase activity by doxycycline: Relationship to structure of the enzyme. *Arthritis & Rheumatism*. 42:1140–1146.

Smith, Z.D., I. Nachman, A. Regev, and A. Meissner. 2010. Dynamic single-cell imaging of direct reprogramming reveals an early specifying event. *Nat. Biotechnol.* 28:521–526.

Soncin, F., M. Lisa, E. Dominik, R. Sarah, M.E. Angela, B. Nicoletta, R. Angela, D. Steve, K. Rolf, L.R.M. Catherine, and M.W. Christopher. 2009. Abrogation of E-Cadherin-Mediated Cell-Cell Contact in Mouse Embryonic Stem Cells Results in Reversible LIF-Independent Self-Renewal. *Stem Cells*. 27:2069–2080.

Song, Y.-A., M. Chan, C. Celio, S.R. Tannenbaum, J.S. Wishnok, and J. Han. 2010. Free-flow zone electrophoresis of peptides and proteins in PDMS microchip for narrow pI range sample prefractionation coupled with mass spectrometry. *Anal. Chem.* 82:2317–2325.

Sporn, M.B., and G.J. Todaro. 1980. Autocrine secretion and malignant transformation of cells. *N. Engl. J. Med.* 303:878–880.

Squires, T.M., R.J. Messinger, and S.R. Manalis. 2008. Making it stick: convection, reaction and diffusion in surface-based biosensors. *Nat. Biotechnol.* 26:417–426.

Stavridis, M.P., J.S. Lunn, B.J. Collins, and K.G. Storey. 2007. A discrete period of FGF-induced Erk1/2 signalling is required for vertebrate neural specification. *Development*. 134:2889 –2894.

Stetler-Stevenson, W.G., S. Aznavoorian, and L.A. Liotta. 1993. Tumor Cell Interactions with the Extracellular Matrix During Invasion and Metastasis. *Annual Review of Cell Biology*. 9:541–573.

Stewart, C.L., P. Kaspar, L.J. Brunet, H. Bhatt, I. Gadi, F. Kontgen, and S.J. Abbondanzo. 1992. Blastocyst implantation depends on maternal expression of leukaemia inhibitory factor. *Nature*. 359:76–79.

Sun, X., E.N. Meyers, M. Lewandoski, and G.R. Martin. 1999. Targeted disruption of Fgf8 causes failure of cell migration in the gastrulating mouse embryo. *Genes Dev.* 13:1834–1846.

Taipale, J., and J. Keski-Oja. 1997. Growth factors in the extracellular matrix. *The FASEB Journal*. 11:51 –59.

Takahashi, K., K. Tanabe, M. Ohnuki, M. Narita, T. Ichisaka, K. Tomoda, and S. Yamanaka. 2007. Induction of pluripotent stem cells from adult human fibroblasts by defined factors. *Cell*. 131:861–872.

Takahashi, K., and S. Yamanaka. 2006. Induction of Pluripotent Stem Cells from Mouse Embryonic and Adult Fibroblast Cultures by Defined Factors. *Cell*. 126:663–676.

Tamkun, J.W., D.W. DeSimone, D. Fonda, R.S. Patel, C. Buck, A.F. Horwitz, and R.O. Hynes. 1986. Structure of integrin, a glycoprotein involved in the transmembrane linkage between fibronectin and actin. *Cell*. 46:271–282.

Taylor, K.R., and R.L. Gallo. 2006. Glycosaminoglycans and their proteoglycans: host-associated molecular patterns for initiation and modulation of inflammation. *FASEB J.* 20:9–22.

Tesar, P.J., J.G. Chenoweth, F.A. Brook, T.J. Davies, E.P. Evans, D.L. Mack, R.L. Gardner, and R.D.G. McKay. 2007. New cell lines from mouse epiblast share defining features with human embryonic stem cells. *Nature*. 448:196–199.

Thomson, J.A., J. Itskovitz-Eldor, S.S. Shapiro, M.A. Waknitz, J.J. Swiergiel, V.S. Marshall, and J.M. Jones. 1998. Embryonic Stem Cell Lines Derived from Human Blastocysts. *Science*. 282:1145 –1147.

Thomson, J.A., J. Kalishman, T.G. Golos, M. Durning, C.P. Harris, R.A. Becker, and J.P. Hearn. 1995. Isolation of a primate embryonic stem cell line. *Proceedings of the National Academy of Sciences*. 92:7844 –7848.

Toh, Y.-C., K. Blagovic, H. Yu, and J. Voldman. 2011. Spatially organized in vitro models instruct asymmetric stem cell differentiation. *Integrative Biology*. in press.

Toh, Y.-C., and J. Voldman. 2011. Fluid shear stress primes mouse embryonic stem cells for differentiation in a self-renewing environment via heparan sulfate proteoglycans transduction. *The FASEB Journal*. 25:1208 –1217.

Toyooka, Y., D. Shimosato, K. Murakami, K. Takahashi, and H. Niwa. 2008. Identification and characterization of subpopulations in undifferentiated ES cell culture. *Development*. 135:909 – 918.

Tremml, G., M. Singer, and R. Malavarca. 2008. Culture of Mouse Embryonic Stem Cells.

Ulrich, T.A., E.M. de Juan Pardo, and S. Kumar. 2009. The mechanical rigidity of the extracellular matrix regulates the structure, motility, and proliferation of glioma cells. *Cancer Res.* 69:4167–4174.

Unger, M.A., H.-P. Chou, T. Thorsen, A. Scherer, and S.R. Quake. 2000. Monolithic Microfabricated Valves and Pumps by Multilayer Soft Lithography. *Science*. 288:113 –116.

Villa-Diaz, L.G., Y. Torisawa, T. Uchida, J. Ding, N.C. Nogueira-de-Souza, K.S. O'Shea, S. Takayama, and G.D. Smith. 2009. Microfluidic culture of single human embryonic stem cell colonies. *Lab on a Chip*. 9:1749.

Vu, T.H., and Z. Werb. 2000. Matrix metalloproteinases: effectors of development and normal physiology. *Genes Dev.* 14:2123–2133.

Wegenka, U.M., J. Buschmann, C. Lütticken, P.C. Heinrich, and F. Horn. 1993. Acute-phase response factor, a nuclear factor binding to acute-phase response elements, is rapidly activated by interleukin-6 at the posttranslational level. *Mol. Cell. Biol.* 13:276–288.

Wells, R.G., and D.E. Discher. 2008. Matrix Elasticity, Cytoskeletal Tension, and TGF-{beta}: The Insoluble and Soluble Meet. *Sci. Signal.* 1:pe13.

Wernig, M., A. Meissner, R. Foreman, T. Brambrink, M. Ku, K. Hochedlinger, B.E. Bernstein, and R. Jaenisch. 2007. In vitro reprogramming of fibroblasts into a pluripotent ES-cell-like state. *Nature*. 448:318–324.

Wichterle, H., I. Lieberam, J.A. Porter, and T.M. Jessell. 2002. Directed Differentiation of Embryonic Stem Cells into Motor Neurons. *Cell*. 110:385–397.

Williams, R.L., D.J. Hilton, S. Pease, T.A. Willson, C.L. Stewart, D.P. Gearing, E.F. Wagner, D. Metcalf, N.A. Nicola, and N.M. Gough. 1988. Myeloid leukaemia inhibitory factor maintains the developmental potential of embryonic stem cells. *Nature*. 336:684–687.

Xiao, L., X. Yuan, and S.J. Sharkis. 2006. Activin A Maintains Self-Renewal and Regulates Fibroblast Growth Factor, Wnt, and Bone Morphogenic Protein Pathways in Human Embryonic Stem Cells. *STEM CELLS*. 24:1476–1486.

Xu, R.-H., T.L. Sampsell-Barron, F. Gu, S. Root, R.M. Peck, G. Pan, J. Yu, J. Antosiewicz-Bourget, S. Tian, R. Stewart, and J.A. Thomson. 2008. NANOG Is a Direct Target of TGF[beta]/Activin-Mediated SMAD Signaling in Human ESCs. *Cell Stem Cell*. 3:196–206.

Yamada, K.M., and K. Olden. 1978. Fibronectins--adhesive glycoproteins of cell surface and blood. *Nature*. 275:179–184.

Yamaguchi, T.P., K. Harpal, M. Henkemeyer, and J. Rossant. 1994. fgfr-1 is required for embryonic growth and mesodermal patterning during mouse gastrulation. *Genes Dev.* 8:3032–3044.

Yamanaka, Y., F. Lanner, and J. Rossant. 2010. FGF signal-dependent segregation of primitive endoderm and epiblast in the mouse blastocyst. *Development*. 137:715 –724.

Ying, Q.-L., J. Nichols, I. Chambers, and A. Smith. 2003a. BMP Induction of Id Proteins Suppresses Differentiation and Sustains Embryonic Stem Cell Self-Renewal in Collaboration with STAT3. *Cell*. 115:281–292.

Ying, Q.-L., M. Stavridis, D. Griffiths, M. Li, and A. Smith. 2003b. Conversion of embryonic stem cells into neuroectodermal precursors in adherent monoculture. *Nat Biotech*. 21:183–186.

Ying, Q.-L., J. Wray, J. Nichols, L. Batlle-Morera, B. Doble, J. Woodgett, P. Cohen, and A. Smith. 2008. The ground state of embryonic stem cell self-renewal. *Nature*. 453:519–523.

Yoshida, K., I. Chambers, J. Nichols, A. Smith, M. Saito, K. Yasukawa, M. Shoyab, T. Taga, and T. Kishimoto. 1994. Maintenance of the pluripotential phenotype of embryonic stem cells through direct activation of gp130 signalling pathways. *Mechanisms of Development*. 45:163–171.

Yu, J., M.A. Vodyanik, K. Smuga-Otto, J. Antosiewicz-Bourget, J.L. Frane, S. Tian, J. Nie, G.A. Jonsdottir, V. Ruotti, R. Stewart, I.I. Slukvin, and J.A. Thomson. 2007. Induced pluripotent stem cell lines derived from human somatic cells. *Science*. 318:1917–1920.

Zandstra, P.W., H.V. Le, G.Q. Daley, L.G. Griffith, and D.A. Lauffenburger. 2000. Leukemia inhibitory factor (LIF) concentration modulates embryonic stem cell self-renewal and differentiation independently of proliferation. *Biotechnol Bioeng*. 69:607–617.

Zhu, J. 2010. Bioactive modification of poly(ethylene glycol) hydrogels for tissue engineering. *Biomaterials*. 31:4639–4656.

Van Zoelen, E.J.J., I. Koornneef, J.C.M.T. Holthuis, M.J.W. Oostwaard, A. Feijen, T.L. De Poorter, C.L. Mummery, and S.C. Van Buul-Offers. 1989. Production of Insulin-Like Growth Factors, Platelet- Derived Growth Factor, and Transforming Growth Factors and Their Role in the Density-Dependent Growth Regulation of a Differentiated Embryonal Carcinoma Cell Line. *Endocrinology*. 124:2029–2041.

Appendix **General Methods**

ESC culture and cell lines

Mouse ESCs (CCE, ABJ1 (Bortvin et al., 2004), Sox2-GFP, 7xTCF-eGFP (ten Berge et al., 2008), Brachyury-GFP (Fehling et al., 2003), H2A-GFP (a gift from the Boyer lab), and H2B-GFP (Foudi et al., 2009) lines) were routinely cultured in medium consisting of DMEM supplemented with 15% defined fetal bovine serum (Hyclone), 4 mM L-glutamine, 1 mM non-essential amino acids, 1X penicillin-streptomycin, 100 μM β-mercaptoethanol (Sigma) and 10 ng/mL LIF (ESGRO, Chemicon). All cell culture reagents were from Invitrogen unless otherwise noted. Cells were grown at 37°C in a humidified incubator with 7.5% CO_2. For serum-free culture, N2B27 medium with 10 ng/mL LIF and 10 ng/mL BMP-4 (R and D Systems) was used (Ying et al., 2003a) and wells were pre-coated with gelatin. All additives to cell cultures are listed below.

Culture media additives

Additive	**Concentration**	**Source**
Inhibitors		
PD0325901	1 μM	Stemgent
CHIR99021	3 μM	Stemgent
sodium chlorate	20 mM	Sigma-Aldrich
JAK inhibitor I	1 μM	Calbiochem
Batimastat	10 μM	Tocris
Ro 32-3555	50 μM	Tocris
Bay 11-7085	50 μM	Tocris
IWP2	2 μM	Sigma
SB431542	1 μM	Sigma
Recombinant proteins		
Activin	30 ng/ml	Peprotech
FGF2	12 ng/ml	Peprotech
FGF4	5 ng/ml	R and D Systems
TGFβ	40 ng/ml	Peprotech
TIMP1	50 ng/ml	Peprotech
MMP1	50 ng/ml	Peprotech

MMP2	50 ng/ml	Peprotech
MMP3	50 ng/ml	Peprotech
Dkk	100 ng/ml	Peprotech
Wnt3a	100 ng/ml	Peprotech
CT-1	10 ng/ml	Peprotech
CNTF	10 ng/ml	Peprotech
OSM	10 ng/ml	Peprotech
Antibodies		
Phospho-Stat3	1:100	Cell Signaling Technology
Phospho-ERK1/2	2.5 μg/ml	BD Biosciences
Secondary antibodies	2 μg/ml	Invitrogen
HepSS	10 μg/ml	Lifespan Biosciences
Oct4	5 μg/ml	Abcam
LIF blocking antibody	500 ng/ml	R and D Systems
CT-1 blocking antibody	7.5 μg/ml	R and D Systems
CNTF blocking antibody	7.5 μg/ml	R and D Systems
OSM blocking antibody	7.5 μg/ml	R and D Systems
Other		
heparin	1 μg/ml	Sigma
collagenase	1 ng/ml - 20 μg/ml	Sigma #C9722
Retinoic Acid	1 μM	Sigma
Doxycycline	2 μg/ml	Sigma
Hoechst	100 ng/ml	Sigma

Quantitative RT-PCR

Cells were harvested using TrypLE Express trypsin replacement (Invitrogen) and total RNA was isolated using the RNeasy Mini Kit (Qiagen), according to manufacturer's instructions. RNA was converted to cDNA using the DyNAmo cDNA synthesis kit with Oligo(dT) primer or the ProtoScript cDNA synthesis kit with Oligo(dT) primer (New England Biolabs). Quantitative PCR reactions were set up using the DyNAmo SYBR Green qPCR kit (New England Biolabs) or the iQ SYBR green supermix (Bio-Rad), according to manufacturer's instructions. Reactions were run on an MJ Opticon DNA Engine thermal cycler or on a Bio-Rad C1000 thermal cycler using a CFX96 real-time system. Primers are listed below.

Quantitative RT-PCR primers

Gene	qRT-PCR forward primer	qRT-PCR reverse primer
FGF5	GAAAAGACAGGCCGAGAGTG	GAAGTGGGTGGAGACGTGTT
Nanog	CTGCTCCGCTCCATAACTTC	TTTCCCTAGTGGCTTCCAAA
Gapdh	CACTGAGCATCTCCCTCACA	GTGGGTGCAGCGAACTTTAT
T	CAGCCCACCTACTGGCTCTA	GAGCCTGGGGTGATGGTA
Dnmt3b	GCATGAAGGCCAGATCAAAT	GCTTCCACCAATCACCAAGT
AFP	CCTGTGAACTCTGGTATCAG	GCTCACACCAAAGCGTCAAC
Gata4	TCTCACTATGGGCACAGCAG	GGGACAGCTTCAGAGCAGAC
Sox17	CTTTATGGTGTGGGCCAAAG	GCTTCTCTGCCAAGGTCAAC
Klf4	CAGGCTGTGGCAAAACCTAT	CGTCCCAGTCACAGTGGTAA
Sox1	CCTGAAAATGATGCTGCTGA	GGAGTAGCTGTGGGTGTGGT
Nestin	GATCGCTCAGATCCTGGAAG	AGTTCTCAGCCTCCAGCAGA
Sox2	AACGCCTTCATGGTATGGTC	TCTCGGTCTCGGACAAAAGT
Oct4	CACGAGTGGAAAGCAACTCA	TTCATGTCCTGGGACTCCTC
Rex1	CCCCCTGGAAGTGAGTCATA	CCACTTGTCTTTGCCGTTTT
Eomes	TTCCGGGACAACTACGATTC	GACCTCCAGGGACAATCTGA
Nodal	ACCATGCCTACATCCAGAGC	ATGCTCAGTGGCTTGGTCTT
Lefty1	TATGTGGCCCTGCTACAACA	GGAGGTCTCTGACACCAGGA
Gata6	CAAAAGCTTGCTCCGGTAAC	TGAGGTGGTCGCTTGTGTAG
Wt1	ATCCGCAACCAAGGATACAG	GGTCCTCGTGTTTGAAGGAA
Hbb-y	GGCCTGTGGAGTAAGGTCAA	GCAGAGGACAAGTTCCCAAA
Hba-x	ATGCGGTTAAGAGCATCGAC	GGGACAGGAGCTTGAAGTTG
Stat3	AGGACATCAGTGGCAAGACC	TGGTCGCATCCATGATCTTA
Socs3	GAGATTTCGCTTCGGGACTA	GGAGCCAGCGTGGATCTG
Vim	AGGAGGCCGAGGAAT GGT	CATCGTTGTTCCGGTTGG

Igfbp2	CCCCTGGACATCTCTACTCC	GGGTTCACACACCAGCACTC
MMP1a	ATTCATGCCAGAACCTGAGC	TGCCTTTGAAATAGCGGACT
MMP2	ATGACATCAAGGGGATCCAG	GGAGTGACAGGTCCCAGTGT
MMP3	TCAGTACCTTCCCAGGTTCG	TTTCAATGGCAGAATCCACA
MMP8	CTTTCAACCAGGCCAAGGTA	GAGCAGCCACGAGAAATAGG
MMP9	CATTCGCGTGGATAAGGAGT	TCACACGCCAGAAGAATTTG
MMP13	ACACTGGCAAAAGCCATTTC	TTTTGGGATGCTTAGGGTTG
Axin2	CCAACACTTTGGCACAGCTA	TTCCTGTCCCTCTGCTGACT
Cdx1	CAACGCCTAGAGCTGGAAAA	GATCTTTACCTGCCGCTCTG
C-myc	CCAGATCCCTGAATTGGAAA	TCGTCTGCTTGAATGGACAG
Gp130	ACCAGATTCCTGTGGACGAC	AGAATCCACATGCACAACCA

Statistical analysis

All results were analyzed by student's T-test and the resulting pairwise p-values are reported. Significance was established at $p<0.05$, and was evaluated up to the level of $p<0.001$.